THE HISTONE DEACETYLASE INHIBITOR PANOBINOSTAT AS A RADIOSENSITISER IN BLADDER CANCER

Blaž Grošelj

Wolfson College

Thesis submitted to the University of Oxford

in accordance with the requirements for the degree of

Doctor of Philosophy

Trinity Term, 2013

University of Oxford

Supervisor

Anne E. Kiltie MA DM MRCP FRCR

Co-Supervisor

Martin Kerr PhD

Assessment Committee

Valentine Macaulay PhD MRCP

Robert Huddart PhD MRCP FRCR









The study presented in this thesis was performed at the Gray Institute for Radiobiology and Radiation Oncology, Department of Oncology, University of Oxford. This work was supported by a scholarship from the Slovene Human Resources Development and Scholarship Fund, and grants from Cancer Research UK.

ABSTRACT

Muscle invasive bladder cancer (MIBC) has a poor prognosis. Currently, therapy consists of radical radiotherapy or cystectomy with or without chemotherapy. The average age of patients with MIBC is high and older patients are less able to tolerate surgery or chemoradiation due to their impaired physical fitness and generally poor renal function. There is an urgent need to find new treatment regimes that are both tolerable and effective.

The aims of this project were to investigate the radiosensitising effects of the histone deacetylase (HDAC) inhibitor panobinostat in bladder cancer cell lines, with the ultimate goal of proposing a novel radiosensitising therapy for MIBC, and to study the effects of panobinostat on the major DNA double strand break (DSB) repair pathways, homologous recombination (HR) and non-homologous end joining (NHEJ), to determine the predominant pathway targeted and to look further upstream at effects on the MRE11/RAD50/NBS1 (MRN) complex.

The HDAC inhibitor panobinostat was found to be toxic in the low nanomolar range and significant radiosensitising effects were demonstrated at doses lower than IC_{50} in all the bladder cell lines studied. The radiosensitising effect of panobinostat was not influenced by *TP53* status, which is generally regarded as an important determinant of bladder cancer response to radiotherapy.

In the “synthetic lethality” bladder cancer cell model, panobinostat predominantly targets the HR pathway, reportedly the only proficient DNA repair pathway in MIBC. HR proteins RAD51 and CtIP were downregulated upon panobinostat treatment in a dose-dependent manner. Upstream, MRE11 and NBS1 proteins were also targeted by panobinostat, with levels slightly decreased in RT112 and T24 cells and in CAL29 cells post-ionising radiation.

In summary, the HDAC inhibitor panobinostat was shown to be an efficient radiosensitiser in bladder cancer cells at low toxic doses and to predominantly target the HR pathway. These findings are promising and may contribute towards establishing a novel combination therapy of panobinostat with IR for MIBC patients.

Zastonj ste prejeli, zastonj dajajte.
Mt 10, 8

Staršema
(to my parents)

ACKNOWLEDGEMENTS

First of all, I would like to thank the two key people without whom this thesis would never have been possible. I am truly grateful to my great supervisor, Dr Anne Kiltie, for giving me the life-changing opportunity to work in her lab and be part of this great Oxford environment. I am grateful for her trust, guidance, advice and time, throughout the thesis process. All her immense help will never be forgotten.

For his constant help, advice and excellent good humour, I could not thank enough my co-supervisor and friend, Dr Martin Kerr. Martin's immense knowledge of biology and his wide experience of lab skills were always inspirational. I can say that I was taught by "the best".

I also want to thank other "lab mates", Sarah, Eva, Helen, Alexa, Katalin, Jackie, Naomi, Becky, Chelsea, and Giulia, Daniel, Selva, Monica, Sophia K, Sophia Z, Aswin, Nikola, Angelos, Anika and Georgina for their happy dispositions and all the amusing gossip we shared. It was a great fun working and talking with them. Of course, I am also grateful for their many useful snippets of scientific advice and helpful explanations.

There were many people at the Gray Institute who were always able to answer even my most illogical questions. I am most grateful to Dr Anderson Ryan for all of his advice over the years and his good humour and trust when they were needed.

I am grateful to Professor Matjaž Zwitter from the Institute of Oncology in Ljubljana, who foresaw my interest in oncology a decade ago and has always actively encouraged me to pursue it.

I wish to thank to my parents Zvonka and Ciril, who were always connected to me in spirit and supportive of my decisions. Words here could not thank them enough! Also, I wish to thank my brothers Urh and Jon and to the one and only Jera, and their families, for their

visits and numerous hilarious phone conversations, which made life abroad so much easier. The same goes for my second family in Šentjošt, headed by Fani and Franci. Hvala vam za vse!

Finally, I want to thank my wife, Darja, for having the great idea of us moving abroad. Also for being a great life-companion. I cannot even begin to mention all her help in the last three years, as there is not enough space to describe it.

TABLE OF CONTENTS

CHAPTER 1: INTRODUCTION 17

1.1 Bladder cancer 17

1.1.1 Epidemiology 17

1.1.2 Histopathology 18

1.1.3 Staging of bladder cancers 19

1.1.4 Molecular basis of bladder carcinogenesis 21

1.1.5 Diagnosis 23

1.1.5.1 Clinical presentation and diagnosis 23

1.1.6 Treatment of non-muscle invasive bladder cancer 24

1.1.6.1 Transurethral resection of bladder cancer (TURBT) 24

1.1.6.2 Intravesical therapies 25

1.1.7 Treatment of muscle invasive bladder cancer (MIBC) 27

1.1.7.1 Radical radiotherapy 28

1.1.7.2 Radical cystectomy 30

1.1.7.3 Radical cystectomy versus radical radiotherapy 31

1.2 Epigenetic cancer therapy 33

1.2.1 Histone deacetylases 33

1.2.2 Histone deacetylase inhibitors 34

1.2.3 HDAC inhibitors and radiation in clinical trials 35

1.3 Irradiation induced double strand break damage 39

1.3.1 IR and DNA damage 40

1.3.2 IR and cell death 40

1.3.3 The “5Rs” of radiobiology and the concept of the therapeutic window 41

1.4 DNA double strand break damage detection, signalling and repair 42

1.4.1 Non-homologous end joining 46

1.4.2 Homologous recombination 49

1.5 HDAC inhibitors and effects on DNA damage signalling and repair 50

1.5.1 HDAC inhibitors in normal human cells.....50

1.5.2 HDAC inhibitors in cancer cells.....51

1.6 HDAC inhibitors and effects on gene transcription.....55

1.7 Aims and objectives.....58

CHAPTER 2: MATERIALS AND METHODS 59

2.1 Materials 59

2.1.1 Cell Lines.....59

2.1.2 Cell culture media and materials.....59

2.1.3 Cytotoxic agents.....61

2.1.4 Irradiation source.....61

2.1.5 Western blotting.....61

2.1.6 Flow cytometry 61

2.1.7 Immunofluorescence microscopy.....62

2.1.8 Real-time PCR reagents.....62

2.1.9 Agarose gel electrophoresis 62

2.2 Buffers/Solutions 63

2.2.1 Freezing solution 63

2.2.2 Protein lysis buffer 63

2.2.3 Phosphate-buffered saline.....63

2.2.4 0.05% PBS-Tween 64

2.2.5 Blocking buffer.....64

2.2.6 10 X Running buffer for electrophoresis.....64

2.2.7 10 X Transfer buffer for electrophoresis.....64

2.2.8 10 X Tris-borate EDTA (TBE) buffer 64

2.3 Methods 65

2.3.1 Cell Culture.....65

2.3.2 Cell cryopreservation 66
2.3.3 Irradiation of cells 66
2.3.4 Chemosensitivity and radiosensitivity clonogenic assays 66
2.3.5 Western blotting 67
2.3.5.1 Preparation of cell lysates 67
2.3.5.2 Protein concentration determination 68
2.3.5.3 Gel running 68
2.3.6 Cell cycle fluorescence-activated cell sorting (FACS) analysis 69
2.3.7 Immunofluorescence microscopy and analysis of γH2AX foci 70
2.3.8 Real-time PCR 71
2.3.8.1 RNA extraction 71
2.3.8.2 cDNA preparation 71
2.3.9 qPCR data analysis 74
2.3.10 Reverse-transcriptase PCR for *TP53* variants 75
2.3.11 Gel Electrophoresis 76

2.4 Statistics and data analysis 77
2.4.1 Clonogenic assay 77
2.4.2 Combination index analysis of radiosensitisers 78
2.4.3 Western blot analysis 79

CHAPTER 3: RADIOSENSITISING EFFECTS OF PANOBINOSTAT 80

3.1 Introduction 80

3.2 Results 83
3.2.1 Cytotoxicity of panobinostat 83
3.2.2 Panobinostat causes acetylation of histone H3 lysine residues 84
3.2.3 Panobinostat incubation time and radiosensitising effects 86
3.2.4 HDAC-specific class effects on chemosensitisation 89
3.2.5 HDAC-specific class effects on radiosensitisation 90
3.2.6 Cell cycle effects on RT112 cells 91

3.2.7 Effects of panobinostat on *TP53* 93
3.2.8 Transcription of *TP53* after panobinostat treatment 96
3.2.9 *TP53* alternative promoter and panobinostat 97

3.3 Discussion 101
3.3.1 Cytotoxicity of panobinostat 101
3.3.2 Acetylation of lysine residues and radiosensitising effects 102
3.3.3 Effects on the cell cycle 105
3.3.4 Effects on p53 protein 105

CHAPTER 4: EXPLOITING "SYNTHETIC LETHALITY" IN BLADDER CANCER CELLS 108

4.1 Introduction 108

4.2 Results 110
4.2.1 Effects of imatinib on RT112 cell proliferation 110
4.2.2 Imatinib's effects on HR and radiosensitisation of Ku80KD cells 110
4.2.3 Ku80KD cells are the most sensitive to panobinostat 113
4.2.4 Effects of panobinostat on key HR and NHEJ proteins 115
4.2.4.1 Effects of panobinostat on the key HR proteins post-IR 116
4.2.4.2 Effects of panobinostat on NHEJ proteins post-irradiation 118
4.2.5 Effects on NHEJ and HR proteins in RAD51KD and Ku80KD cells 120
4.2.6 Panobinostat and transcriptional regulation of *RAD51* and *CtIP* genes 121

4.3 Discussion 124

CHAPTER 5: PANOBINOSTAT AND DNA DAMAGE: EFFECTS UPSTREAM OF NHEJ AND HR PATHWAYS 129

5.1 Introduction 129

5.2 Results 131
5.2.1 Panobinostat and effects on the MRE11/RAD50/NBS1 complex 131

5.2.2 Panobinostat increases the amount of γH2AX in cells 133
5.2.3 Panobinostat induces an increase in γH2AX foci 134
5.2.4 Panobinostat delays γH2AX foci repair post-irradiation.....136
5.2.5 Effects of panobinostat on NBS1 and MRE11.....138
5.2.6 Panobinostat and transcription of *MRE11/NBS1/RAD50* genes.....140
5.2.7 Modulation of *HDAC* gene transcription by panobinostat 143

5.3 Discussion.....148

CHAPTER 6: GENERAL DISCUSSION AND FUTURE PLANS..... 154

6.1 General discussion 154

6.2 Future Plans 156

REFERENCES..... 158

APPENDICES..... 178

Appendix A.....178

Appendix B. Melting temperature profiles for *HDAC1-11* primers 180

Appendix C. Published papers 185

LIST OF TABLES

Table 1.1. 2004 WHO grading classification of bladder neoplasms. 19

Table 1.2. 2009 Tumour-Node-Metastasis classification of bladder cancer. 21

Table 1.3. Recurrence and progression score for non-muscle invasive bladder cancer. ..26

Table 1.4. Clinical trials using combination of HDAC inhibitors and radiation. 38

Table 2.1. Antibodies used for western blotting. 69

Table 2.2. cDNA preparation components per reaction. 72

Table 2.3. qPCR experiment components. 72

Table 2.4. qPCR primers for *HDAC* expression. 73

Table 2.5. Primers used in qPCR experiments. 73

Table 2.6. cDNA preparation components per reaction. 75

Table 2.7. PCR primers used for ∆133p53 variant detection. 75

Table A.1. Cell lines *TP53* status, grade and stage characteristics. 178

Table A.2. Plating efficiencies for cell lines used in this thesis. 178

Table A.3. The combination index analysis of 10 nM panobinostat in RT112 cells. 178

Table A.4. The combination index analysis of 25 nM panobinostat in RT112 cells. 179

LIST OF FIGURES

Figure 1.1. Presentation of non-muscle and muscle invasive bladder cancers. 20
Figure 1.2. Bladder cancer carcinogenesis. 23
Figure 1.3. Therapeutic options for metastatic or non-metastatic MIBC. 28
Figure 1.4. Ionising radiation causes DNA damage directly or indirectly. 39
Figure 1.5. The therapeutic window. 42
Figure 1.6. The MRN complex structure and function in DSB repair. 44
Figure 1.7. The MRN complex domains. 46
Figure 1.8. Classical (D-NHEJ) and alternative (B-NHEJ) NHEJ DNA repair pathways. 48
Figure 1.9. The homologous recombination pathway. 49
Figure 1.10. HDAC inhibitors and effects on the major NHEJ and HR proteins. 54
Figure 1.11. Gene transcription and the interplay of HDAC and HAT. 55
Figure 3.1. Evaluation of panobinostat's cytotoxicity in bladder cancer cell lines. 83
Figure 3.2. Acetylation of histone H3 lysine residues post-panobinostat treatment. 85
Figure 3.3. Radiosensitisation clonogenic assay following 1 hour panobinostat treatment. 86
Figure 3.4. Panobinostat radiosensitises bladder cancer cells following 24 hour treatment. 88
Figure 3.5. Evaluation of mocetinostat's cytotoxicity in bladder cancer cell lines. 89
Figure 3.6. Mocetinostat only mildly radiosensitises bladder cancer cells. 91
Figure 3.7. Cell cycle effects of panobinostat in RT112 cells. 92
Figure 3.8. Cell cycle effects of panobinostat and irradiation in RT112 cells. 93
Figure 3.9. Panobinostat downregulates levels of p53 protein in a dose-dependent manner. 95
Figure 3.10. Transcription of *TP53* after panobinostat treatment alone or in combination with 5 Gy irradiation. 97
Figure 3.11. *TP53* gene ∆133p53 variants. 98
Figure 3.12. Panobinostat downregulates levels of p53 protein and ∆133p53 in a dose-dependent manner. 100
Figure 4.1. Chemical structure of imatinib and cells depleted for RAD51 and Ku80. 111

Figure 4.2. Cytotoxicity and “synthetic lethality” in bladder cancer and imatinib. 112
Figure 4.3. “Synthetic lethality’’ in bladder cancer and panobinostat. 114
Figure 4.4. Panobinostat downregulates RAD51 and CtIP proteins. 115
Figure 4.5. Panobinostat downregulates RAD51.....117
Figure 4.6. Panobinostat attenuates upregulation of CtIP protein.....118
Figure 4.7. Panobinostat does not cause any marked effects on NHEJ protein levels. ..119
Figure 4.8. Effects of panobinostat on the major HR and NHEJ proteins in cells depleted for RAD51 or Ku80. 120
Figure 4.9. *RAD51* gene expression after panobinostat treatment. 122
Figure 4.10. Expression of CtIP in RT112 and CAL29 cells after panobinostat treatment. 123
Figure 5.1. Panobinostat causes downregulation of MRE11 and NBS1 proteins in a dose-dependent manner.....132
Figure 5.2. Induction of γH2AX after panobinostat treatment and irradiation.....133
Figure 5.3. Panobinostat causes an increase in γH2AX foci in a dose-dependent manner. 135
Figure 5.4. Panobinostat causes post-irradiation γH2AX foci resolution delay. 137
Figure 5.5. Effects of panobinostat on MRE11 and NBS1 protein expression in bladder cancer cells.....139
Figure 5.6. Control western blot for MRN complex in cells, treated with DMSO. 140
Figure 5.7. Transcription of *MRE11/RAD50/NBS1* genes after panobinostat alone or in combination with 5 Gy irradiation. 142
Figure 5.8. *HDAC* expression in normal human urothelial (NHU) and RT112, CAL29 and T24 bladder cancer cell lines. 143
Figure 5.9. Comparisons of *HDAC* gene expressions between the cell lines. 144
Figure 5.10. Expression of 11 *HDAC* genes with or without panobinostat treatment. 146
Figure 5.11. Effects of panobinostat on *HDAC* gene expression.....147

LIST OF ABBREVIATIONS

ATLD: ataxia-telangiectasia-like-disorder

ATM: ataxia telangiectasia-mutated

BCA: bicinchoninic acid assay

BC: bladder cancer

BSA: bovine serum albumin

CDK: cyclin-dependent kinase

CI: confidence interval

CIS: *carcinoma in situ*

CON: carbogen and nicotinamide

C_T: threshold cycle

CTCL: cutaneous T-cell lymphoma

DAPI: 4',6-diamidino-2-phenylindole

DFS: disease-free survival

DMEM: Dulbecco's modified eagle medium

DMSO: dimethyl sulfoxide

DNA: deoxyribonucleic acid

DNA-PK: DNA protein kinase

DSB: double strand breaks

EMSA: electrophoretic mobility shift assay

FCS: fetal calf serum

HAT: histone acetylatransferases

HDAC: histone deacetylase

HR: homologous recombination

IR: ionising radiation

LOH: loss-of-heterozygosity

MC: mitotic catastrophe

MTD: maximum-tolerated dose

MIBC: muscle-invasive bladder cancer

MMC: mitomycin C

MMEJ: microhomology-mediated end joining

MRN: MRE11-RAD50-NBS1 complex

NaB: sodium butyrate

NBS: Nijmegen breakage syndrome

NBSLD: Nijmegen breakage syndrome-like disorder

NSCLC: non-small cell lung cancer

NHEJ: non-homologus end joining

NHU: normal human urothelial

NMIBC: non-muscle invasive bladder cancer

NTCP: normal tissue complication probability

PBS: phosphate-buffered saline

PCR: polymerase chain reaction

PE: plating efficiency

PI: propidium iodide

PTM: post-translational modification

RNA: ribonucleic acid

ROS: reactive oxygen species

RPM: revolutions per minute

RT: radiotherapy

RT-PCR: reverse-transcriptase PCR

SER_{10}: sensitisation enhancement ratio at 10% survival

SF: cell surviving fraction

SSB: single strand DNA breaks

TCC: transitional cell carcinoma

TCP: tumour control probability

TNM: tumour-node-metastasis

TSA: trichostatin A

TURBT: transurethral resection of bladder tumour

UC: urothelial carcinoma

VPA: valproic acid

WHO: World Health Organisation

CHAPTER 1: INTRODUCTION

1.1 Bladder cancer

1.1.1 Epidemiology

Bladder cancer is a common disease. Worldwide, it is the 9th commonest cancer. Each year more than 330,000 patients develop bladder cancer and 130,000 people die from it. It is more frequent in men, with a male to female ratio of 3.8:1 (Stenzl et al, 2011). In the UK it is the 4th most common cancer in men and 11th most common in females, with approximately 11,000 new patients diagnosed per annum (male to female ratio of 5:2), and more than 4,900 patient deaths. Eight in 10 newly diagnosed patients are older than 65 years of age (Cancer Research UK 2010). Bladder cancer is also the most costly cancer to treat from diagnosis to death (Sievert et al, 2009), with a big financial burden to the UK health system (Sangar *et al*, 2005).

The major risk factor for bladder cancer in the developed world is tobacco smoking, causing more than 50% of bladder cancers in males and 20% in females. Smokers have a 2-4 times higher risk of getting bladder cancer compared with non-smokers (Pelucchi *et al*, 2006; Freedman *et al*, 2011). Occupational exposure to chemicals in the rubber, plastics, paint, leather, dye and other industries is another major risk factor (Brown *et al*, 2012); about 7% of male and 2% of female bladder cancers can be attributable to these factors (Parkin, 2011). However, in the Middle East and Africa the major cause of bladder cancer is chronic inflammation due to the parasitic infection, schistosomiasis. Moreover, because of the endemic nature of this infection, Egypt has the highest incidence of bladder cancer in the world (Gouda *et al*, 2007; Ploeg *et al*, 2009).

Racial differences and familial predisposition also contribute to the bladder cancer occurrence and survival. The incidence of bladder cancer in the white USA population is twice as high as in the black population (Mueller *et al*, 2008; Burger *et al*, 2013), but with a

lower disease specific 5-year survival in the black population (Yee *et al*, 2011). The risk for first-degree relatives of affected individuals is also increased, at 1.35-fold in men and 2.29-fold in women in a Swedish cohort (Plna & Hemminki, 2001), and 1.8-fold in the Dutch population (Aben *et al*, 2002).

1.1.2 Histopathology

Tumours originating from the bladder urothelial epithelium are called urothelial carcinomas (UC), previously called transitional cell carcinoma (TCC), and these represent more than 90% of bladder tumours. There are other less frequent types. Squamous cell carcinoma, accounts for around 3% of all cases in the West but more than 50% in schistosomiasis endemic areas (Ghoneim *et al*, 1997). Adenocarcinoma represents only about 1% of the cases, but is more frequent in the developing world where it accounts for around 10% of bladder tumours (Chalasani *et al*, 2009; Valerio *et al*, 2011). Another rare bladder cancer is small cell carcinoma, accounting for less than 1% of all bladder cancer cases (Chalasani *et al*, 2009). This thesis will focus only on the UC type.

These tumours present as either flat or papillary lesions. Microscopically, histological grading depends on the urothelium thickness, cell polarity, nuclear size and pleomorphism, presence of cellular mitoses, inflammation and some other characteristics (Montironi *et al*, 2008; Mazzucchelli *et al*, 2012). The WHO 2004 classification is currently used for the purpose of histological grading of benign and malignant bladder neoplasms (see Table 1.1) (Lopez-Beltran, 2008; Grignon, 2009).

Table 1.1. 2004 WHO grading classification of bladder neoplasms.
Adapted from Lopez-Beltran (2008) and Grignon (2009).

Normal
Hyperplasias
Flat lesions with atypia
Reactive (inflammatory) atypia
Atypia of unknown significance
Dysplasia (low-grade intra-urothelial neoplasia)
Carcinoma *in situ* (high-grade intra-urothelial neoplasia)
Papillary neoplasms
Papilloma
Inverted papilloma
Papillary urothelial neoplasm of low malignant potential
Papillary carcinoma, low grade
Papillary carcinoma, high grade
Invasive neoplasms

1.1.3 Staging of bladder cancers

For the purposes of clinical treatment, bladder cancers (BC) are divided according to their depth of invasion into the layers of the bladder (Figure 1.1). Non-muscle invasive bladder cancers (NMIBC), are confined to the bladder mucosa or sub-mucosa (*lamina propria*) and are staged as Ta, T1 and Tis *(Carcinoma in situ, CIS)*. They affect approximately 80% of all the patients; the remaining 20% of patients have muscle-invasive disease (MIBC, stages T2-T4) with potentially N+ (local lymph nodes invaded) and/or M+ (metastases in distant organs) dissemination, see also Table 1.2 (Knowles, 2006; Lopez-Beltran, 2008).

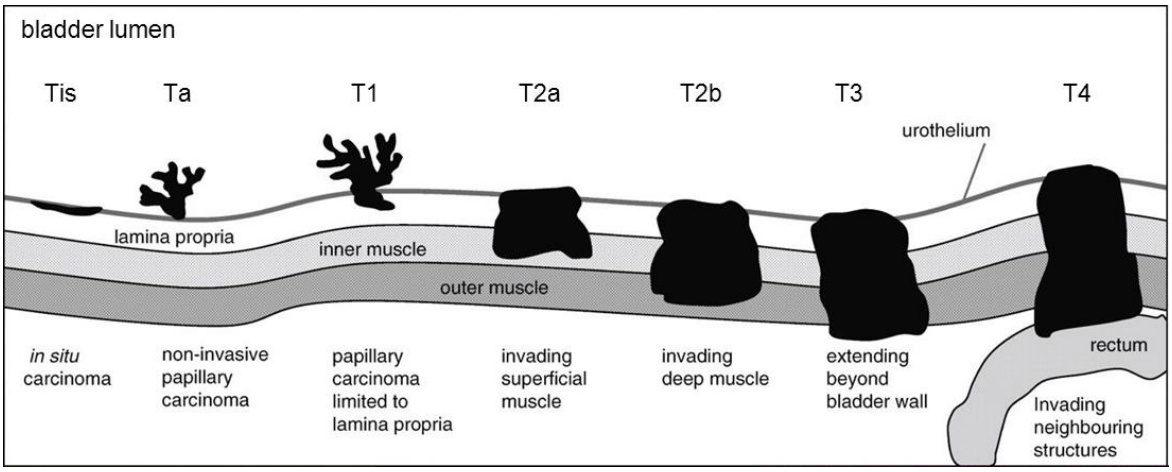


Figure 1.1. Presentation of non-muscle and muscle invasive bladder cancers. Non-muscle invasive bladder cancers are confined to the bladder mucosa or sub-mucosa (*lamina propria*). They are staged either as Ta, T1 or Tis *(Carcinoma in situ, CIS)*. Muscle-invasive disease presents as stages T2a, T2b or T3, or T4, where the cancer invades structures adjacent to the bladder. Adapted from Knowles (2006).

Table 1.2. 2009 Tumour-Node-Metastasis classification of bladder cancer.
Adapted from Stenzl *et al* (2011).

	T - Primary tumour	
TX	Primary tumour cannot be assessed	
T0	No evidence of primary tumour	
Ta	Non-invasive papillary carcinoma	
Tis	*Carcinoma in situ*: “flat tumour”	
T1	Tumour invades subepithelial connective tissue	
T2	Tumour invades muscle	
	T2a	Tumour invades superficial muscle (inner half)
	T2b	Tumour invades deep muscle (outer half)
T3	Tumour invades perivesical tissue	
	T3a	Microscopically
	T3b	Macroscopically (extravesical mass)
T4	Tumour invades any of the following: prostate, uterus, vagina, pelvic wall, abdominal wall	
	T4a	Tumour invades prostate, uterus or vagina
	T4b	Tumour invades pelvic wall or abdominal wall
	N - Lymph nodes	
NX	Regional lymph nodes cannot be assessed	
N0	No regional lymph node metastasis	
N1	Metastasis in a single lymph node in the true pelvis (hypogastric, obturator, external iliac, or presacral)	
N2	Metastasis in multiple lymph nodes in the true pelvis (hypogastric, obturator, external iliac, or presacral)	
N3	Metastasis in common iliac lymph node(s)	
	M - Distant metastasis	
M0	No distant metastasis	
M1	Distant metastasis	

1.1.4 Molecular basis of bladder carcinogenesis

In order for a bladder cancer to develop, several different molecular alterations have to occur. Tumour suppressor genes are inactivated and oncogenes activated (Höglund, 2012). Genetic alterations in bladder cancer defined so far point to mutations in genes involved in cell cycle regulation, and genes coding for growth factor receptors and various signalling pathway components. Furthermore, chromosomal deletions leading to loss-of-

heterozygosity (LOH) are also frequent. Some of those characteristics are specific for NMIBC, whereas others are specific for MIBC, indicating at least two different pathways of carcinogenesis, presented in Figure 1.2 (Goebell & Knowles, 2010).

Low grade and low stage tumours are genomically stable, but tend to recur. Common biological features are deletions of chromosome 9q (chromosome 9 long arm) and activating mutations or overexpression of the fibroblast growth factor receptor 3 *(FGFR3)* oncogene, with 50% to 80% of Ta tumours having this mutation. These mutations were also correlated with favourable clinical outcome (Knowles, 2006, 2008; Junker *et al*, 2008). FGFR3 activates the RAS-MAPK signalling pathway; interestingly, in Ta tumours *FGFR3* and *RAS* mutations are mutually exclusive (Knowles, 2008).

Losses of chromosome 9 are also seen in high grade and MIBC tumours. These tumours have a broad spectrum of mutations and deletions, with *TP53* being mutated or deleted in more than 70% of cases. LOH in *Rb* gene is seen in more than 50% of MIBC. Also frequent are *PTEN* gene LOH and mutations and deletions of chromosome 17 (Knowles, 2008). Bakkar *et al* (2003) also established in a set of 81 newly diagnosed bladder tumours that the *FGFR3* and *TP53* mutations are almost mutually exclusive.

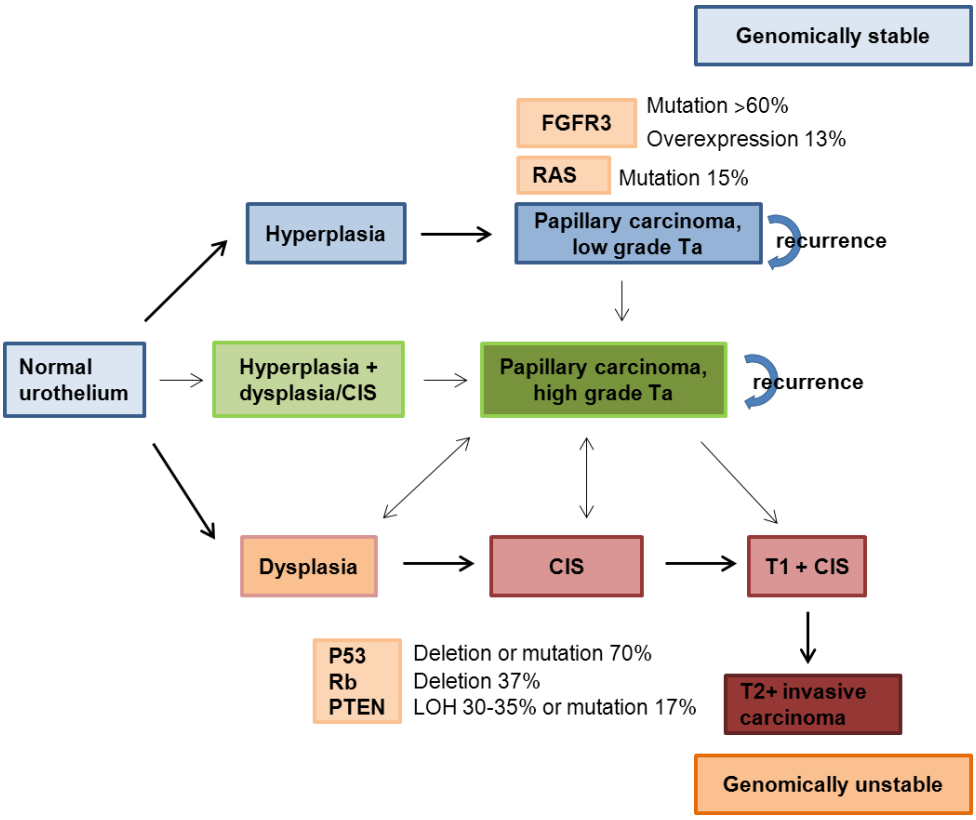


Figure 1.2. Bladder cancer carcinogenesis.
The normal urothelium can develop low grade Ta tumours (in blue), having high instances of *FGFR3* and *RAS* mutations. They are genomically stable, but frequently recur. Another pathway of progression is to invasive carcinoma, with frequent *TP53*, *Rb* and *PTEN* mutations. These tumours are genomically unstable. Thin lines represent other potential pathways of tumour progression. CIS = *carcinoma in situ*; LOH = loss-of-heterozygosity. Adapted from Goebell and Knowles (2010).

1.1.5 Diagnosis

1.1.5.1 Clinical presentation and diagnosis

The first presentation of bladder cancer in three-quarters of all cases is with painless, intermittent gross haematuria (Lopez-Beltran, 2008). Around 20% of people having those symptoms are found to have bladder cancer. Haematuria can also be microscopic, due to many different causes such as inflammation, kidney disease and many other non-cancerous reasons (McDonald *et al*, 2006). Since only a small proportion of those people are later diagnosed with bladder cancer, the usefulness of microscopic haematuria as a bladder cancer indicator remains controversial (Lopez-Beltran, 2008; Sharma *et al*, 2009).

Patients can also experience urgency and dysuria, and with more advanced tumours, pelvic pain and urinary tract obstruction are also frequently seen (Stenzl *et al*, 2011).

The first investigation performed in a patient presenting with haematuria is usually a flexible cystoscopy, to identify the cause of the bleeding (Lopez-Beltran, 2008). Since the bleeding could also come from elsewhere in the urinary tract, CT urography is also frequently used (O'Connor & Maher, 2010).

Once the UC is macroscopically confirmed, a transurethral resection of bladder tumour (TURBT) is performed, to sample the tumour for pathological staging and also to assess the tumour size, location and shape. Moreover, maximal tumour resection at TURBT is also an important first therapeutic step (described below) (Sexton *et al*, 2010).

1.1.6 Treatment of non-muscle invasive bladder cancer

1.1.6.1 Transurethral resection of bladder cancer (TURBT)

The TURBT procedure is an important component of the treatment of bladder cancer. In NMIBC the lesion should be completely removed and the resection should include bladder wall muscle (*muscularis propria*), for the pathologist to give an accurate grade and stage (Mariappan *et al*, 2010). If the removal is incomplete, and histopathology reveals high grade or stage T1 disease, another TURBT is performed, usually 2-6 weeks later, to lower the chance of recurrence and to confirm that the tumour is not muscle-invasive (Babjuk *et al*, 2011, 2013). The skills of the surgeon performing the TURBT can also impact on the recurrence rate (Brausi *et al*, 2002). Finally, the findings acquired with the TURBT will indicate the risk of recurrence and dictate future therapeutic options (Herr & Donat, 2008; British Uro-oncology Group (BUG) and British Association of Urological Surgeons (BAUS) Section of Oncology and Action on Bladder Cancer (ABC), 2013).

1.1.6.2 Intravesical therapies

The role of intravesical therapy is to prevent local tumour recurrence and to eradicate any tumour that was incompletely resected (British Uro-oncology Group (BUG) and British Association of Urological Surgeons (BAUS) Section of Oncology and Action on Bladder Cancer (ABC), 2013). As such, it reduces recurrence risk in Ta and T1 bladder tumours by 39% compared with TURBT alone (Sylvester *et al*, 2004). One adjuvant intravesical instillation of chemotherapy is therefore recommended for all patients (Babjuk *et al*, 2011). Sylvester *et al*, have proposed a recurrence and progression score algorithm, where the NMIBC patients are divided into three groups, according to the chance of their cancer progressing (see Table 1.3). This score also aids therapeutic decision making (Sylvester *et al*, 2006). In patients with low recurrence risk, mitomycin C (MMC), epirubicin or doxorubicin all show beneficial effects and this constitutes definitive treatment, whereas in the intermediate recurrence risk group, this intravesical instillation is the first stage of potential further intravesical therapies (Babjuk *et al*, 2011). Patients with intermediate or high risk of recurrence should be treated with either MMC or BCG immunotherapy (Malmström *et al*, 2009). BCG therapy has lower recurrence rates but is more toxic than MMC, but it needs to be maintained for 3 years (Babjuk *et al*, 2011; British Uro-oncology Group (BUG) and British Association of Urological Surgeons (BAUS) Section of Oncology and Action on Bladder Cancer (ABC), 2013).

Table 1.3. Recurrence and progression score for non-muscle invasive bladder cancer.

A) Factors contributing to the recurrence or progression score. B) Short- and long-term recurrence and progression risk in NMIBC. According to the score, patients are divided into low, medium and high risk groups. Adapted from Sylvester *et al* (2006) and Babjuk *et al* (2011).

A)

Factor	Recurrence	Progression
No. of tumours		
Single	0	0
2–7	3	3
≥8	6	3
Tumour diameter		
<3 cm	0	0
≥3 cm	3	3
Prior recurrence rate		
Primary	0	0
≤1 recurrence per year	2	2
>1 recurrence per year	4	2
Category		
Ta	0	0
T1	1	4
Concomitant CIS		
No	0	0
Yes	1	6
Grade (1973 WHO)		
G1	0	0
G2	1	0
G3	2	5
Total score	**0–17**	**0–23**

CIS = *carcinoma in situ*; WHO = World Health Organisation.

B)

Recurrence score	Probability of recurrence at 1 yr		Probability of recurrence at 5 yr		Recurrence risk group
	%	(95% CI)	%	(95% CI)	
0	15	(10–19)	31	(24–37)	Low risk
1–4	24	(21–26)	46	(42–49)	Intermediate risk
5–9	38	(35–41)	62	(58–65)	
10–17	61	(55–67)	78	(73–84)	High risk

Progression score	Probability of progression at 1 yr		Probability of progression at 5 yr		Progression risk group
	%	(95% CI)	%	(95% CI)	
0	0.2	(0–0.7)	0.8	(0–1.7)	Low risk
2–6	1	(0.4–1.6)	6	(5–8)	Intermediate risk
7–13	5	(4–7)	17	(14–20)	High risk
14–23	17	(10–24)	45	(35–55)	

CI = confidence interval.

1.1.7 Treatment of muscle invasive bladder cancer (MIBC)

MIBC therapy consists either of potentially curative treatment with radical radiotherapy (RT) or cystectomy with or without neoadjuvant chemotherapy, in organ-confined disease, or palliative systemic chemotherapy with or without radiotherapy for advanced, metastatic disease as seen in Figure 1.3.

The use of neoadjuvant chemotherapy aims to treat micrometastatic deposits of disease and causes down-staging of the disease. Furthermore, it prolongs disease-specific and overall survival. The therapy is usually administered as three cycles of cisplatinum-based chemotherapy (Stenzl *et al*, 2011; Griffiths, 2013).

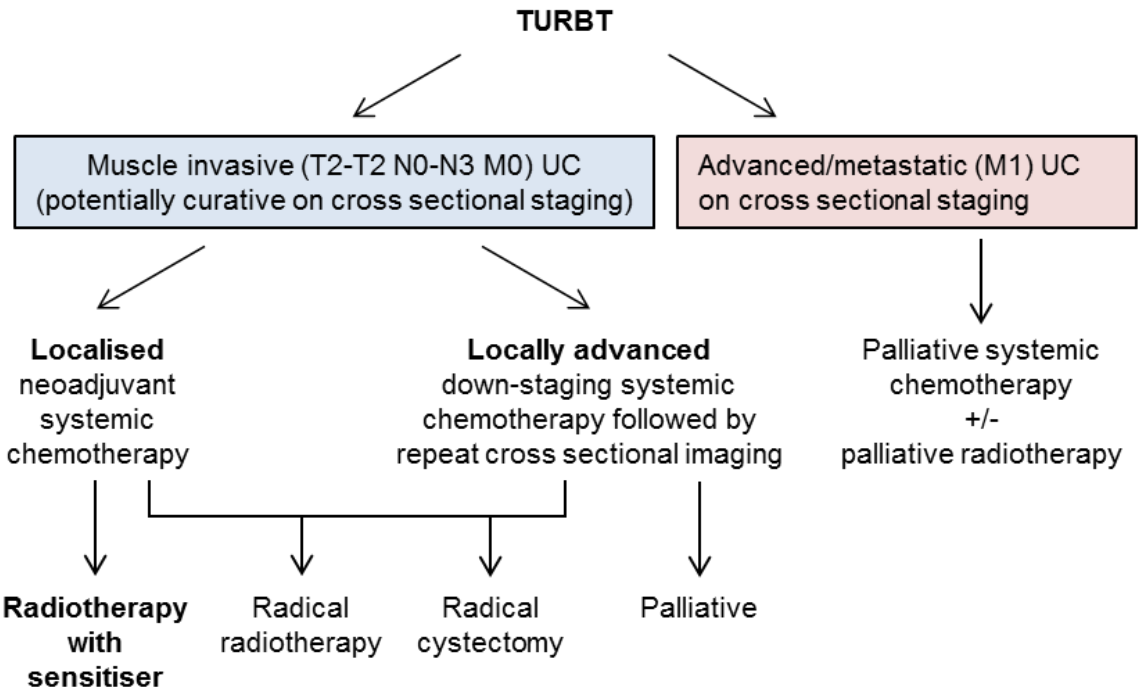


Figure 1.3. Therapeutic options for metastatic or non-metastatic MIBC.
Adapted from Griffiths (2013). TURBT = transurethral resection of bladder cancer; UC = urothelial carcinoma.

1.1.7.1 Radical radiotherapy

Radical RT is a curative treatment for patients with MIBC. The biggest advantage over radical cystectomy treatment is preservation of the bladder, such that a high proportion of those surviving long-term post radical RT treatment still have a well-functioning bladder (Choueiri & Raghavan, 2008).

Prior to radical RT, a visible complete TURBT is performed. This step is crucial for therapy response and survival (Rodel *et al*, 2002; Heney *et al*, 2009; Efstathiou *et al*, 2012). For external beam radiotherapy, the bladder receives a dose of 64 Gy in 32 fractions or a hypofractionated schedule of 55 Gy in 20 fractions, with a 1.5-2.0 cm safety margin (Stenzl *et al*, 2011; British Uro-oncology Group (BUG) and British Association of Urological Surgeons (BAUS) Section of Oncology and Action on Bladder Cancer (ABC), 2013). A dose of 45-50 Gy is used for pelvic lymph node treatment (Kragelj *et al*, 2005; Ott *et al*, 2009).

Adverse effects of radical RT for MIBC can be acute or late. The most frequent acute adverse effects are cystitis, urinary frequency, dysuria, diarrhoea, tenesmus, proctitis and lethargy. The late adverse effects include bladder atrophy, diarrhoea and impotence (Majewski & Tarnawski, 2009; British Uro-oncology Group (BUG) and British Association of Urological Surgeons (BAUS) Section of Oncology and Action on Bladder Cancer (ABC), 2013).

As reported in a retrospective analysis by Majewski and Tarnawski (2009), the rate of patients with very severe toxicities (grade 3 or more) is relatively low. Only 5% of patients experienced severe acute bladder toxicities, such as frequency with urgency, pelvic pain and haematuria and 3% of patients experienced severe bowel toxicities, such as severe diarrhoea or bowel obstruction.

Patients with MIBC are also at great risk of having occult distant metastases. Wallmeroth *et al* (1999) showed in a large autopsy study, that the occurrence of metastases correlated with the MIBC stage, where 36% of T2, 45% T3a, 69% T3b and 79% of T4 patients were positive for tumour metastases. It is therefore clinically rational to combine radical RT therapy with chemotherapeutic agents.

In an important randomised phase III trial, BC2001, published by James *et al* (2012) results comparing radiotherapy alone or radiotherapy and 5-fluorouracil and MMC chemotherapy (chemoradiation) for MIBC, established a greater locoregional-recurrence free survival in the chemoradiation group (but not overall survival).

Promising combinations of chemotherapeutics and radiotherapy have also been reported in several other studies. Hoskin *et al* (2010) reported on the outcome of the BCON (Bladder CarbOgen Nicotinamide) phase III trial, where concurrent carbogen and nicotinamide (CON) were tested as radiosensitisers compared to a radiotherapy-only group. The results were promising, with an improvement in 3-year overall survival, from 46% in the RT-alone group, to 59% in the radiotherapy plus CON group. An 11% absolute improvement in 3-year relapse-free survival was also seen in the RT plus CON group.

In a phase II study, Choudhury *et al* (2011) tested concurrent weekly low dose gemcitabine (100 mg/m^2) and radiotherapy over 4 weeks. The treatment combination produced a very high response rate and durable local control, with 3-year cancer-specific and overall survivals of 82% and 75%, respectively.

1.1.7.2 Radical cystectomy

Radical cystectomy is a treatment in which the bladder is removed and a pelvic lymphadenectomy performed along with removal of prostate and seminal vesicles in men and the uterus and adnexae in women (Stenzl *et al*, 2005; Griffiths, 2013). Patients who receive radical cystectomy include those who fail to respond to BCG therapy or have carcinomas of non-urothelial origin. Furthermore, patients who have previously received bladder sparing treatment but in whom the tumour has recurred may undergo salvage cystectomy (Stenzl *et al*, 2011).

There are three major methods of urinary diversion post-radical treatment, the choice being dependent on factors such as the patient's health, preference, age and available surgical experience (Kim *et al*, 2013a). The most common procedures are abdominal diversions, such as an ileal conduit, where a continence pouch is made from a part of the intestine and urine is drained through the abdominal wall as a stoma. Other options include rectal reservoirs, designed to collect urine (Cody *et al*, 2012). An increasingly important possibility, that is judged feasible according to distal urethra frozen section examination by the pathologist and the patient's clinical status, is a urethral diversion, such as construction of a neobladder, where the urine can be passed normally through the patient's intact urethra (Gakis & Stenzl, 2010; Stenzl *et al*, 2011).

Approximately 28% of patients experience some complications after radical cystectomy in a population based study reported by Konety *et al* (2006). The most common complications included gastrointestinal, cardiac and respiratory complications, disrupted wound healing and postoperative infections. Younger patients were less likely to experience complications (British Uro-oncology Group (BUG) and British Association of Urological Surgeons (BAUS) Section of Oncology and Action on Bladder Cancer (ABC),

2013). The mortality rate for radical cystectomy is approximately 3% (Stein & Skinner, 2006). Mortality within 90 days from cystectomy was also addressed in a large population-based cohort and elderly patients tend to have a higher mortality, compared with those less than 70 years old. Mortality in the under-70 year old population was 2%, whereas it was found to be 5% in septuagenarians and 9% in octogenarians (Liberman *et al*, 2011).

1.1.7.3 Radical cystectomy versus radical radiotherapy

Traditionally, the gold standard worldwide for MIBC treatment has been radical cystectomy and lymphadenectomy. However, only limited data exist to support the use of radical cystectomy over radical radiotherapy with or without radiosensitising chemotherapy, since the disease free survivals (DFS) for both modalities are similar (Griffiths, 2013).

Clinical evidence so far exists from only non-randomised trials. To address this issue and to directly compare these two treatment modalities, the phase III clinical trial, “Selective bladder preservation against radical excision, SPARE” was initiated in the UK. Unfortunately despite a promising start, patient accrual was poor and the trial was stopped early, after the pilot phase (Huddart *et al*, 2010).

In the UK, selection for either radical radiotherapy or radical cystectomy is based on patient preference in consultation with the treating urologist and oncologist. Importantly, factors such as large tumour volume, *CIS* distant to the tumour, poor bladder function, lower urinary tract symptoms or previous radiotherapy in the pelvic region favour cystectomy, whereas a patient’s poor fitness for surgery (which could be due to many factors) favours radical radiotherapy (British Uro-oncology Group (BUG) and British Association of Urological Surgeons (BAUS) Section of Oncology and Action on Bladder Cancer (ABC), 2013).

An important study by Rödel *et al* addressing the long term survival outcomes in patients has shown that radiotherapy or chemoradiotherapy can have similar outcomes to cystectomy treatment (Rodel *et al*, 2002). Kotwal *et al* (2008) addressed this in a

retrospective study for radical bladder cancer treatment in Leeds, West Yorkshire. The authors did not detect any significant difference in the 5-year cause-specific survival (CSS), or regional or distant recurrence rates between the treatments. In the Massachusetts General Hospital (MGH) cohort, treated with bladder preserving TURBT followed by radiotherapy and radiosensitising chemotherapy, the outcomes were comparable to the cystectomy series (Efstathiou *et al*, 2012).

Nielsen *et al* (2007) have established that in MIBC patients, age is a negative prognostic factor for disease recurrence. Furthermore, as reported by Noon *et al* (2013) older patients are more likely to die due to their cancer compared to younger patients. Older patients should therefore be given a more aggressive treatment for their MIBC than is presently the case.

Due to an aging population, radical radiotherapy will inevitably become a more important therapeutic modality in these increasingly elderly patients. The aim of this thesis was therefore to explore the use of a novel biological targeted agent panobinostat as a radiosensitiser at low-toxicity doses in MIBC patients.

1.2 Epigenetic cancer therapy

1.2.1 Histone deacetylases

Chromatin is a structure composed from the basic unit, the nucleosome, where around 146 base pairs of DNA molecule are wrapped around a globular histone protein octamer, formed from two copies each of H2A, H2B, H3 and H4 (Luger *et al*, 1997). The histone proteins have N-terminal tails that protrude from the globular octamer and can be subjected to various post-translational modifications (PTM), such as acetylation, methylation, phosphorylation, sumoylation and ubiquitylation and thereby influence the chromatin function, by changing its structure or by forming new binding sites for various proteins (Cosgrove *et al*, 2004). These PTM are thought to form the "histone code" (Jenuwein & Allis, 2001), that can be "read" by the chromatin-associated proteins, resulting in reorganised chromatin and modulated gene regulation (Cosgrove *et al*, 2004; Cosgrove & Wolberger, 2005). As the main focus of this thesis is the action of panobinostat on cancer cells (described below), here only acetylation/deacetylation PTM will be discussed.

One of the most studied PTM, known for decades, is acetylation of histone and non-histone lysine residues, regulated by histone acetylatransferases (HAT), which transfer the acetyl group from acetyl-CoA to the histone lysine residue (Allfrey *et al*, 1964; Pogo *et al*, 1966). Acetylation of the lysine residue neutralises the positive lysine charge, reducing the affinity of the lysine residue for negatively charged DNA, resulting in relaxation of the chromatin. This allows the DNA to be more accessible for various transcription factors and other proteins. Over time it became evident that other, non-histone proteins can also be acetylated, leading to the increasing list of acetylated proteins, forming the "acetylome" (Minucci & Pelicci, 2006).

The overall cell acetylation status is also regulated by another group of proteins, the histone deacetylases (HDAC), with opposing function to HATs. As the name suggests, this family of proteins remove the acetyl group from the acetylated histone lysine residues

and other acetylated proteins (Peserico & Simone, 2011). There are 18 different HDAC enzymes, grouped into four different classes, according to the structure similarity to their yeast homologues. Class I (HDAC1, 2, 3, 8; yeast homologue group RPD3); class IIa (HDAC4, 5, 7 and 9 are related to yeast homologue HDA1) and IIb (HDAC6 and 10); and class IV (HDAC11), all need Zn^{2+} for their catalytic activity (are "Zn^{2+}-dependent"), whereas class III (yeast homologue SIR2) need nicotinamide adenine dinucleotide (NAD+) for their catalytic activity (Spiegel *et al*, 2012) (since HDAC inhibitors do not act on this class of HDAC, these enzymes will not be discussed further).

The interplay of acetylation and deacetylation plays a crucial role in dynamic chromatin structural changes and also in gene expression, two major components of the response to ionising radiation (Camphausen & Tofilon, 2007). Moreover, histone acetyltransferase inactivation (HAT) and also aberrant HDAC expression are linked to oncogenesis and tumour formation and upregulated in cancers, such as bladder (Ozawa *et al*, 2010; Xu *et al*, 2011b; Niegisch *et al*, 2012), vulvar (Samartzis *et al*, 2011), mesenchymal (Pacheco & Nielsen, 2012) and hepatocellular cancer (Camphausen & Tofilon, 2007; Quint *et al*, 2011; Lachenmayer *et al*, 2012). Histone deacetylases (HDAC) have recently become considered important targets in tumour therapies.

1.2.2 Histone deacetylase inhibitors

HDAC inhibitors have been well tolerated in clinical studies using HDAC inhibitors as single agents or in combination with radiotherapy.

In urological malignancies, the first HDAC inhibitor to show a radiosensitising effect was the class I specific inhibitor entinostat (MS-275), tested in prostate cancer cells *in vitro* and in a mouse xenograft model (Camphausen *et al*, 2004a, 2004b), and reviewed in Sharma *et al* (2013). Belinostat has been used in superficial bladder cancer, and valproic acid (VPA) inhibited invasiveness in invasive bladder tumours (Chen *et al*, 2006; Buckley *et al*, 2007; Ozawa *et al*, 2010).

Panobinostat is one of the most potent pan-HDAC inhibitors, showing strong HDAC inhibitory effects *in vitro* in comparison with other HDAC inhibitors (Atadja, 2009). It has also shown synergy with gemcitabine and with paclitaxel in human ovarian cancer cell lines and with sorafenib in hepatocellular carcinoma (Budman *et al*, 2011; Lachenmayer *et al*, 2012), cytotoxicity in triple-negative breast cancer cells (Tate *et al*, 2012) and has been found to induce radiosensitisation in non-small-cell lung carcinoma (NSCLC) (Geng *et al*, 2006; Storch *et al*, 2010).

1.2.3 HDAC inhibitors and radiation in clinical trials

HDAC inhibitors have been successfully introduced into clinical use over the last few years, as a single agent to treat different types of haematological malignancies. Vorinostat was the first HDAC inhibitor to be granted approval by the US Food and Drug Administration (FDA) for the treatment of cutaneous T-cell lymphoma (CTCL) (Mann *et al*, 2007). Two years later another HDAC inhibitor, romidepsin, was also approved by the FDA for the treatment of CTCL (VanderMolen *et al*, 2011).

Panobinostat has also been tested in early clinical studies of CTCL, lymphomas and myeloid malignancies (Prince & Bishton, 2009), and it was well tolerated by patients in either oral or intravenous formulation and also a clinical response was achieved. The most common dose-dependent adverse effects, were fatigue and thrombocytopenia, but these were quickly reversible after drug cessation and were not seen at lower doses.

In a phase II trial, treating patients with CTCL with oral vorinostat (400 mg daily), 30 % of patients had a partial response and there was a reduction in debilitating pruritus in 32% of patients (Duvic *et al*, 2007). In another phase II trial of CTCL patients, romidepsin at 14 mg/m^2 iv achieved a similar response rate, with four complete responses and 20 partial responses (34%) (Prince & Dickinson, 2012). Whittaker *et al* (2010), addressed the efficacy of romidepsin in a large multi-centre clinical trial of patients with advanced CTCL. Thirty four percent of patients responded to the therapy, including 6% of patients with complete response. However, panobinostat had a lower overall response rate (17%) in

CTCL and a shorter response duration, and it was not approved for use in CTCL patients (Prince & Dickinson, 2012).

Most other clinical trials using HDAC inhibitors alone or in combination have only been phase I or II studies, with many yet to publish. Therefore only a limited amount of information on clinical efficacy of HDAC inhibitors has been collected to date.

The rapidly expanding knowledge both regarding HDAC inhibitors and their possible clinical implications, in addition to promising results in preclinical reports of the radiosensitising effects of HDAC inhibitors, has led to combined HDAC inhibitor and radiation therapy being tested clinically over recent years, reviewed in Groselj *et al* (2013) (see Table 1.4).

The first clinical report was published by Noguchi *et al* (2009), showing efficient treatment of an aggressive and highly lethal anaplastic thyroid carcinoma with a combination of valproic acid (VPA), cisplatin/doxorubicin and a total of 40 Gy radiotherapy over three 3-4 week cycles, followed by surgical resection and 15 Gy intra-operative radiation. Two years later, the patient was still disease-free. As though the treatment approach was very aggressive and the effects of VPA on the outcome hard to prove, this case report showed that HDAC inhibitors can be safely combined with radiotherapy.

Ree *et al* (2010) published the first phase I clinical study of combined HDAC inhibitor and radiation therapy, the Pelvic Radiation and Vorinostat (PRAVO) trial, combining vorinostat and palliative pelvic radiotherapy. Sixteen patients with gastrointestinal malignancies, received a total dose of 30 Gy in 10 fractions over 2 weeks, to target the primary tumour lesions and also abdominal wall and pelvic bone metastases. Vorinostat was given 3 hours before each radiotherapy and relatively well tolerated, with toxicities of grade 1 and 2, mostly fatigue and gastrointestinal adverse effects. Six of the patients also experienced grade 3 adverse effects, with fatigue, anorexia, and hyponatraemia and hypokalaemia, but in three this was unrelated to the treatment received (Bratland *et al*, 2011). Biological activity of vorinostat was measured by testing the acetylation of histones H3 and H4, on

the third day of treatment 2.5 hours post-vorinostat, in a tumour biopsy. The PRAVO study was also important from the perspective of future similar studies, with recommendations from the authors as to what should also be considered when designing this type of clinical study (Ree & Hollywood, 2013).

In a preliminary report of another phase I report of an ongoing study by Kamrava *et al* (2008), the authors have shown that VPA can be safely combined with radiotherapy (and temozolomide) in glioblastoma patients, with no additional toxicities, compared with either therapy alone.

Candelaria *et al* (2010) have conducted a safety and tolerability study of a combination of cisplatin-based chemoradiation and the HDAC inhibitor VPA and the DNA methylation inhibitor hydralazine, in patients with cervical carcinoma. The efficacy was not tested, but the therapeutic combination was reportedly well tolerated.

Vorinostat and VPA have been the only HDAC inhibitors used in clinical trials in combination with radiation until recently, when panobinostat was also introduced in combination with external radiotherapy for localised prostate, head and neck and oesophageal cancer. The phase I study is already completed, with as yet unpublished results, and the phase II study is still ongoing (http://clinicaltrials.gov; NCT00670553). In another proposed phase I study (NCT01324635), patients with recurrent glioma, high-grade meningioma or brain metastasis will receive oral panobinostat combined with stereotactic radiation. These studies will determine panobinostat's maximally tolerated dose and dose-limiting toxicity levels in combination with radiotherapy, and provide guidance for future clinical studies.

Table 1.4. Clinical trials using combination of HDAC inhibitors and radiation.
Adapted from Groselj *et al* (2013).

HDAC inhibitor	Other combination therapy	Malignancy type (no. of patients)	Phase and status	Reference/ trial identifier
VPA	Surgery	High-grade sarcoma	I (Ongoing recruitment)	NCT01010958
VPA	Cisplatin, doxorubicin, surgery	Anaplastic thyroid	Case report	Noguchi *et al* (2009)
VPA	—/Variety	Glioma	Retrospective (4 out of 66 patients)	Masoudi *et al* (2008)
VPA	Cisplatin	Cervical	II (Completed, well-tolerated)	Candelaria *et al* (2010)
VPA	Temozolomide	Brain metastases in solid tumours	I (Terminated, lack of enrolment)	NCT00437957
VPA	Temozolomide	Glioblastoma	II (Ongoing)	Kamrava *et al* (2008); NCT00302159
Vorinostat	—	Gastrointestinal	I (Completed, MTD 300 mg daily)	Ree *et al* (2010); NCT00455351
Vorinostat	—	Pancreatic	I/II (Terminated, unknown reason)	NCT00831493
Vorinostat	—	NSCLC	I (Completed, unpublished)	NCT00821951
Vorinostat	Cisplatin, pemetrexed	NSCLC	I (Ongoing recruitment)	NCT01059552
Vorinostat	—	Brain metastases	I (Ongoing)	NCT00838929
Vorinostat	5-FU	Pancreas	I/II (Ongoing)	NCT00948688
Vorinostat	Paclitaxel	NSCLC	I/II (Terminated, unknown reason)	NCT00662311
Vorinostat	Cisplatin	Oropharyngeal	I (Ongoing recruitment)	NCT01064921
Vorinostat	Temozolomide, bevacizumab	Glioma	II/III (Ongoing recruitment)	NCT01236560
Vorinostat	Capecitabine	Pancreatic	I (Ongoing)	NCT00983268
Vorinostat	—	Glioma	I/II (Ongoing recruitment)	NCT01189266
Vorinostat	Temozolomide	Glioblastoma	I/II (Ongoing)	NCT00731731
Vorinostat	Stereotactic radiosurgery	Brain metastases in NSCLC	I (Ongoing)	NCT00946673
LBH589	—	Prostate, head and neck, oesophageal	I (Completed, unpublished); II (Ongoing)	NCT00670553
Vorinostat	—	Glioma	Upcoming phase I (Including fractionated stereotactic radiation therapy)	NCT01378481
LBH589	Stereotactic radiation	Patients with brain tumours	I (Ongoing recruitment)	NCT01324635

Abbreviations: HDAC = histone deacetylase; HDACi = HDAC inhibitors; NSCLC = non-small cell lung cancer; MTD = maximum-tolerated dose; 5-FU = 5-fluorouracil; VPA = valproic acid.

1.3 Irradiation induced double strand break damage

The most toxic damage to the DNA molecule is the double strand break (DSB). The DNA phosphodiester backbone is broken on both strands, within a distance of 10 base pairs (Lomax *et al*, 2013). DSB can be induced endogenously during cellular metabolism or exogenously by cytotoxic therapy which can act through inhibition of replication or in a radiomimetic fashion (induction of DSB through a free radical mechanism), such as bleomycin (Khanna & Jackson, 2001; Povirk, 2012). However, a major therapeutic modality used in many cancers is the use of ionising radiation (IR) in the form of external beam radiotherapy, which causes many DNA DSB in targeted cells, leading to cell inactivation and death (Khanna & Jackson, 2001; Mladenov *et al*, 2013). When the IR photons enter the cell, they cause ionisations, ejecting electrons from atoms in the cell. These electrons can damage the DNA directly, or indirectly through creation of free radicals mainly by water radiolysis, resulting in DNA base damage, and single strand and double strand DNA breaks (Figure 1.4) (Wouters & Begg, 2009).

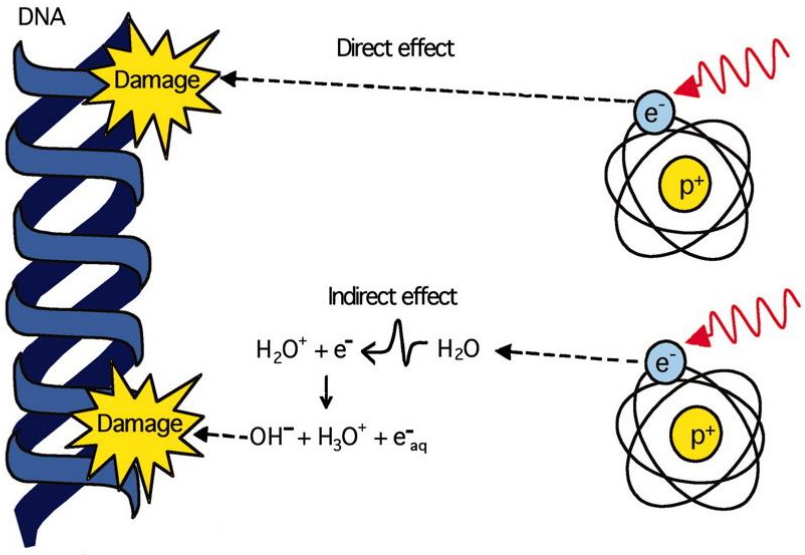


Figure 1.4. Ionising radiation causes DNA damage directly or indirectly.
Photons (red wave) cause ionisations, ejecting electrons from atoms in the cells. These can harm DNA directly. Alternatively, ejected electrons can cause radiolysis of water, and free radicals can harm the DNA molecule indirectly. Adapted from Morgan and Sowa (2005).

1.3.1 IR and DNA damage

Every day, tens of thousands of DNA lesions are formed per cell due to the reactive oxygen species (ROS) produced during cell aerobic metabolism. Each Gy of IR per cell will also cause lesions to the DNA that are chemically similar to those formed endogenously, such as 850 pyrimidine base and 450 purine base damage lesions, approximately 1,000 SSB and approximately 20-40 of the most toxic and deleterious lesions, namely DSB (Wouters & Begg, 2009; Lomax *et al*, 2013). The major difference between metabolically-induced lesions and IR-induced DNA lesions is the spatial distribution, which is evenly distributed in the first case and concentrated in a close spatial distribution, known as “clustered” in the case of IR. These clustered lesions rarely occur endogenously and often lead to formation of DNA DSB (Lomax *et al*, 2013). Homogenously distributed lesions can be efficiently repaired by cells, whereas the clustered DNA damage is a much greater repair problem. The most problematic lesions are so-called “complex” DSB lesions, in which guanine, adenine or cytosine bases are oxidised (Nikjoo *et al*, 2001; Lomax *et al*, 2013). The “complex” DSB frequently have damage on the 3’-sugar, in the form of a phosphoglycolate, and a 5’-OH, and these prevent direct end-ligation of DNA (Schipler and Iliakis, 2013). Cancer cells are frequently unable to properly repair IR-induced DSB, eventually causing their death.

1.3.2 IR and cell death

Low levels of DNA damage can induce activation of the DNA damage response, resulting in cell-cycle checkpoint arrest (G1, S or G2-phase arrests). Cell cycle arrest allows the cell time for the damage to be repaired before the cell progresses in mitosis (Kastan & Bartek, 2004). When the damage is too deleterious, cells can switch towards one of the cell-death programs, such as apoptosis, mitotic catastrophe (MC), senescence or necrosis (Surova & Zhivotovsky, 2013).

Cancers frequently have deficient cell-cycle checkpoints and damage to the DNA, such as IR-induced DSB, can persist as cells enter mitosis. Cell division without adequate repair

occurring results in MC is a well-established mode of cell death (Jonathan *et al*, 1999), where cells with unrepaired DNA damage enter mitosis. Morphological alterations, such as chromosomal fragmentations, multinucleation and giant cells can be visible in those cells under the microscope (Surova & Zhivotovsky, 2013).

1.3.3 The "5Rs" of radiobiology and the concept of the therapeutic window

Radiotherapy has a large impact on cancer cells. The main factors that modulate local cancer control after fractionated radiotherapy are described by the "5Rs" of radiobiology. These are: repair of DNA damage following irradiation fractions which differs between cancer and non-cancerous cells; repopulation of cells (cell division) and redistribution into more (G2/M phase) or less (S phase) radiosensitive cell cycle phases; tumour reoxygenation, with higher tissue oxygen tension contributing to higher radiosensitivity, and intrinsic cellular radiosensitivity (Steel *et al*, 1989; Harrington *et al*, 2007).

Generally, very high doses of radiotherapy can kill tumour cells, but these would also inevitably lead to unwanted consequences in non-cancerous cells (see Figure 1.5). In order to maintain the balance between maximal cancer cell kill, while still maintaining acceptable levels of toxicity towards normal cells, radiotherapy treatment planning has to take into account the "therapeutic window", depicted in Figure 1.5. A sufficient irradiation dose has to be given to achieve good tumour control, but with acceptable normal-tissue side effects. So, for a 5% late normal tissue complication probability (NTCP), which is acceptable in most tissues except for the spinal cord, radiotherapy alone might only confer a 70% tumour control probability (TCP). However, radiosensitising agents may be used to shift the balance between TCP and NTCP by shifting the tumour cell kill curve to the left, and therefore expanding the "therapeutic window". Hence for a 5% NTCP the TCP increases to over 90% in this hypothetical example (Figure 1.5).

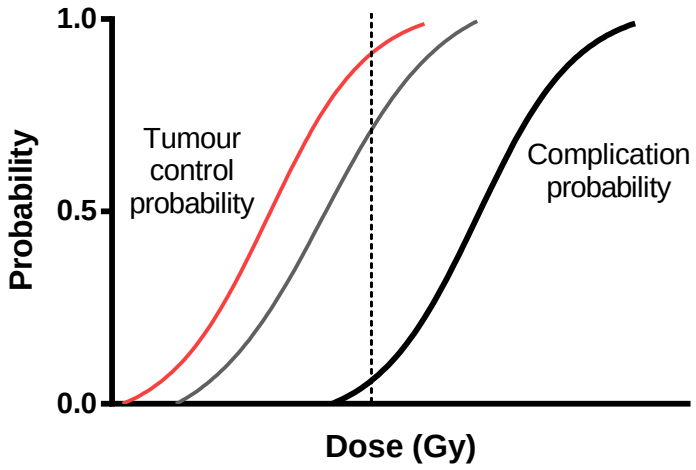


Figure 1.5. The therapeutic window.
The tumour control probability (TCP) versus normal tissue complication probability (NTCP) per irradiation dose is depicted. The right curve represents the NTCP and the middle curve the TCP for irradiation alone. The red line to the left represents the TCP when a radiosensiting agent is added to the radiotherapy regimen. Adapted from Baumann *et al* (2002).

1.4 DNA double strand break damage detection, signalling and repair

DNA DSB are first detected by a complex involved in DSB detection, signalling and DNA repair, consisting of three different proteins, MRE11, RAD50 and NBS1 (the MRN complex) (Rupnik *et al*, 2010). The MRN complex is crucial for the activation of the ATM signalling pathway (Lee & Paull, 2005), where the interaction of NBS1 and ATM is crucial for ATM phosphorylation and its recruitment to the sites of DSB (Falck *et al*, 2005; Berkovich *et al*, 2007) (Figure 1.6). Here ATM phosphorylates the serine 139 residue of the H2AX histone, to become γH2AX (Jakob *et al*, 2011). In a very short time this signal gets amplified and these phosphorylations form foci, to which all the proteins and chromatin modifiers involved in DSB repair can be attracted. These foci therefore form a DNA repair platform. Eventual DSB resolution also causes γH2AX foci to disappear (Rogakou *et al*, 1999; Bonner *et al*, 2008).

In vivo, MRE11 forms a complex as an MRE11 dimer, with two RAD50 proteins, each binding to one MRE11, and each MRE11 protein has a binding site for an NBS1 protein (Lamarche *et al*, 2010). MRE11 has several biochemical activities, e.g. using its' 5'–3' endonuclease activity in resection of DSB ends, to initiate homologous recombination (HR) and using its 3'–5' exonuclease activity to resect the broken DSB ends (Figure 1.6) (Paull & Gellert, 1998; Trujillo, 1998). Moreover, it facilitates the processing of DNA by other factors, such as CtIP (Williams *et al*, 2008, 2010; Park *et al*, 2011; Buis *et al*, 2012).

MRE11 protein-deficient cells are highly radiosensitive. Humans with mutations in the *MRE11A* gene suffer from ataxia-telangiectasia-like-disorder (ATLD); these cells have increased ionising radiation sensitivity and high chromosomal instability (Stewart *et al*, 1999). The cancer predisposition is difficult to prove directly, since there are only a small number of patients with this disorder, but two patients with ATLD have been diagnosed with lung adenocarcinoma (Uchisaka *et al*, 2009). On the other hand, reports exist correlating mutations, both germline and somatic in the *MRE11A* gene and predisposition to breast cancer (Bartkova *et al*, 2008), lymphomas (Fukuda *et al*, 2001), and colorectal cancer (Giannini *et al*, 2002).

RAD50 can bind to and unwind DSB termini in an ATP-dependent manner, by using an ATP-binding cassette, a structure made from RAD50's N- and C- terminal nucleotide binding domains (Walker A and B domain) (see Figures 1.6 and 1.7) (Hopfner *et al*, 2001). Moreover, the two coils with a zinc hook at the ends can interact with another RAD50 coil, providing an important mechanism for bringing together two DNA molecules (Hopfner *et al*, 2002). *RAD50* mutations result in Nijmegen breakage syndrome-like disorder (NBSLD), manifesting as mental retardation, short stature, bird-like face, but probably not malignancies. Cells from a patient are highly radiosensitive, and do not form MRN foci at DNA DSB sites (Waltes *et al*, 2009).

NBS1 does not have any known enzymatic functions, but it has a role in cell-cycle checkpoint protein-protein interactions and, also, since it has a nuclear localisation signal, a role in translocating the complex into the nucleus (Desai-Mehta *et al*, 2001). *NBS1* gene

mutations cause Nijmegen breakage syndrome (NBS), with a high incidence of lymphomas (Hiel *et al*, 2000). Cell lines from these patients do not exhibit MRE11/RAD50 focus formation (Carney *et al*, 1998; Hiel *et al*, 2000; Desai-Mehta *et al*, 2001).

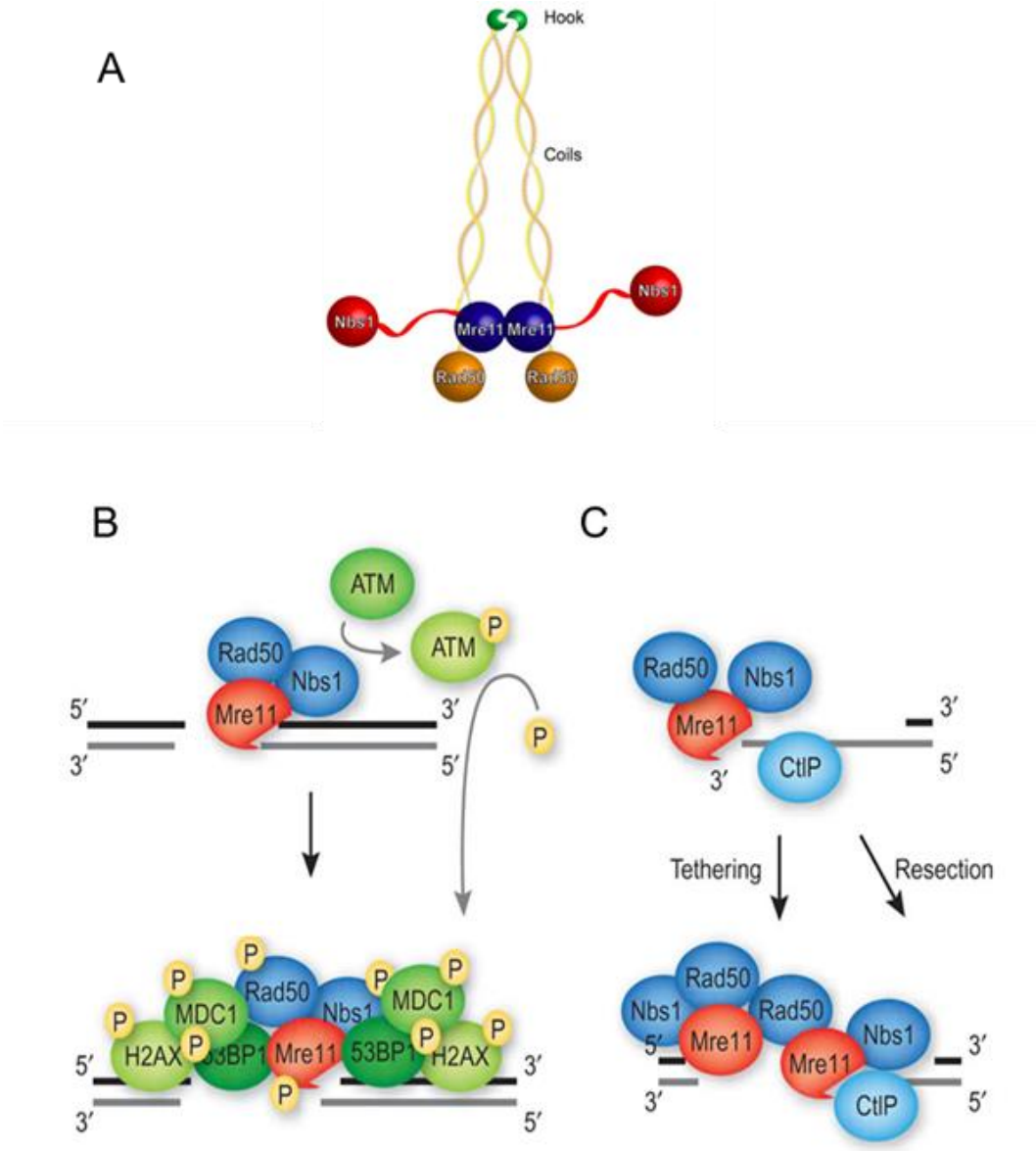


Figure 1.6. The MRN complex structure and function in DSB repair.
A) In vivo, the MRN complex comprises an MRE11 dimer and two RAD50 proteins, with each MRE11 protein possessing a binding site for the NBS1 protein. B) The complex recruits the ATM protein to sites of DSB. ATM then auto-phosphorylates and this further activates the DNA damage response. ATM targets are recognised and phosphorylated, including the histone variant H2AX (termed γH2AX when phosphorylated). C) The MRN complex binds to the DNA DSB ends, where end-resection can be initiated by the MRE11 and CtIP proteins or ends can be tethered, using the RAD50 hook domain. Adapted from Zha *et al* (2009) and Williams *et al* (2010).

Two major mechanisms for repairing DNA DSB exist, non-homologous end joining (NHEJ) and homologous recombination (HR) (Mladenov *et al*, 2013). Furthermore, NHEJ is divided into two pathways: classical (DNA-PK dependent) and alternative NHEJ. NHEJ repairs DSB much faster than HR (Mao *et al*, 2008). Pathway choice for repair of DSB is not fully understood, but it depends on the cell cycle phase when DSB occur, the cell type and also direct competition between various NHEJ or HR repair proteins (Shao *et al*, 2012).

In the second half of the cell cycle (S- and G2-phase), HR is promoted through the elevated expression of proteins including RAD51, BRCA1, BRCA2 and CtIP (Flygare *et al*, 1996; Wang *et al*, 1997; Shrivastav *et al*, 2008). Another important component in pathway choice is the phosphorylation of proteins by cyclin dependent kinases (CDKs). For example, CDK phosphorylation of CtIP promotes the interaction between BRCA1 and CtIP, which is important for HR pathway initiation (Yu & Chen, 2004), and phosphorylation of NBS1 can enhance the action of HR in an MRN-dependent manner (Falck *et al*, 2012). CtIP can also be phosphorylated by ATM, to promote HR (Li *et al*, 2000).
Another important protein regulating pathway choice is the p53 binding protein 1 (53BP1) and its downstream effector, RIF1, which can inhibit DNA end-resection and favours NHEJ (Chapman *et al*, 2013; Panier & Boulton, 2014). 53BP1 also has an inhibitory function on HR in BRCA1-deficient cells (Bunting *et al*, 2010), thus further promoting the NHEJ pathway. Ku proteins (NHEJ) directly compete with MRN or PARP1 for the pathway choice (Wang *et al*, 2006; Cheng *et al*, 2011; Mladenov *et al*, 2013).

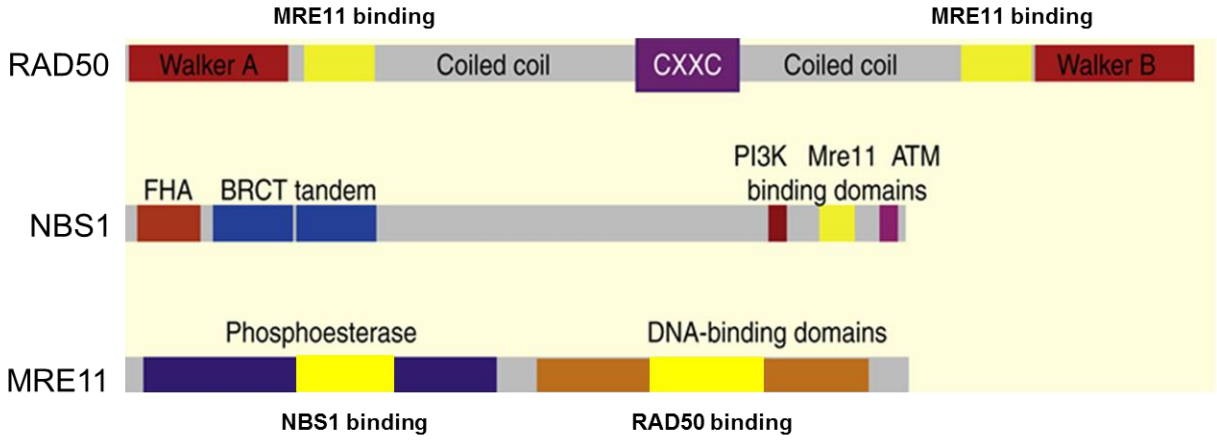


Figure 1.7. The MRN complex domains.
Structure of RAD50, NBS1 and MRE11 proteins. CXXC = zinc hook; FHA = Forkhead associated domain; BRCT = BRCA1 carboxyl terminus domain. Adapted from Rupnik *et al* (2008).

1.4.1 Non-homologous end joining

NHEJ is active throughout the cell cycle, but is predominant in G1 and early S-phase. The repair process may be accurate when the ends of the breaks are compatible, but can be error prone in "difficult lesions" created by IR, such as damaged bases (see IR and DNA damage section). NHEJ does not require a DNA template to be used for DSB repair. The repair starts with the DNA-PK complex, when the Ku70 and Ku80 proteins are recruited and loaded onto the site of the lesion to form a heterodimer Ku70/Ku80, and then the DNA-PKcs (catalytic subunit) is recruited to the heterodimer and is autophosphorylated in order to bring both DNA ends together. If the DNA ends need processing (small base pair deletions or insertions) it can activate the nuclease Artemis. Subsequently, the Ligase IV complex (Ligase IV/XRCC4/XLF) is attracted to the site and the DNA is ligated end-to-end (Chan *et al*, 2002; van Gent & van der Burg, 2007; Fattah *et al*, 2010; Shao *et al*, 2012).

DNA-PKcs is not always required for end joining. A backup pathway to classical NHEJ exists. In situations where DNA-PK or Ligase IV is absent, inhibited or aberrantly active, alternative/backup NHEJ (B-NHEJ) may come into play. As this pathway frequently utilises small regions of microhomology for end-joining, is also frequently referred to as microhomology mediated end-joining (MMEJ) (McVey & Lee, 2008; Mladenov *et al*, 2013).

It is also active throughout the cell cycle, with an increased activity in G2 phase of cell cycle. The pathway is more error-prone than NHEJ, with the use of microhomologies, typically 5-30 nucleotides long and up to 1Kb from the DSB, which can result in long deletions. It starts with PARP-1 and MRN resection of the ends and ends with end-ligation using XRCC1 and DNA Ligase III (Figure 1.8). Bentley *et al* (2004) have shown that high grade bladder tumours use MMEJ as a preferential repair pathway, and this fact might contribute to the high level of mutations and deletions seen in bladder cancers (Bentley *et al*, 2004; Fattah *et al*, 2010; Manova *et al*, 2012; Mladenov *et al*, 2013).

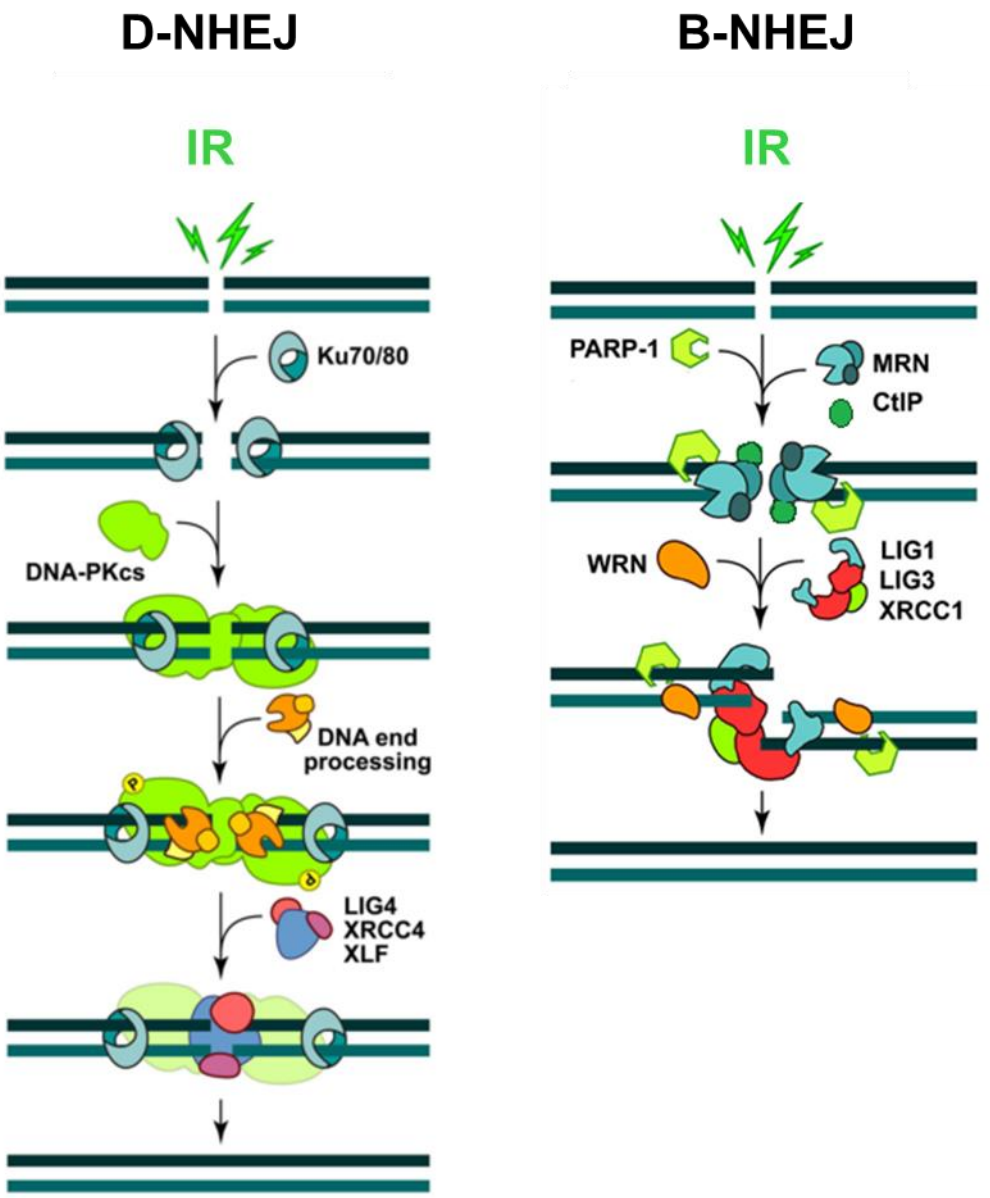


Figure 1.8. Classical (D-NHEJ) and alternative (B-NHEJ) NHEJ DNA repair pathways. In classical NHEJ (also referred to as D-NHEJ), Ku70 and Ku80 proteins form a heterodimer and bind to the DNA ends. DNA-PKcs is then recruited to form an active heterotrimeric holoenzyme. Various proteins, such as Artemis, are subsequently attracted to the DSB sites where they help with DNA end-processing. Finally, the Ligase IV complex (Ligase IV/XRCC4/XLF) is attracted to the site and the DNA is ligated end-to-end. The alternative NHEJ pathway (B-NHEJ) starts with PARP-1 and MRN resection of DNA ends. The resected end ligation is mediated by XRCC1 and DNA Ligase I or III enzymes. As this pathway frequently utilises small regions of microhomology for end-joining, is also frequently referred to as microhomology mediated end-joining (MMEJ). IR = ionising radiation. Adapted from Mladenov et al (2013).

1.4.2 Homologous recombination

HR is a more complex mechanism than NHEJ, but is error-free. It is predominant in late G2/S phase as it needs the sister chromatid as a template (or, more rarely, the homologous chromosome) (Iijima *et al*, 2008). The MRN complex and CtIP facilitate 5'-3' strand resection at the DSB ends, to create a long single stranded DNA (ssDNA) 3'-overhang (Sartori *et al*, 2007). The BRCA1 protein has a crucial role in MRN-CtIP binding (Chen *et al*, 2008). Next, the RPA protein which has a very high affinity for ssDNA is loaded onto the ssDNA at the 3'-overhang. The RPA molecules are replaced by RAD51 molecules which form a nucleoprotein filament, leading to strand invasion and the search for homologous sequence, thus creating a D-loop. This reaction is facilitated by PALPB and BRCA2 (Figure 1.9) (Buisson *et al*, 2010; Rassool & Tomkinson, 2010).

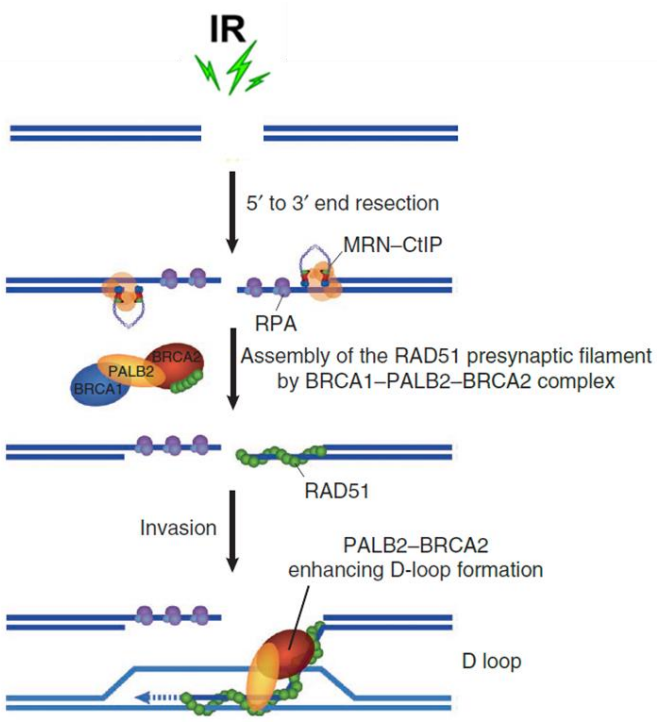


Figure 1.9. The homologous recombination pathway.
It starts with MRN-CtIP DNA resection, creating single stranded DNA. RPA proteins are loaded onto the ssDNA and replaced by the RAD51 protein, that initiates sister chromatid strand invasion and D-loop formation, a step facilitated by PALP2-BRCA2 proteins. Note, that only early steps of homologous recombination are shown. IR = ionising radiation. Adapted from Buisson *et al* (2010).

1.5 HDAC inhibitors and effects on DNA damage signalling and repair

A role for HDACs in the DNA damage response has been identified. Miller *et al* (2010) have recently demonstrated accumulation of HDAC1 and HDAC2 at sites of DNA damage. Furthermore, the authors demonstrated that depletion of HDAC1 and HDAC2 in cells results in impaired NHEJ and an increased sensitivity to IR. Kotian *et al* (2011) have reported that depleting HDAC9 or HDAC10 results in HR impairment. Taken together, these results suggest that HDACs have distinct roles in the repair of DSBs.

1.5.1 HDAC inhibitors in normal human cells

Evidence to date shows that normal cells are not affected by HDAC inhibition as much as cancer cells (discussed below), either when treated with inhibitor alone or in combination with ionising radiation (IR). This is important especially from a clinical perspective, since radiotherapy treatment inevitably affects some normal (noncancerous) tissue.

Lee *et al* found that vorinostat induced γH2AX signalling in normal human foreskin fibroblasts, indicating DNA DSB formation, as detected on both western blot and immunofluorescence, but cells showed efficient repair at later timepoints (loss of γH2AX signal), even though the drug was still present in the incubation medium. Furthermore, these fibroblasts did not show any reduction in the levels of the DNA damage signalling and repair proteins (RAD50, MRE11, phosphorylated-ATM) or reduced viability, in contrast to vorinostat treated non-small cell lung and prostate cancer cells (Lee *et al*, 2010). Blattmann *et al* (2010) found no radiosensitising effects of vorinostat in normal human fibroblast and osteoblasts. Munshi *et al* did not detect any decrease in levels of NHEJ Ku70, Ku80 and DNA-PK proteins in normal human lung fibroblasts treated with sodium butyrate (NaB), but these effects were detected in cancer cells. Moreover, NaB did not cause any radiosensitising effects (Munshi *et al*, 2005b). Konsoula et *al.* found that H6CAHA-treated normal prostate epithelial cells did not show decreased viability.

Furthermore, using γH2AX- and RAD51-foci assays there was little effect on DNA repair capability in treated normal cells (compared with effects on prostate malignant cells, see below). Their finding of an increased survival fraction after IR in a clonogenic assay even implied that HDAC inhibition resulted in radio-protection (Konsoula *et al*, 2011).

1.5.2 HDAC inhibitors in cancer cells

When DNA damage signalling and repair proteins are supressed, this results in greater sensitivity to ionising radiation (Zhang *et al*, 2005; O'Driscoll & Jeggo, 2006). As some cancer cells show great radiosensitisation when treated with HDAC inhibitors, it is possible that HDAC inhibitors might target DNA damage signalling and repair proteins.

In lung adenocarcinoma and prostate cancer cells, treatment with vorinostat as a single therapy (compared with normal fibroblasts, see previously) resulted in persistent γH2AX signalling (Lee *et al*, 2010) as did treatment with TSA and irradiation in squamous carcinoma cells (Zhang *et al*, 2007), indicative of delayed DNA repair. Downregulation of RAD50 and MRE11 protein levels was detected after treatment with H6CAHA in prostate cancer cells in parallel with attenuated induction of phosphorylated-ATM foci and radiosensitisation of cells (Konsoula *et al*, 2011).

In terms of NHEJ, vorinostat and NaB can cause downregulation of Ku70 and Ku80 proteins and NaB has also been shown to cause a decrease in DNA-PK levels in melanoma cells (Munshi *et al*, 2005b, 2006). TSA had a similar effect on these proteins in non-small cell lung carcinoma cells (Zhang *et al*, 2009).

In terms of HR, Adimoolam *et al* (2007) observed RAD51 downregulation in colon cancer cells and radiosensitisation after PCI-24781 treatment, and, in mouse xenografts models, decreased RAD51 protein levels were found in PCI-24781 treated mice. In prostate (Chinnaiyan *et al*, 2005), osteosarcoma and rhabdomyosarcoma cells, upon vorinostat treatment (Blattmann *et al*, 2010), RAD51 levels decreased causing radiosensitisation.

TSA reduced levels of BRCA1 and BRCA2 proteins in squamous cancer cells. In this study there were no radiosensitising effects in BRCA1-null cells. However, after ectopic BRCA1 expression, TSA's radiosensitising effects were restored, demonstrating that TSA exerts its radiosensitising effects through inhibition of DNA DSB repair (Zhang *et al*, 2007). In prostate cells, H6CAHA caused radiosensitisation and attenuation of phosphorylated-BRCA1 foci (Konsoula *et al*, 2011). These effects are graphically summarized in Figure 1.10.

In order to compare radiosensitising effects of various drugs and cancers, the SER_{10} value (sensitisation enhancement ratio at 10% survival) can be used. These are not always stated in preclinical radiosensitising studies on HDAC inhibitors, but in cases where they were not stated, I have estimated them from published graphs.

Kim *et al* (2004), have tested the HDAC inhibitor TSA as a radiosensitiser in human glioblastoma cells. They provide SER_{10} values, which were in the range of 1.27-1.53 for 18 h TSA incubation at concentrations of 50 to 200 nM, respectively. Similarly, the SER_{10} for VPA treated glioblastoma cells was 1.3, using a 24 h incubation protocol at a 1.5 mM dose (Camphausen *et al*, 2005). Chinnaiyan *et al* (2008), report on glioma cells to be radiosensitised with SER_{10} of 1.4 after 24 h incubation with VPA. Kim *et al* (2005), tested TSA as a radiosensitiser in a human adenocarcinoma cell line. After 18 h incubation, the SER_{10} (estimated) was approximately 1.1 for 50 nM and 1.5 for 200 nM treatment. Similar values can be estimated for the cervical adenocarcinoma, with SER_{10} of 1.2-1.3 for the same TSA doses of 100 nM and 200 nM. Another HDAC inhibitor, NaB, has proved to be an efficient radiosensitiser in two melanoma cell lines, with 24 h incubation of 3 mM NaB producing an SER_{10} of 1.3 in one cell line and 2.1 in the other, while the normal cells were not radiosensitised (Munshi *et al*, 2005b).

In human chronic myelogenous leukemia cells, 24 h incubation at doses of 100 nM – 1 μM gave radiosensitisation SER_{10} of 1.1-2.1(Karagiannis *et al*, 2005). 18 h incubation with vorinostat, radiosensitised human colorectal carcinoma cell lines, with estimated SER_{10} of 1.3-1.6 (Flatmark *et al*, 2006). Longer, 48 h incubations of pancreactic cells with vorinostat

caused radiosensitisation with SER_{10} values estimated to be in the range of 1.4-1.6 (Deorukhkar *et al*, 2010). Adimoolam *et al* (2007), used abexinostat (PCI-24781) in clonogenic assays. 24 h incubation of large cell lung cancer cells caused radiosensitisation (estimated SER_{10} of 1.4) and similar treatment also caused radiosensitisation of colorectal carcinoma cells (estimated SER_{10} of 1.4). Ovarian and breast adenocarcinoma cell lines were also tested with 500 nM vorinostat for radiosensitising effects. Cells were incubated for 18 hours pre-IR and the drug was left in the medium after irradiation for the duration of the experiment. The SER_{10} was 1.2 for the breast and 1.5 for the ovarian adenocarcinoma cell line (Baschnagel *et al*, 2009).

In terms of urological malignancies, prostate carcinoma cells were radiosensitised after 48 h incubation with VPA with estimated SER_{10} values in the range of 1.15-1.40 (Kachhap *et al*, 2010). Konsoula *et al* (2011), have tested a novel HDAC inhibitor, H6CAHA, that proved to be an efficient radiosensitiser in prostate carcinoma cells (with estimated SER_{10} of 1.4 after 16 h incubation with 1 μM).

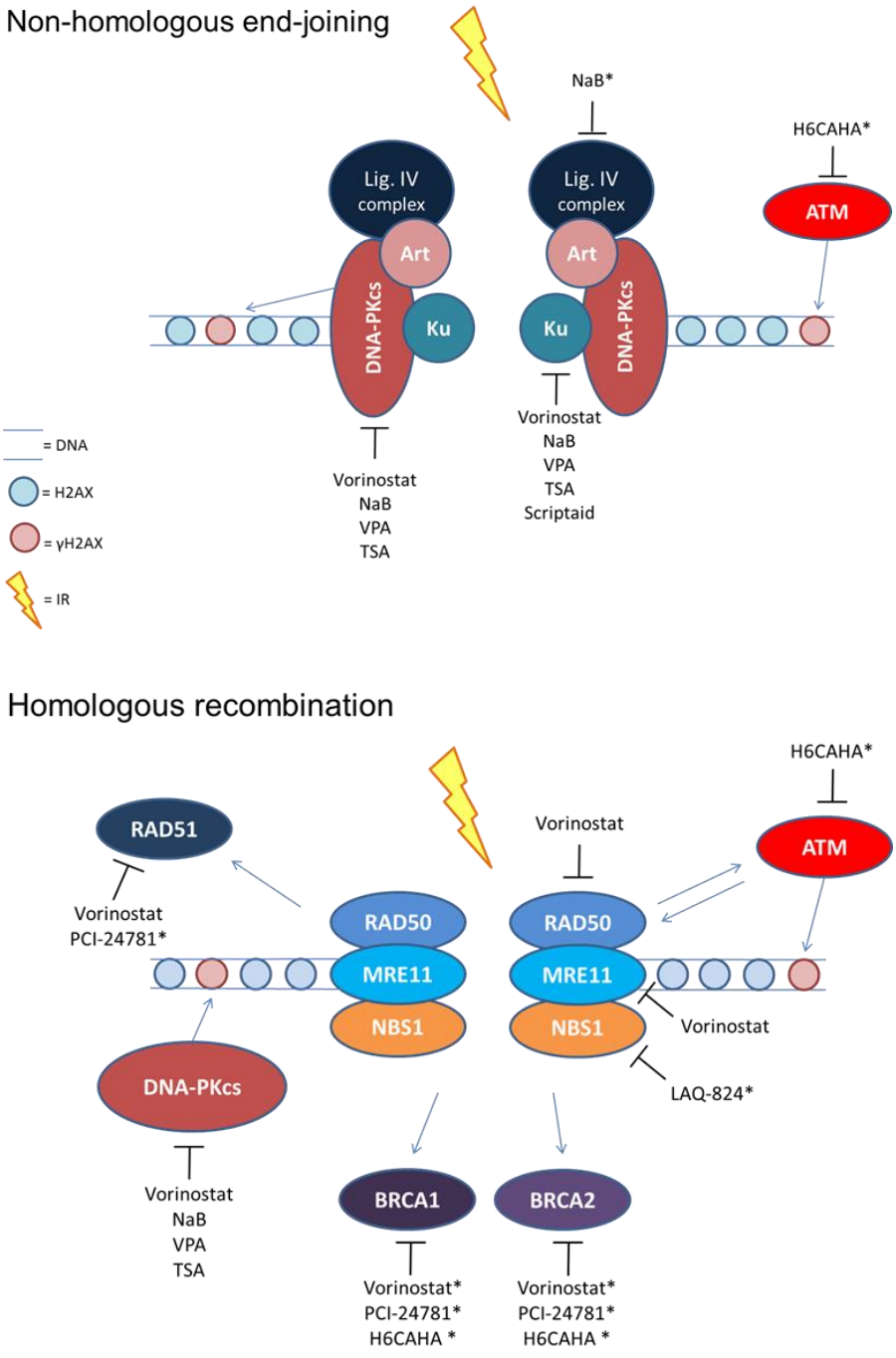


Figure 1.10. HDAC inhibitors and effects on the major NHEJ and HR proteins. Schematic presentation of the key repair proteins involved in either NHEJ (top) or HR proteins (bottom) and effects of HDAC inhibitors on the proteins. * = HDAC inhibitor downregulates the mRNA levels. Abbreviations: γH2AX = phosphorylated histone H2AX; NaB = sodium butyrate; VPA = valproic acid; TSA = trichostatin A. Adapted from Groselj et *al* (2013).

1.6 HDAC inhibitors and effects on gene transcription

The acetylation and deacetylation of lysines on histone proteins is a dynamic process, dependent on the interplay between HATs and HDACs (Figure 1.11) (Wang *et al*, 2009; Dickinson *et al*, 2010). Acetylation of histone lysine residues has long been known to be associated with relaxation of chromatin (due to the neutral charge on the histone tails), and activation of gene transcription (Allfrey *et al*, 1964; Pogo *et al*, 1966; Hebbes *et al*, 1988; Wang *et al*, 2009). On the other hand, deacetylated lysine residues are positively charged and the DNA molecule becomes more firmly bound to histones, resulting in less relaxed chromatin, thus preventing transcription machinery from accessing gene promoter regions (Ropero & Esteller, 2007). An additional mechanism for transcriptional regulation could be creation of the new binding surfaces by acetylated histone lysines, particularly for the protein bromodomain binding (Clayton *et al*, 2006). HDAC inhibitors can also inhibit large HDAC-associated complexes, recruited to chromatin to act as transcriptional repressors (Nagy *et al*, 1997; Ropero & Esteller, 2007; Kachhap *et al*, 2010).

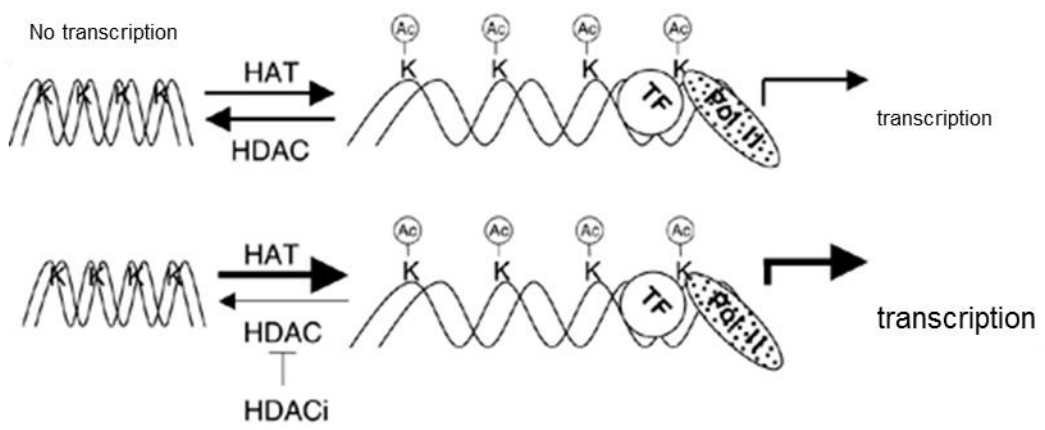


Figure 1.11. Gene transcription and the interplay of HDAC and HAT.
The balance between deacetylated and acetylated chromatin has a key role in determining gene expression. In a simplified model, HDAC inhibitors (HDACi) shift the balance towards the more acetylated and transcriptionally active chromatin. Furthermore, transcription factors (TF) and the enzyme polymerase II (Pol II) can access the gene promoter regions, enhancing gene transcription. Adapted from Glozak *et al* (2007).

Whilst it is logical to generalise that (due to effects on chromatin) HDAC inhibitors activate gene expression, several gene expression microarrays studies have come to the conclusion, that upon treatment with HDAC inhibitors, gene expression can also be suppressed. Kortenhorst *et al* (2008) have shown in a cDNA microarray global gene expression analysis, using SAHA or VPA-treated prostate cells that only about 3-10% of the genes studied were affected, with 51-73% of genes being upregulated and 28-49% downregulated. The result was cell type-and-treatment specific.

In another study, bladder and breast cancer cell lines were treated with the HDAC inhibitors vorinostat, TSA and MC-275 (entinostat) (Glaser *et al*, 2003). Only about 10% of studied genes were affected, with as many genes upregulated as downregulated, and results varying between the cells and HDAC inhibitors used. The authors speculated that the repressive effect on gene expression caused by the HDAC inhibitors could result in activated transcription of factors involved in negative regulation of gene transcription (Glaser *et al*, 2003).

Recently, Kim *et al* (2013b) established a mechanism for the transcriptional repression caused by HDAC inhibitors targeting highly expressed genes and high copy genes. In cancer cells those are usually oncogenes, that have occurred through multiplication of various chromosomal segments. The authors established that the HDAC inhibitors TSA and vorinostat target elongation of RNA polymerase II, in breast cancer cells.

HDAC inhibitors have also been found to suppress transcription of genes involved in DNA DSB damage signalling, detection and repair in various cancer cells. For the genes of the MRN complex, *NBS1* gene downregulation was observed after melanoma cells were treated with the HDAC inhibitor NaB (Munshi *et al*, 2005b); the *ATM* gene was transcriptionally repressed by the HDAC inhibitor H6CAHA in prostate cancer cells (Konsoula *et al*, 2011). Various HDAC inhibitors also affect expression of genes involved in the HR and NHEJ pathway. Transcription of the key HR gene transcription, *RAD51* has been found to be downregulated upon SAHA and VPA treatment in prostate carcinoma cells (Kachhap *et al*, 2010), and in colorectal cancer cells, after PCI-24781 (Adimoolam *et*

al, 2007). The inhibitors H6CAHA (Konsoula *et al*, 2011), PCI2478 (Adimoolam *et al*, 2007), VPA (Kachhap *et al*, 2010) and TSA (Zhang *et al*, 2007) had suppressive effects on *BRCA1* and *BRCA2* gene expressions in prostate, colon or squamous cancer, respectively. The NHEJ genes were targeted in melanoma cells treated with NaB, resulting in decreased expression of *Ku70, K80*, *DNA-PKcs*, *Ligase IV* and *XRCC4* genes (Munshi *et al*, 2005b).

Currently the mechanisms underlying the repressive effects of HDAC inhibitors on gene transcription are still not well understood, as these effects are cell type-and HDAC inhibitor-dependent.

1.7 Aims and objectives

The main aims of this project were:

1. To investigate the radiosensitising effects of the histone deacetylase inhibitor panobinostat in bladder cancer cell lines, with the ultimate goal of proposing a novel radiosensitising therapy for muscle invasive bladder cancer.

The following objectives were set to achieve this aim:

i. To determine the cytotoxicity of panobinostat and to determine the optimum incubation timing for radiosensitisation.

ii. To test if panobinostat affects p53 protein levels in *TP53* wild-type and *TP53* mutant bladder cancer cell lines and to determine whether expression of the Δ133p53 variant influenced panobinostat treatment.

2. To study the effects of panobinostat on homologous recombination and non-homologous end joining, to determine the predominant pathway targeted and to look further upstream at effects on the MRE11/RAD50/NBS1 complex.

The following objectives were set to achieve this aim:

i. To use bladder cancer cells impaired in either homologous recombination or non-homologous end joining and to establish whether panobinostat targeted the unimpaired pathway thus exploiting the synthetic lethality concept in bladder cancer cells.

ii. To establish the effects of panobinostat on proteins upstream of HR or NHEJ (MRE11/NBS1/RAD50) and to determine whether its effects on DNA repair damage signalling proteins are transcriptional or post-transcriptional.

CHAPTER 2: MATERIALS AND METHODS

2.1 Materials

2.1.1 Cell Lines

The bladder cancer cell line RT112 and the normal human urothelial (NHU) cell line 1754 were kindly provided by Prof. MA Knowles (Leeds Institute of Molecular Medicine, UK) and T24 and CAL29 cell lines were purchased from the DSMZ (Braunschweig, Germany; https://www.dsmz.de/). Stably transfected RT112-derived cell lines pSil8 (transfected with circular negative control pSilencer neovector), C13 (transfected with pSilencer-Ku80, target sequence: 5'-AAC TCC ATT CCT GGT ATA GAA-3') and 795J (transfected with pSilencer-RAD51, target sequence: 5'-AAT CAC TAA TCA GGT GGT AGC-3') were made by Dr. Boling Qiao (Leeds Institute of Molecular Medicine, Leeds, UK), (Qiao *et al*, 2013).

The *TP53* wild-type RT112 bladder cancer cell line has been extensively characterised (microsatellite typing, MFISH, karyotypic analysis) in the laboratory of Prof. MA Knowles. Of the other two cell lines used in experiments, T24 bladder cancer cell line is known to be *TP53* mutant, with the in frame deletion of tyrosine 126 (exon 5), as established by Cooper *et al* (1994). This mutation has also been confirmed in Anne Kiltie's laboratory (Dr. Martin Kerr, personal communication). CAL29 is also known to be *TP53* mutant (exon 8, p.R282W), with the mutation described as "highly destabilising", leading to dominant-negative function (Xu *et al*, 2011a) (http://p53.iarc.fr). See also Table A.1 in Appendix A (for cell line *TP53*, grade and stage characteristics).

2.1.2 Cell culture media and materials

RT112 and T24 cells were cultured in RPMI medium containing 0.3 g/l L-glutamine (Sigma-Aldrich, Dorset, UK). The CAL29 cell line was cultured in Dulbecco's Modified

Eagle Medium (DMEM) and GlutaMAX (Gibco, Paisley, UK). Both cell culture media were supplemented with 10% fetal bovine serum (FBS; Gibco, Paisley, UK). The NHU cell line 1754 was cultured in Keratinocyte Growth Medium Kit 2 (PromoCell, Heidelberg, Germany), containing supplemented Bovine Pituitary Extract 0.004 ml/ml, Epidermal Growth Factor 0.125 ng/ml, insulin 5 µg/ml, hydrocortisone 0.33 µg/ml, epinephrine 0.39 µg/ml, transferrin 10 µg/ml and $CaCl_2$ at a final concentration of 0.09 mM. All media were stored at 4°C. pSil8, C13 and 795J were cultured in RPMI containing 300 µl (600 µg/ml) of G-418 Solution (Roche, Indianapolis, IN). All cell lines were cultured at 37°C, 5% CO_2 in a humified incubator.

Trypsin was bought as pre-prepared, gamma irradiated 0.12% w/v trypsin-EDTA from SAFC Global (Gillingham, UK). For the NHU cells, the trypsin solution was diluted in PBS (GIBCO, Paisley, UK) to 0.05% v/v trypsin-EDTA. Trypsin inhibitor at 10 mg/ml was obtained from Sigma (Dorset, UK) and dissolved in PBS to 1% (w/v) working solution. Cholera toxin for NHU cell attachment was purchased from Sigma (Dorset, UK) and prepared at 30 µg/ml stock concentration in growth medium and used at a final concentration of 30 ng/ml. All the stocks and working solutions were stored at 4°C.

Conical plastic 50 ml and 15 ml centrifuge tubes were purchased from Corning Inc. (Corning, NY). Tissue culture T75 and T175 cm^2 flasks were purchased from Appleton Woods (Birmingham, UK). Cells were frozen in 2 ml cryogenic vials from Corning Inc. (Corning, NY) and transferred to an isopropranol-filled Nalgene Cryo 1°C Freezing Container from VWR (Lutterworth, UK). DMSO for cell freezing was purchased from Sigma (Gillingham, UK).

For cell pellet collection and western blot sample preparation, 1.5 ml microcentrifuge tubes were used (STARLAB, Ahrensburg, Germany).

For cell pellet collection and clonogenic assay experiments, 10 cm CellStar cell culture dishes were used (Greiner Bio-One Ltd., Stonehouse, UK).

2.1.3 Cytotoxic agents

Panobinostat (LBH-589) was purchased from Selleck Chemicals (Houston, TX) and dissolved in DMSO (Sigma-Aldrich, Irvine, UK) to a 1 mM stock concentration. Mocetinostat (MGCD0103) was purchased from Selleck Chemicals (Houston, TX). It was dissolved in DMSO to a 2.5 mM stock concentration. Imatinib was purchased from Stratech Scientific (Newmarket, UK) and dissolved in DMSO to a 10 mM stock concentration. Single use aliquots were stored at -80°C.

2.1.4 Irradiation source

For irradiation experiments, a Caesium-137 source (GSR D1, Gamma-Service Medical GmbH, Leipzig, Germany) was used.

2.1.5 Western blotting

The Pierce BCA protein assay kit and the bovine serum albumin standard were purchased from Thermo Scientific (Rockford, IL) and stored at room temperature. Protein absorbance was measured on a POLARstar Omega plate reader (BMG LABTECH, Aylesbury, UK). The 2 x Laemmli Sample buffer was obtained from Sigma-Aldrich (St. Louis, MO) and stored at -20°C. Samples were heated on an Accublock Digital Dry Bath from Labnet International Inc. (Edison, NJ). Four to 20% tris-glycine gels were purchased from Biorad (Hempstead, UK) and stored at 4°C. Nitrocellulose membrane with 0.45 µm pores was purchased from Thermo Scientific (Rockford, IL). Blots were scanned using a Li-cor Odyssey Detection System (Li-cor Biosciences UK Ltd., Cambridge, UK).

2.1.6 Flow cytometry

Propidium iodide was purchased from Sigma-Aldrich (St. Louis, MO) at 40 µg/ml and RNaseA at 10mg/ml from Novagen (San Diego, CA) and stored at 4°C and -20°C

respectively. Cell cycle distribution was measured using a laser detection FACScan or FACSort from Becton Dickinson (Oxford, UK).

2.1.7 Immunofluorescence microscopy

Sixteen percent paraformaldehyde was bought from Thermo Scientific (Cramlington, UK) and stored at room temperature. Bovine serum albumin powder was obtained from VWR International (Lutterworth, UK) and stored at room temperature. Fluoromount G and DAPI were purchased from Sigma (Dorset, UK) and stored at 4°C. A Zeiss LSM 780 confocal microscope was used (Zeiss Ltd., Cambridge, UK).

2.1.8 Real-time PCR reagents

RNAeasy mini kit from Qiagen (Hilden, Germany) was used and all the kit components stored at room temperature. In the RNA extraction process, 21G needles from Terumo (Leuven, Belgium) and BD Plastipak syringes (Beckton Dickinson, Madrid, Spain) were used. RNase-free distilled water was obtained from Qiagen (Hilden, Germany) and stored at room temperature. The concentration of RNA was determined using a Nanodrop (Thermo Scientific, Wilmington, DE).

2.1.9 Agarose gel electrophoresis

Molecular grade agarose was obtained from Sigma (St. Louis, MO). The required gel density was prepared (typically 1% w/v) in 1 X TBE buffer (see Buffers/Solutions). GelRed Nucleic Acid Stain was bought from Bioutium (Hayward, CA). The gels were imaged using a Molecular Imager FX ProPlus (Bio-Rad Laboratories, Hemel Hempstead, UK).

2.2 Buffers/Solutions

2.2.1 Freezing solution

One hundred microlitres of DMSO, 500 µl of FBS and 400 µl of appropriate serum free medium were mixed together and added to the cell pellet. Cells were gently resuspended in the solution by pipetting and put into a 2 ml cryogenic vial.

2.2.2 Protein lysis buffer

5.957 g HEPES (Sigma, St. Louis, MO)

1.461 g NaCl (Fisher Scientific, Loughborough, UK)

10 ml of 500 mM EDTA (Sigma, St. Louis, MO)

5 ml Triton X-100 (Sigma, Dorset, UK)

20 ml of 100 mM sodium pyrophosphate (AppliChem, Darmstadt, Germany)

5 ml of 200 mM sodium orthovanadate (Sigma, St. Louis, MO)

5 ml of 1 M sodium fluoride (Sigma, St. Louis, MO)

50 ml of 500 mM β-glycerophosphate (Sigma, St. Louis, MO)

5 g sodium dodecyl sulphate (SDS) (Fisher Scientific, Loughborough, UK)

Chemicals were dissolved in 450 ml dH_2O, pH adjusted to 7.5 with 10 M NaOH (Sigma, St. Louis, MO), and made to the final volume of 500 ml with dH_2O and stored at 4°C.

2.2.3 Phosphate-buffered saline

To make up a 1 X solution, two PBS tablets (Gibco, Paisley, UK) were added to 1 litre of dH_2O. The solution was then autoclaved.

2.2.4 0.05% PBS-Tween

Two hundred and fifty microliters of Tween-20 (Promega, Madison, WI) was added to a sterile bottle of 500 ml of PBS.

2.2.5 Blocking buffer

0.05% PBS-Tween was mixed with Li-Cor buffer (Li-Cor Biosciences UK Ltd, Cambridge, UK) 1:1 v/v.

2.2.6 10 X Running buffer for electrophoresis

To 700 ml of dH_2O, 121 g Tris base (Fisher Scientific, Rockford, IL), 10 g SDS and 238 g HEPES (Sigma) were added. When the chemicals were dissolved, the volume was made up to 1 l with dH_2O.

For 1 X running buffer, 100 ml of 10 X Running buffer was added to 900 ml of dH_2O.

2.2.7 10 X Transfer buffer for electrophoresis

To 700ml dH_2O, 30 g of Tris base and 144 g of glycine (Fisher Scientific, Rockford, IL) were added and dH_2O added to the total volume of 1 l.

For 1 X transfer buffer, 100 ml of 10 X Transfer buffer and 200 ml of 100% Methanol (Fisher Scientific, Rockford, IL) were added to 700 ml dH_2O.

2.2.8 10 X Tris-borate EDTA (TBE) buffer

Tris-borate EDTA buffer was purchased as 10 X from Bio-Rad (Bio-Rad Laboratories, Hempstead, UK).

For 1 X TBE buffer, 100 ml of 10 X TBE buffer was added to 900 ml of dH_2O.

2.3 Methods

2.3.1 Cell Culture

For sub-culturing RT112, CAL29 and T24 bladder cancer cells, complete growth medium was warmed to 37°C in a water bath, then growth medium was removed by aspiration from the flasks and 5 ml of 0.12% trypsin-EDTA added to the cell monolayer for 3-6 minutes incubation at 37°C, in 5% CO_2 to allow detachment of cells. Then 25 ml of complete growth medium was added and mixed and the cells transferred to a plastic 50 ml centrifuge tube. Cells were pelleted by centrifugation in an Heraeus Labofuge 400 centrifuge (Thermo Fisher Scientific, Waltham, MA) at 1,300 rpm (200 g) for 3 minutes. Once the supernatant was removed, 10 ml of complete growth medium was used to gently resuspend the pellet by pipetting up and down. For the maintenance of cells, 2 x 10^6 RT112, 3 x 10^6 CAL29 or 1 x 10^6 T24 cells were added to 20 ml complete medium in a T175 cm^2 flask and the medium topped up to 25 ml.

NHU cells were sub-cultured in a similar way but T75 cm^2 flasks were used. The initial step was aspiration of medium, but this was followed by incubation in 5 ml pre-warmed 0.1% EDTA in PBS, for 5 minutes at 37°C, in 5% CO_2. The EDTA solution was removed by aspiration and 1 ml trypsin added for 3 min. Then 5 ml of complete growth medium plus trypsin inhibitor was used to resuspend the cells by gently pipetting up and down before transfer to a plastic 15 ml centrifuge tube. Cells were pelleted by centrifugation in an Heraeus Labofuge 400 centrifuge (Thermo Fisher Scientific, Waltham, MA) at 1,400 rpm for 4 minutes. Once the supernatant was removed, 10 ml complete growth medium was used to gently resuspend the pellet. Cells were routinely passaged at 2 x 10^5 in 10 ml medium in a T75 cm^2 tissue culture flask.

For all the experimental work, cell cultures in mid-log phase were used and treated with the drug, or equal volumes of DMSO for the control group.

2.3.2 Cell cryopreservation

For freezing, log-phase cells were prepared as described above, but the post-centrifugation cell pellet was resuspended in 1 ml of freezing solution (see Buffers/Solutions) and transferred to a 2 ml cryogenic vial and then to an isopropranol-filled Nalgene Cryo 1°C Freezing Container and allowed to cool to -80°C at 1°C/min. The next day cells were transferred to liquid nitrogen for long-term storage.

2.3.3 Irradiation of cells

In irradiation experiments, a Caesium-137 γ-ray source was used at a dose-rate of 1.7 Gy per minute. In the panobinostat clonogenic assay, cells were irradiated in 10 cm dishes at room temperature and then transferred to the incubator as soon as possible (5-10 minutes). For the imatinib clonogenic assay, cells were irradiated in 15 cm falcon tubes containing 10 ml of medium and immediately put on ice after irradiation.

In γH2AX foci experiments, studying DSB repair at different timepoints post-irradiation, cells were plated onto slides at the bottom of 5 cm dishes in 3 ml of medium and irradiated. After irradiation the medium was aspirated, the dishes washed twice with PBS and fresh complete medium added.

2.3.4 Chemosensitivity and radiosensitivity clonogenic assays

The cytotoxic effect of panobinostat and mocetinostat on tumour cells was assessed by the chemosensitivity clonogenic assay. Six hundred to 1,000 cells (for the experiments in T24, RT112, pSil, C13 and 795J cell lines) and 3,000-5,000 cells (CAL29) were plated in 10 cm dishes in 10 ml medium and exposed to appropriate increasing concentrations of

panobinostat, mocetinostat or imatinib for 24 hours. The next day, the medium was aspirated, and the dishes washed twice with 10 ml warm, sterile PBS. Finally, 10 ml of fresh medium was added to each dish and the dishes incubated at 37°C in 5% CO_2 for 14 days.

In the radiosensitisation clonogenic assay, 7.5 x 10^5 cells were plated in 10 cm dishes, and the following day treated either with DMSO or panobinostat at appropriate concentrations. After 24 h further incubation, cells were trypsinised and appropriate numbers plated in 10 cm dishes. Cells were then irradiated immediately after plating as described above.

Eight to fourteen days later (dependent on cell type), the medium was decanted from all dishes and replaced with 93% methanol:7% acetic acid to both wash and fix colonies. After fixing the colonies, 5 ml of Brilliant Blue R Concentrate (0.25% Brilliant blue R:40% methanol:7% acetic acid; Sigma-Aldrich, St. Louis, MO), diluted 1:1 with distilled H_2O, was added for 30 minutes to stain colonies. The stain was poured away and the dishes were rinsed in running water before being left to dry overnight. The number of colonies (containing more than 50 cells) per dish was counted automatically using an Oxford Optronix Colcount (Oxford Optronics, Oxford, UK).

2.3.5 Western blotting

2.3.5.1 Preparation of cell lysates

Cells were seeded at a density of 1 x 10^5/ml, in 10 ml of medium and plated onto 10 cm dishes. The next day dishes were treated with drug (or DMSO vehicle control), as necessary. Then, cells from the dishes were scraped in ice-cold PBS and lysed with protein lysate buffer containing 1% w/v SDS (see Buffers/Solutions), using a volume approximately equal to the volume of the cell pellet (typically 50 µl), supplemented with 0.1 g/ml protease inhibitor Complete Mini (Roche, Mannheim, Germany). The samples were then mechanically sonicated twice for 3 seconds on ice in 1.5 ml microcentrifuge

tubes. Samples were left for a further 5 minutes on ice and then spun for 7 minutes at 14,000 rpm (19,000 g) in an Eppendorf centrifuge 5430R (Eppendorf, Hamburg, Germany), pre-cooled to 4°C.

2.3.5.2 Protein concentration determination

Protein concentration was quantified by bicinchoninic acid assay, using a Pierce BCA protein assay kit. First, 10 µl of a dilution series (0.1 to 2 mg/ml) of bovine serum albumin standard and 1 µl of the lysed protein samples were loaded onto a 96-well plate (Corning Inc., Corning, NY). Next, 200 µl of Reagent A and B from the assay kit were added to each well, and the plate incubated for 45 minutes in the incubator. Following incubation, absorbance was measured at 562 nm on a POLARstar Omega plate reader. The protein concentration of each sample was then calculated by plotting absorbance against the standard curve of a dilution series of bovine serum albumin. Then 50 µg of the protein lysates were mixed with equal volumes of 2 x Laemmli Sample buffer and incubated on an Accublock Digital Dry Bath at 95ºC for 5 min.

2.3.5.3 Gel running

The samples were loaded on a 4 to 20% tris-glycine gel with at least one Amersham Full Range Rainbow Marker lane (GE Healthcare Life Sciences, Little Chalfont, UK) and run at 100 V for 70 minutes to separate samples according to molecular weight. Next, the gel was soaked in ice cold transfer buffer for 5 min. Proteins were then transferred from the gel onto a nitrocellulose membrane with 0.45 µm pores for 120 minutes at 40 V. The membrane was placed in 10 ml membrane blocking buffer for 30 minutes on a mini gyro-rocker SSM3 (Stuart, Stone, UK), at 24 revolutions per minute (RPM), and then incubated with primary antibody overnight at 4ºC on a See-saw rocker SS24 (Stuart, Stone, UK), at 24 RPM. The following day, the membrane was washed for 10 minutes three times in 0.05% PBS-T and incubated in secondary fluorochrome-conjugated (Li-cor Biosciences UK Ltd., Cambridge, UK) mouse or rabbit antibody (see Table 2.1) for 1 hour at room temperature on a mini gyro-rocker SSM3. The membrane was washed again three times for 10 minutes in PBS-T. Finally, blots were scanned using an infrared Li-cor Odyssey

Detection System. All antibodies were diluted in 50% PBS-T and 50% Li-Cor blocking buffer. All mouse antibodies were diluted 1:10,000 and rabbit antibodies 1:5,000.

Table 2.1. Antibodies used for western blotting.

Antibody	Source (Product code)	Primary Antibody	Species
β-ACTIN	Abcam (ab8227)	1:5,000	Rabbit
CtIP	Millipore (07-1010)	1:2,500	Rabbit
DNA-PK	Abcam (ab230)	1:2,000	Rabbit
γH2AX	Millipore (05-636)	1:2,000	Mouse
H3K9	Cell Signaling (9671)	1:1,000	Rabbit
H3K18	Cell Signaling (9675)	1:1,000	Rabbit
H3K23	Cell Signaling (9674)	1:1,000	Rabbit
Ku70	Abcam (ab314)	1:4,000	Mouse
Ku80	NeoMarkers (MS285-P1)	1:4,000	Mouse
MRE11	Abcam (ab30725)	1:5,000	Rabbit
NBS1	Abcam (ab398)	1:2,500	Rabbit
p53 (DO-12)	Mouse serum, obtained from Prof. Borivoj Vojtesek	1:50	Mouse
p53 (DO-1)	Santa Cruz Biotechnology (H2702)	1:2,000	Mouse
RAD50	Abcam (ab89)	1:2,000	Mouse
RAD51	Santa Cruz Biotechnology (sc-8349)	1:2,000	Rabbit

2.3.6 Cell cycle fluorescence-activated cell sorting (FACS) analysis

Cells were plated and treated with drug or an equivalent amount of DMSO and irradiated as required. Subsequently, cells were scraped using a cell scraper (Greiner Bio-one, Frickenhausen, Germany) in ice-cold PBSA and centrifuged in 15 ml polypropylene tubes in an Heraeus Labofuge 400 centrifuge (Labcare, Hamburg, Germany) at 1,300 rpm (200 g) for 3 minutes. The supernatant was discarded and the cell pellet resuspended in 250 µl of ice cold PBS. The pellet was constantly vortexed using a Vortex Mixer (Labnet International, Inc., Edison, NJ) and 5 ml of ice-cold 70% ethanol was added slowly to avoid cell clumping. Samples were then stored at -20°C, for at least 1h. Just prior to processing, samples were centrifuged in the Heraeus Labofuge 400 centrifuge at 1,300 rpm (200 g) for 3 minutes and the supernatant discarded and replaced with 700 µl of

propidium iodide and 250 µl RNaseA (as described in Materials). Samples were then incubated in a water bath at 37°C for 1 hour and vortexed immediately before running the samples. Stained cells were detected and the cell cycle distribution profiled using laser detection (FACScan or FACSort, Becton Dickinson, Oxford, UK). The results were analysed by model fitting using ModFit software (Verity Software House, Topsham, ME).

2.3.7 Immunofluorescence microscopy and analysis of γH2AX foci

Ionising radiation-induced γH2AX focus formation was used as a surrogate marker for DNA damage (Kuo & Yang, 2008). For the immunofluorescence experiments, 2.5 x 10^5 cells were plated onto sterile glass coverslips in 5 cm dishes in 3 ml medium, and the following day treated with panobinostat or DMSO for 24 hours. Then, cells were either fixed or irradiated with 5 Gy prior to fixation, at required timepoints. Cells were fixed by incubation in 1 ml 4% paraformaldehyde/0.1% Triton X-100 for 20 minutes at room temperature, followed by three PBS washes. Then cells were permeabilised by incubating in 1 ml 0.5% Triton/PBS for 15 minutes, followed by three further PBS washes. Cells were blocked for 30 minutes at room temperature in 5% bovine serum albumin (BSA). Mouse monoclonal anti-γH2AX antibody (05-636, Millipore, Billerica, MA) in 1 ml 5% BSA and 0.1% Triton were added and the cells incubated overnight at 4ºC.

The following day, the coverslips were washed three times in PBS for 10 minutes on a mini gyro-rocker SSM3, and the cells were incubated in secondary anti-mouse (Alexa 488, Invitrogen) antibody for 1 hour. Coverslips were rinsed with PBS three more times and once with distilled H_2O. Coverslips were mounted onto slides with Fluoromount G containing 0.1 µg/ml DAPI. The slides were left to dry overnight and finally scanned using a Zeiss LSM 780 confocal microscope. For each condition two slides were prepared independently and 70-100 cells counted per slide.

2.3.8 Real-time PCR

2.3.8.1 RNA extraction

For real-time PCR (qPCR), 7.5 x 10^5 RT112, 9.0 x 10^5 CAL29, 8.0 x 10^5 T24 or 1.0 x 10^6 NHU cells were plated in 10 cm dishes in 10 ml medium and the following day treated with DMSO or panobinostat for 24 hours. Cells were then trypsinised, spun down and the pellets collected for RNA extraction using the RNAeasy mini kit. Alternatively, in the case of the *MRE11/RAD50/NBS1* and *TP53* transcription experiments, cells were also irradiated at 5 Gy, the medium changed and cells collected 4 hours later, followed by the RNA extraction step. Briefly, cells were lysed using the kit's buffer and the lysate passed through a 21G needle five times, using a 5 ml BD Plastipak syringe. Next, one volume of 70% ethanol was added to the sample and mixed by pipetting. The entire sample was loaded into a column and centrifuged and washed several times using the required buffers as per manufacturer's instructions. Lastly, 30 µl RNase-free distilled water was added, and spun down into a clean 1.5 ml microcentrifuge tube, to elute the RNA. The concentration of RNA was determined using a Nanodrop, by loading 1 µl of RNA sample and the concentration automatically determined. For determining RNA purity, the measurements of absorbance at 260 nm and 280 nm and the ratio between them (260/280) was used and the ratio of 2.0-2.1 regarded as pure RNA.

2.3.8.2 cDNA preparation

cDNA was prepared from 3 µg or 5 µg RNA (see details below), using a High Capacity cDNA reverse transcription kit (Applied Biosystems, Foster City, CA) as per manufacturer's instructions (see Table 2.2). The RNA made up to a total volume of 10 µl with RNase-free distilled water. The final reaction volume was 20 µl.

Table 2.2. cDNA preparation components per reaction.

Component	Volume
10x RT buffer	2.0 µl
25x dNTP (100 mM)	0.8 µl
Oligo random primers	1.0 µl
RT enzyme (MultiScribe™ Reverse transcriptase, 50 U/µL)	1.0 µl
RNase-free distilled water	4.2 µl

In the case of ∆133p53 variant detection, cDNA was prepared as per protocol from 5 µg RNA, but instead of Oligo random primers, 1 µl of RE11 and 1 µl ATP5B reverse primers were used and 3.2 µl of RNase-free distilled water.

The following conditions were used to make the cDNA:
10 min at 25°C, 120 min at 37°C, 5 min at 85°C, then 4°C hold. The cDNA was either used immediately or stored at -20°C.

For the qPCR experiments, a mastermix consisting of SybrGreen PCR Mastermix (Applied Biosystems, Paisley, UK), primers (see Tables 2.4 and 2.5) and RNase-free distilled water was made up (Table 2.3):

Table 2.3. qPCR experiment components.

Component	Volume
2X SybrGreen	10.0 µl
RNase-free distilled water	7.8 µl
Forward primers (100 µM stock)	0.1 µl
Reverse primers (100 µM stock)	0.1 µl

Then 18 µl of the mastermix was added to wells in a 96-well MicroAmp Reaction plate (Applied Biosystems, Warrington, UK). cDNA to be used in the experiment was then diluted in RNAse free distilled water, 1:10, and 2 µl were added to the wells. Diluted RNA was stored at -20°C.

Samples were run on a 7500 Fast Real-time qPCR system (Applied Biosystems, Warrington, UK) with the following conditions: 20 s at 50°C, followed by 10 min at 95°C, then 40 cycles of 1 min at 60°C, 15 s at 95°C, 1 min at 60°C, 1 min at 95°C.

Forward and reverse primers are shown in Tables 2.4 and 2.5.

Table 2.4. qPCR primers for *HDAC* expression.

Analysed *HDAC*	Forward primer	Reverse primer
1	AGACAGCTGTGGCCCTGGATAC	CGGCAGCATTCTAAGGTTCTCAA
2	TGCAGTTGCCCTTGATTGTGA	ATCTGGACACCAGGTGCATGAG
3	AGAGTGGCCGCTACTACTGTCTGAA	TGGGTTGGTAGAAGTCCACTACCTG
4	GAGCAGGAGCTGGAGAAG	AATGCAGTGGTTCAGATTCC
5	GTGTCTCGGCTCTGCTCAGTGTAG	TTTGCTGCAAGACTGCCTCATC
6	GTCTACTGTGGTCGTTACATC	GGCCTGACAGTAGTAACAC
7	CGGGTGCACAGTAAATAC	CCAGAGCCTTAGAGATTCATA
8	TGACGGAATGTGCAAAGTAGCAA	TCAAATTTCCGTCGCAATCGTA
9	AAGTAGAGAGGCATCGCAGAGA	TTCGTTGCTGATTTACTCAGTAGG
10	ATGACCCCAGCGTCCTTTACT	CGCAGGAAAGGCCAGAAG
11	CCCCTTGGTCATGGGATTT	CATCCACACCAGTGCCTATAGC

The HDAC intron-spanning primer sequences used were previously described in the literature. Sequences *for HDAC1-8* primers were taken from Kawabata *et al* (2010), HDAC9 primer sequence from Niegisch *et al* (2012) and *HDAC10* and *11* from Duong *et al* (2008).

Table 2.5. Primers used in qPCR experiments.

Analysed gene	Forward primer	Reverse primer
MRE11	GAGGAGGTACGTCGTTTCA	TGGTCATAGCCTCACGGACT
NBS1	TCCATCTGGCATAAATGATGA	GTGGAAGTTTTCCTGCTCCA
RAD50	GAGATTTCCCTCCTGGAACC	ACATCACGAAATTGCAGACG
GAPDH	ACAGTCAGCCGCATCTTCTT	AATGAAGGGGTCATTGATG
RAD51	TGAGGGTACCTTTAGGCCAGA	CACTGCCAGAGAGACCATACC
CtIP	TGAGGGAACAGCAGAAAGTC	TCTGCTGGAGTTGTTCAGAA
TP53	AGGCCTTGGAACTCAAGGAT	CCCTTTTTGGACTTCAGGTG

Intron-spanning primer sequences for *MRE11, NBS1, RAD50* and *GAPDH* were designed by Dr. Rebecca Martin (Gray Institute for Radiation Oncology and Biology, University of Oxford).

Intron spanning primers for *RAD51, CtIP, E2F1* and *TP53* were designed using Roche Applied Science website (http://www.roche-applied-science.com/shop/CategoryDisplay?catalogId=10001&tab=Assay+Design+Center&identifier=Universal+Probe+Library&langId=-1).

See Appendix B for the melting temperature profile of all the primers and qPCR amplification plots.

2.3.9 qPCR data analysis

The qPCR data analysis was performed as described in Livak and Schmittgne (2001). For the analyses of the genes of interest, the C_T (threshold cycle) values were subtracted from the C_T values of the *GAPDH* housekeeping gene (normaliser and calibrator), according to the following formula:

$$\Delta\Delta Ct = \Delta Ct_{calibrator}(Ct_{calibrator} - Ct_{normaliser}) - \Delta Ct_{sample\ of\ interest}(Ct_{sample} - Ct_{normaliser})$$

And the values calculated according the following formula:

$$\text{Relative quantity to calibrator} = 2^{-\Delta\Delta Ct}$$

Further, the relative comparison between the untreated or treated (panobinostat and/or irradiation) were made and compared to the untreated sample (set as 1) or in the case of *HDAC1-11* gene expressions, the relative values were compared to the NHU untreated sample.

2.3.10 Reverse-transcriptase PCR for TP53 variants

For the reverse-transcriptase (RT) PCR reaction, the Crimson Taq Polymerase (5000 U/ml, New England BioLabs, Hitchin, UK) and 5 x Crimson Taq Reaction buffer were used (New England BioLabs, Hitchin, UK) in the reaction, see Table 2.6.

Table 2.6. cDNA preparation components per reaction.

Component	Volume
Forward primer	0.5 µl (from 100 µM stock)
Reverse primer	0.5 µl (from 100 µM stock)
5 x Taq Buffer	4.0 µl
Crimson Taq Polymerase	0.5 µl
DMSO	2.0 µl
RNase-free distilled water	9.5 µl
cDNA	1.0 µl

In the first round of RT-PCR, primers 4b and RE11 were used with the following conditions: 95°C 5 min, then 35 cycles of 95°C 15 s, 55°C 30 s and 72°C 1 min, then 72°C for 7 min and 4°C hold. A similar reaction was also set up with the ATP5B forward and ATP5B reverse primers, to serve as a reaction loading control.

The template was then used for a nested RT-PCR reaction using primers 4b2 and Alpha (for ∆133p53alpha), 4b2 and Beta (for ∆133p53beta) and 4b2 and Gamma (for ∆133p53gamma) (see Table 2.7): with 95°C 5 min, then 25 cycles of 95°C 15 s, 55°C 30 s and 72°C 1 min; then 72°C 7 min and 4°C hold.

Table 2.7. PCR primers used for ∆133p53 variant detection.

Primer name	Primer sequence
ATPB forward	ACCATCAAAGGATTCCAGCA
ATPB reverse	GCTTTTGCCACAGCTTCTTC
RE11	AATGTCAGTCTGAGTCAGGCCCTTCTG
4b	TAGACGCCAACTCTCTCTAG
4b2	TGGGTTGCAGGAGGTGCTTACAC
Alpha	CTCACGCCCACGGATCTGA
Beta	TTGAAAGCTGGTCTGGTCCTGA
Gamma	TCGTAAGTCAAGTAGCATCTGAAGG

All the primer sequences were from Bourdon *et al* (2005). *ATP5B* forward and reverse primers were designed by Dr. Rebecca Martin.

2.3.11 Gel Electrophoresis

The RT-PCR products were run on a 1% agarose gel. The gel was made from 1.8 g agarose and 180 ml 1 X TBE buffer. After heating until the agarose was totally dissolved, 5 µl of GelRed Nucleic Acid Stain was added. The gel was then poured into a mould and a 20 lane comb positioned appropriately. After 30 minutes, the solidified gel was placed in a gel electrophoresis tank, which was filled with 1 X TBE buffer and 20 µl of the PCR reaction loaded into the wells. On each side a DNA 1kb HyperLadder was used. The samples were run at 100V for 60 minutes and the bands visualised using a Molecular Imager FX ProPlus (Bio-Rad Laboratories, Hemel Hempstead, UK).

2.4 Statistics and data analysis

All statistical analyses were performed using GraphPad Prism 6.0 Software (La Jolla, CA). The results were presented as the mean with error bars representing the standard error of the mean (SEM). For the comparison of cell survival curves, a two-way ANOVA with Bonferroni's multiple comparison tests was used. For the comparison of more than two samples, a one-way ANOVA test with Bonferroni correction was used. For comparison of two samples, a Student's two-tailed, unpaired t-test was used. A p-value of 0.05 or less was regarded as statistically significant.

2.4.1 Clonogenic assay

Clonogenic assays were performed in triplicate, three times. The sensitisation enhancement ratio (SER) was used to compare two cell survival fractions at 10% survival (SER_{10}). The plating efficiency (PE) for each cell line was determined as described in Franken *et al* (2006): The table of plating efficiencies for cell lines used in this thesis can be seen in Table A.2 (in Thesis Apendix A).

PE = (No. of colonies formed/No. of cells seeded) x 100%

and the number of treated cells expressed in terms of PE, called cell surviving fraction (SF), was determined as:

SF = No. of colonies formed after treatment/(No. of cells seeded x PE)

The table of plating efficiencies for cell lines used in this thesis can be seen in Table A.2 (Apendix A).

The graphs for the clonogenic survival assays were drawn using GraphPad Prism, using the linear quadratic (LQ) model to plot the curves. The model was described by Douglas

and Fowler (1976), where the yield (Y) of lethal lesions is the sum of lethal lesions produced from a single radiation track (which are linearly related to dose, αD) and lethal lesions produced from two radiation tracks (which are quadratically related to dose, βD^2):

$$Y = \alpha D + \beta D^2$$

Lethal lesions follow Poisson distribution from cell to cell and the surviving fraction (SF) is:

$$SF = \exp -(Y)$$

This leads to the standardized LQ equation:

$$SF = \exp -(\alpha D + \beta D^2)$$

Note: when discussing the pharmacology of a drug, the effect is generally measured as EC_{50} for a 50% stimulatory effect and IC_{50} for a 50% inhibitory effect. Here, the readout for panobinostat effect is clonogenic survival, therefore the IC_{50} and the SF_{50} are synonomous, but inversely related for all other measurements, i.e. IC_{10} is equivalent to SF_{90}. For clarity, in reference to drug effect the terms IC_{50} and IC_{10} were chosen, as opposed to effects of IR, which are measured as surviving fraction (SF).

2.4.2 Combination index analysis of radiosensitisers

The concept of synergy versus additivity was tested in RT112 cells, using the Chou-Talalay method, as described in Chou *et al* (2010). Briefly, the described theorem offers a method for determining if the effect of drug combinations was additive - the combination index (CI) = 1. If the combination is synergistic, then the index is less than 1 (CI < 1), and in case of antagonism the index is greater than 1 (CI > 1).

First, the ratio (Sfb) between the plating efficiency of treated and untreated was calculated:

1. Sfb = PE of treated/PE control
2. Plot survival fraction of untreated cells (Sfa)
3. Plot survival fraction of treated cells (Sfab)

4. Multiply Sfa and Sfb (= Sfa x Sfb)
5. Compare (Sfa x Sfb and Sfab)
6. Sfab = Sfa x Sfb then additive
7. Sfab > Sfa x Sfb then sub-additive
8. Sfab < Sfa x Sfb then supra-additive

2.4.3 Western blot analysis

Western blotting for each experiment was done at least twice. Blots were scanned using the LiCor scanner, with the linear range pixel count.

CHAPTER 3: RADIOSENSITISING EFFECTS OF PANOBINOSTAT

3.1 Introduction

Combining chemotherapy and radiotherapy, compared to using radiotherapy alone, can improve locoregional control, progression-free and also overall survival in many different tumour types (Harrington *et al*, 2011). The median age of bladder cancer patients at diagnosis is 68 years (Gallagher and Milowsky, 2009), and the average age of patients with muscle invasive bladder cancer (MIBC) receiving combination radiotherapy is higher and is increasing (Kotwal *et al*, 2008). Older patients are less able to tolerate chemoradiation due to their impaired physical fitness and generally poor renal function (Dash *et al*, 2006; Nicholson, 2012). Therefore, there is an urgent clinical need to find novel and less toxic therapeutics to be combined with radiotherapy, for use in the elderly.

Histone deacetylase (HDAC) inhibitors are emerging anti-cancer agents, already tested in many preclinical and also clinical studies as single therapeutics or in combination with other agents. In preclinical studies they have been reported as showing low cytotoxicity towards non-cancer cells and also to be good radiosensitisers in cell lines, including prostate and non-small cell lung carcinoma (Zhang *et al*, 2007; Kachhap *et al*, 2010; Konsoula *et al*, 2011) and some others, as reviewed in Groselj *et al* (2013).

The HDAC inhibitor panobinostat emerged in several preclinical studies as very potent, with similar promising reports from some early phase clinical trials. Previous studies have shown panobinostat to be working in a low nanomolar range across a broad range of malignancies. These include lymphoblastic leukaemia (Scuto *et al*, 2008) and lymphoma cells (Hasegawa *et al*, 2011). In small cell and non-small cell lung carcinoma and mesothelioma cells, the cytotoxicity IC_{50} range was from 4-470 nM (median 20 nM) (Crisanti *et al*, 2009), with similar results in another lung cancer study (Edwards *et al*, 2007). Panobinostat demonstrated efficacy in colon carcinoma (Wilson *et al*, 2013),

hepatocellular carcinoma (Lachenmayer *et al*, 2012), renal cancer cells (Cha *et al*, 2009), ovarian cancer (Budman *et al*, 2011), triple-negative breast cancer cells (Tate *et al*, 2012) and anaplastic thyroid carcinoma (Catalano *et al*, 2012).

The expression of HDACs can be aberrantly overexpressed in a broad panel of cancers. This can be associated with poor patient prognosis or contribute to the pathogenesis of the disease (Barneda-Zahonero & Parra, 2012). Class I HDACs have been reported to be aberrantly overexpressed compared to normal tissue in studies of bladder cancer (Junqueira-Neto *et al*, 2013). Niegisch *et al* (2012), have reported on upregulated protein levels of HDAC2 and HDAC8. Ozawa *et al* (2010), have reported that HDAC1 mRNA and protein levels in bladder cancer tissue was significantly higher than in the surrounding normal tissue. Therefore, UC would seem to be a good target for HDAC inhibition.

HDAC inhibitors have so far only been used as single agents in bladder cancer, reviewed in Sharma *et al* (2013). The aim of this study therefore was to test panobinostat as a potential radiosensitiser in bladder cancer cells, at low, non-toxic doses causing less than 50% cell kill, to mimic clinically achievable doses for panobinostat. This has not yet been reported in bladder cancer cells using any HDAC inhibitor.

Acetylation of various histone H3 and H4 lysine residues is a very robust marker of the activity of HDAC inhibitors. For example, in lymphoblastic leukaemia cells, induction of acetylation of H3K9 and H4K8 was detected 24 h post panobinostat treatment (Scuto *et al*, 2008). Moreover, in panobinostat treated T-cell lymphoma patients, hyperacetylation of H3 was detected 4 h post treatment in collected mononuclear cells (Scuto *et al*, 2008).

Only a fraction of cells will survive treatment with the combination of cytotoxic agents and ionising radiation, or either as a single therapy. The gold standard for testing cytotoxicity of treatments is the clonogenic assay, which was used in the experiments in this thesis. Each cell treated is tested for its ability to proliferate further (Franken *et al*, 2006) and to divide at least five more times to form a colony of at least 50 cells. There are several other

options to measure the cytotoxicity of treatments, such as assays measuring the cell's metabolic cell activity e.g. MTT and MTS assays, but with the disadvantage that unlike the clonogenic assay, they detect both cell killing and cytostatic effects (Munshi *et al*, 2005a; Franken *et al*, 2006; Sumantran, 2011). Also, while the endpoint in the clonogenic assay is cell survival at 14 days, the other metabolic assays measure mitochondrial activity. This fact is especially important in radiation-treated cells, when cells are not killed immediately and can keep dividing (with active mitochondrial activity for several days), so the results of the other assays may not be as robust as those for the clonogenic assay.

In this chapter, panobinostat's cytostatic effects were examined in three bladder cancer cell lines and the ability of panobinostat to acetylate histone H3 lysine residues 9, 18 and 23 tested, to determine the rate at which elevated histone acetylation can be detected and also the dynamics of histone acetylation over time. Two different incubation schedules were tested to assess their radiosensitising effects. Since panobinostat is a pan-HDAC inhibitor, the class I specific compound, mocetinostat was also used, to determine if any of panobinostat's radiosensitising effects could be attributed to the specific class of HDACs. Due to the importance of p53 and the high rate of *TP53* mutations seen in bladder cancer, the effect of panobinostat on p53 protein levels and transcription of the gene were also assessed.

3.2 Results

3.2.1 Cytotoxicity of panobinostat

First, the cytotoxicity of panobinostat in bladder cancer cell lines was determined using the clonogenic assay. Three bladder cancer cell lines, RT112, CAL29 and T24, were studied. Seven hundred RT112, 3,000 CAL29 and 600 T24 cells were plated into 10 cm dishes in duplicate and treated with different doses of panobinostat for 24 hours. The following day, the medium was removed and the dishes washed twice with sterile phosphate-buffered saline (PBS). Next, 10 ml of fresh media were added and the dishes incubated for 14 days in the incubator at 37°C, 5% CO_2. Dishes were then collected, stained and counted as per protocol. According to the literature panobinostat was expected to work in the nanomolar range and so dishes were treated at doses of up to 200 nM. The half maximal inhibitory concentration (IC_{50}) values for 24 hour panobinostat incubation were 27 nM in RT112 cells; 11 nM in CAL29 and 40 nM in T24 cells (Figure 3.1).

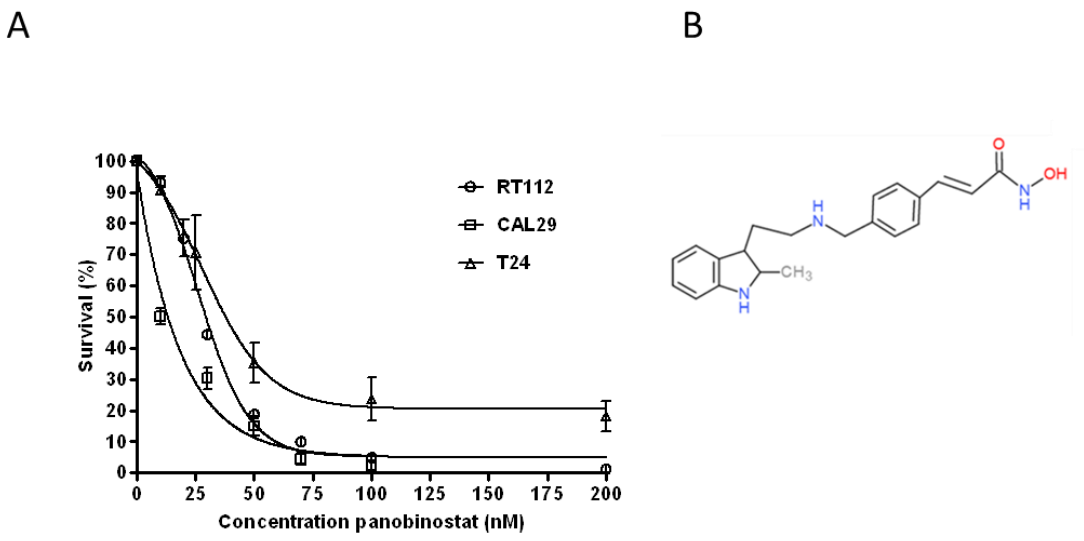


Figure 3.1. Evaluation of panobinostat's cytotoxicity in bladder cancer cell lines. A) RT112, CAL29 and T24 cells were treated with the increasing panobinostat (PAN) doses for 24 h. Cells were washed twice with PBS and fresh medium added for 14 days' incubation before counting. Each point represents the mean ± standard error of the mean (SEM) of at least three experiments. B) Chemical structure of panobinostat.

3.2.2 Panobinostat causes acetylation of histone H3 lysine residues

Since the acetylation of histone lysine residues is one of the most obvious effects of HDAC inhibitors, the goal in these experiments was to determine the incubation time required for histone H3 lysine acetylation and also whether the acetylation levels change over time. Incubation times from 30 minutes to 24 hour were assessed.
Acetylation of the H3 residues K9, K18 and K23 was determined in RT112 cells after treatment with 25 nM panobinostat, the concentration representing the IC_{40} dose. RT112 cells were treated for 0.5, 1, 2, 3, 4 and 5 hours (Figure 3.2A). In the next experiment, the dynamics of histone H3, K9 and K23 acetylation was tested from 20 to 24 hours for H3 K9 (Figure 3.2B) and 23 and 24 h for H3 K23 (Figure 3.2C).

Acetylation of all the tested histone residues was clearly upregulated after only 30 minutes post-incubation with panobinostat, and levels increased at 1 hour but then did not change over longer incubation timepoints (from 2 to 5 hour panobinostat treatment, Figure 3.2A). To determine if acetylation of H3 K9 changes following much longer exposure to panobinostat, cells were treated for 20-24 hours (Figure 3.2B), and levels of acetylation did not change over time and were comparable to the levels of the same lysine residue seen at shorter incubation times. Results were similar for the H3 K23 lysine residue at 23 and 24 h incubation times (Figure 3.2C).

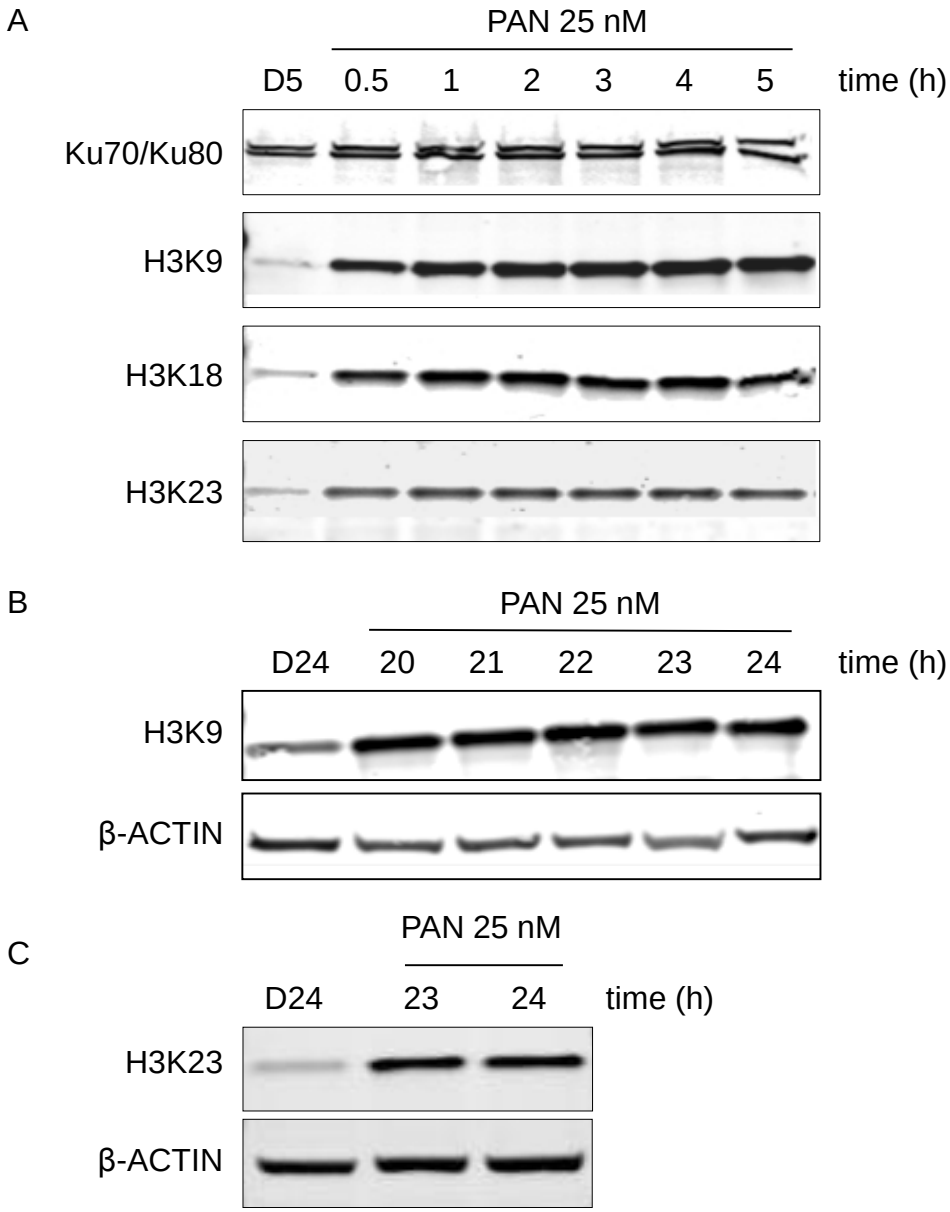


Figure 3.2. Acetylation of histone H3 lysine residues post-panobinostat treatment. A) RT112 cells were treated with 25 nM panobinostat (PAN) for 0.5, 1, 2, 3, 4 and 5 hours and a DMSO (D) treated control was also treated for 5 hours. Western blots were tested for acetylation of histone H3 lysine (K9, K18 and K23). B) RT112 cells were treated with 25 nM panobinostat for 20 to 24 hours and DMSO for 24 h (D24) with western blotting for acetylation of the H3 K9 residue, and C) acetylation of H3 K23, tested over 23 and 24 hours.

3.2.3 Panobinostat incubation time and radiosensitising effects

Panobinostat was shown to quickly acetylate histone lysine residues and therefore a set of radiosensitising clonogenic assays was performed in RT112 cells to determine whether, after 1 hour panobinostat incubation, radiosensitising effects could be detected. RT112 cells were plated in 10 cm dishes and the following day treated with DMSO (mock), 10 nM (IC_{10}), 25 nM (IC_{40}) and 50 nM (IC_{80}) panobinostat for 1 h, after which cells were trypsinised and plated in 10 cm dishes and irradiated from 0 to 8 Gy. They were then incubated at 37°C, 5% CO_2 and harvested after 14 days.

As seen in Figure 3.3, using this protocol no radiosensitisation was detected, not even at the highest, highly cytotoxic dose of 50 nM (IC_{80}).

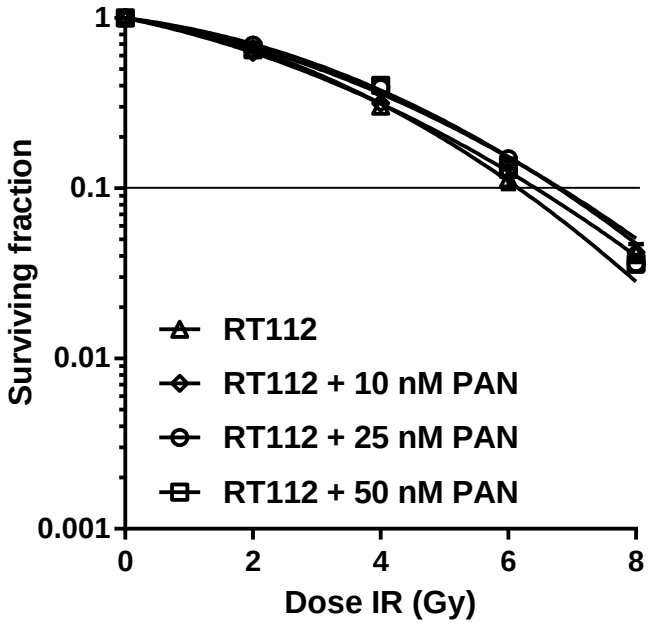
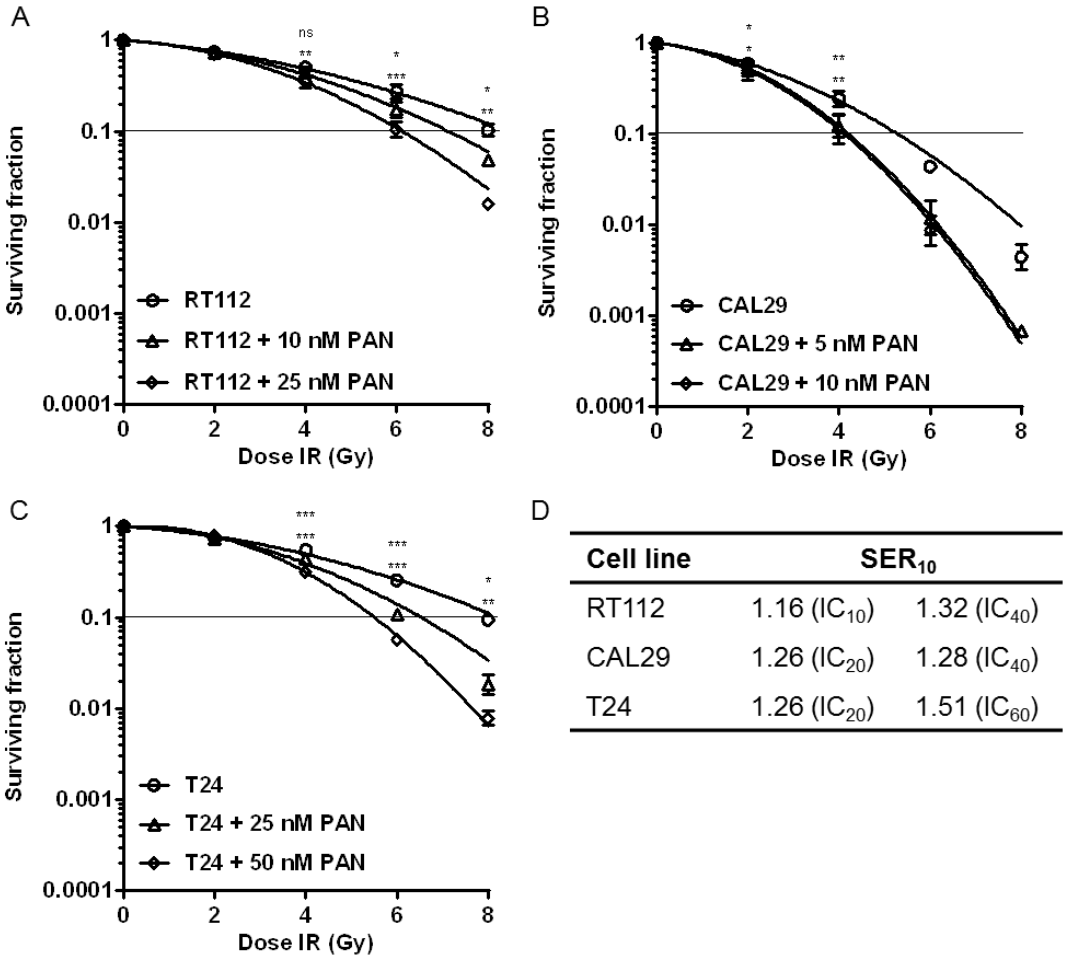


Figure 3.3. Radiosensitisation clonogenic assay following 1 hour panobinostat treatment.
RT112 cells were treated with DMSO, 10, 25 and 50 nM PAN for 1 hour. Dishes were then trypsinised, and cells plated, irradiated and harvested after 14 days. Each point represents the mean ± standard error (SEM) of three experiments. The line represents 10% cell survival.

Therefore a longer panobinostat incubation was tested, with the next clonogenic assays performed 24 h post-panobinostat incubation with the same experimental protocol. RT112 were treated at doses of 10 nM and 25 nM PAN (IC_{10} and IC_{40} respectively) (Figure 3.4A);

5 nM and 10 nM were used in CAL29 (IC_{10} and IC_{40}) (Figure 3.4B); and 25 nM and 50 nM in T24 (IC_{30} and IC_{60}) (Figure 3.4C). Panobinostat proved to be an efficient radiosensitiser in three different bladder cancer cells. The sensitiser enhancement ratio (SER) at 10% cell survival (horizontal lines in Figure 3.4A-C) was used to detect differences between DMSO and panobinostat-treated cells. The SERs for RT112 were 1.16 (10 nM) and 1.32 (for 25 nM) (P=0.05 and P=0.01 respectively). The combination index analysis of radiosensitisers showed, that for both 10 nM and 24 nM panobinostat treatments, effects were synergistic with IR doses of 4 Gy upwards. The SERs for CAL29 were 1.26 and 1.28; T24 were also radiosensitised, with SER's of 1.26 and 1.51 respectively (Figure 3.4D).



D

Cell line	SER_{10}	
RT112	1.16 (IC_{10})	1.32 (IC_{40})
CAL29	1.26 (IC_{20})	1.28 (IC_{40})
T24	1.26 (IC_{20})	1.51 (IC_{60})

E

Cell line	Mean	95% CI	Mean	95% CI	Mean	95% CI
RT112	DMSO		10 nM PAN		25 nM PAN	
	8.0	7.4 - 9.5	7.1	6.4 - 7.9	6.2	5.6 - 6.8
CAL29	DMSO		5 nM PAN		10 nM PAN	
	5.4	4.7 - 6.0	4.1	3.4 - 5.0	4.1	3.2 - 5.1
T24	DMSO		25 nM PAN		50 nM PAN	
	8.2	7.4 - 9.1	6.5	5.9 - 6.8	5.5	5.4 - 5.5

Figure 3.4. Panobinostat radiosensitises bladder cancer cells following 24 hour treatment.
In all the cell lines the same experimental protocol was used: cells were treated for 24h, trypsinised, replated and irradiated in a dose range from 2 to 8 Gy. Dishes were left for 14 days, stained and counted. A) RT112 cells, B) CAL29 and C) T24 cells were treated with DMSO or different doses of panobinostat (PAN). D) Sensitisation enhancement ratios (SER) at 10% survival (line). E) The mean Gy for 0.1 cell surviving fraction (SF) with Confidence intervals (CI) were also calculated for all the three cell lines. Each point represents the mean ± SEM of at least three experiments. Two-way ANOVA, Bonferroni's multiple comparisons test over DMSO control; * $p < 0.05$, ** $p < 0.01$, *** $p < 0.001$; upper row low drug dose, lower row high drug dose. Note that in panel B, 6 Gy and 8 Gy results were not significant.

3.2.4 HDAC-specific class effects on chemosensitisation

Panobinostat is a pan-HDAC inhibitor, acting on all the HDACs. To determine, if panobinostat's radiosensitising effects can be attributed to actions on class I or class II HDAC's, mocetinostat, a class I-specific HDAC inhibitor was used. RT112, CAL29 and T24 cells were incubated in mocetinostat for 24 hours before washing and standard clonogenic incubation, staining and counting. The IC_{50} values for mocetinostat were 1.6 μM in RT112 and 0.75 μM in CAL29; and 1.7 μM in T24 (Figure 3.5), suggesting that either this drug has much lower potency than panobinostat, or that class II inhibition is also required in order to achieve higher cytotoxicity (discussed later). The class II-specific HDAC inhibitor MC1568 was also used in similar experiments, but due to problems with drug solubility in cell culture medium, this approach was abandoned (data not shown).

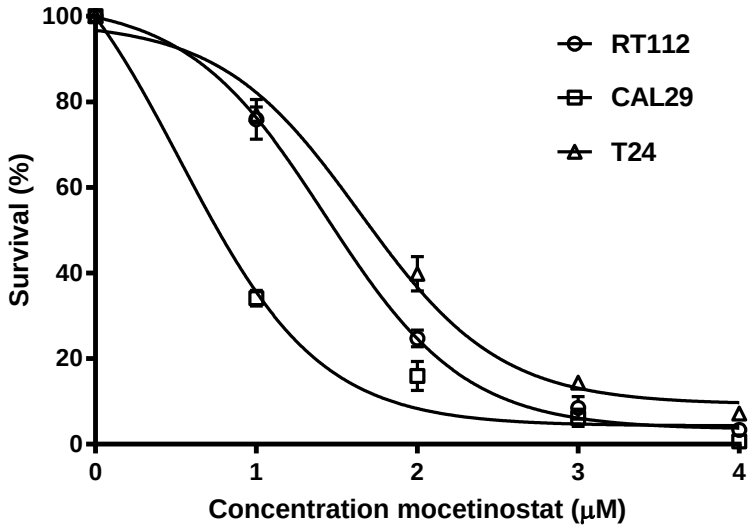
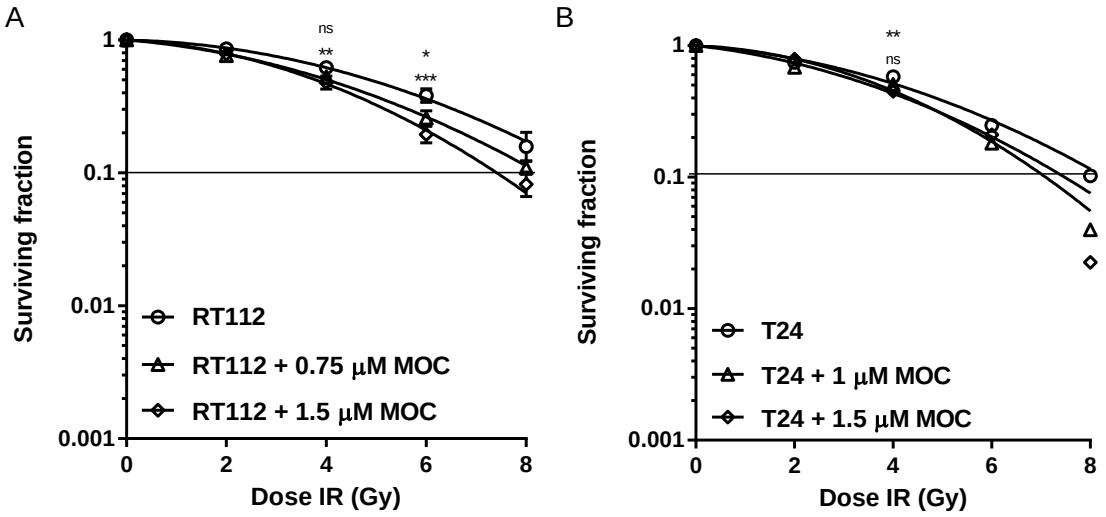


Figure 3.5. Evaluation of mocetinostat's cytotoxicity in bladder cancer cell lines. RT112, CAL29 and T24 cells were treated with the increasing mocetinostat doses for 24 h. Each point represents the mean ± SEM of at least three experiments.

3.2.5 HDAC-specific class effects on radiosensitisation

Once the cytotoxicity of mocetinostat had been established, clonogenic assays were performed in RT112 and T24 cell lines, to test mocetinostat for potential radiosensitising effects. These experiments were also crucial to test whether bladder cancer cells could be efficiently radiosensitised using an HDAC class I–specific agent, to elucidate the role of class I HDACs in cell radiosensitisation. The IC_{20} and IC_{40} doses were used (namely, 0.75 μM and 1.5 μM in RT112; and 1.0 μM and 1.5 μM in T24 cells).

Both cell lines were radiosensitised, although to a lesser degree than that seen in panobinostat-treated cells. The SERs at 10% survival for mocetinostat in RT112 cells were 1.11 (0.75 μM) and 1.24 (1.5 μM). In the case of T24 cells, the SERs were 1.12 (1.0 μM) and 1.17 (1.5 μM) (Figure 3.6).



C

Cell line	SER_{10}	
	IC_{20}	IC_{40}
RT112	1.11	1.24
T24	1.12	1.17

Figure 3.6. Mocetinostat only mildly radiosensitises bladder cancer cells.
RT112 (A) and T24 cells (B) were treated for 24 h with mocetinostat, trypsinised, replated and irradiated in a dose range from 2 to 8 Gy before standard clonogenic assay processing. Each point represents the mean ± SEM of at least three experiments. Sensitisation enhancement ratios at 10% survival are stated in (C). The horizontal lines represent cell survival at 10%. Two-way ANOVA, Bonferroni's multiple comparisons test over DMSO control; * $p < 0.05$, ** $p < 0.01$, *** $p < 0.001$; upper row low drug dose, lower row high drug dose.

3.2.6 Cell cycle effects on RT112 cells

The cell cycle phase is an important determinant of cellular radiosensitivity. Cells in G2/M phase are the most sensitive, those in G1 less so and S-phase cells are the least sensitive (Pawlik & Keyomarsi, 2004). Here, the hypothesis that panobinostat's radiosensitisation of bladder cancer cells could be attributed to the cell accumulation in G2/M phase was tested. RT112 cells were treated for 24 hours at doses up to 100 nM and the cell cycle distribution determined by the FACS analysis.

Panobinostat caused borderline significant accumulation of cells in G2/M at doses of IC_{50} and higher (Figure 3.7A). Quantification of this analysis is represented in the Figure 3.7B. Since the radiosensitising effects of panobinostat are detected at lower doses, which do not affect cell cycle distribution, panobinostat's radiosensitising effects at low doses are unlikely to be determined by its effects on the cell cycle.

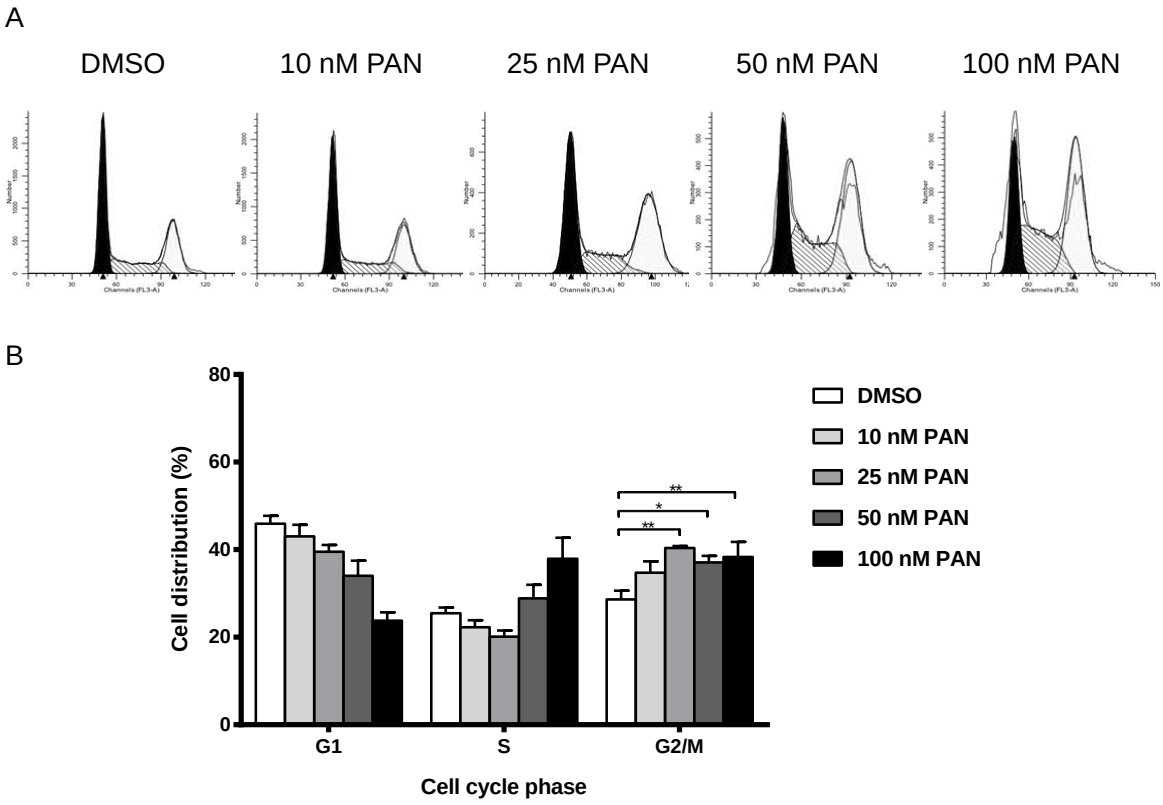


Figure 3.7. Cell cycle effects of panobinostat in RT112 cells.
Cells were treated with panobinostat (PAN) for 24 hours, dishes scraped and cells incubated in ice-cold 70% ethanol and prepared for FACS analysis. A) FACS cell cycle traces and B) quantification. Mean ± SEM of at least three experiments are presented. One-way ANOVA, Bonferroni's multiple comparisons test over DMSO control; * $p < 0.05$, ** $p < 0.01$, *** $p < 0.001$.

To further test the cell cycle distribution post-IR, RT112 cells were treated with 25 nM panobinostat (or DMSO) and harvested, or they were irradiated with 5 Gy, the dishes washed twice with PBS, fresh medium added and samples collected 4, 8 or 24 hours later.

Accumulation of cells in G2/M was observed after irradiation in either panobinostat or DMSO treated samples (Figure 3.8). The differences between 8 h post-IR and control, either DMSO or 25 nM panobinostat, were statistically significant (see Figure 3.8). There were no differences for DMSO control versus panobinostat among all timepoints.

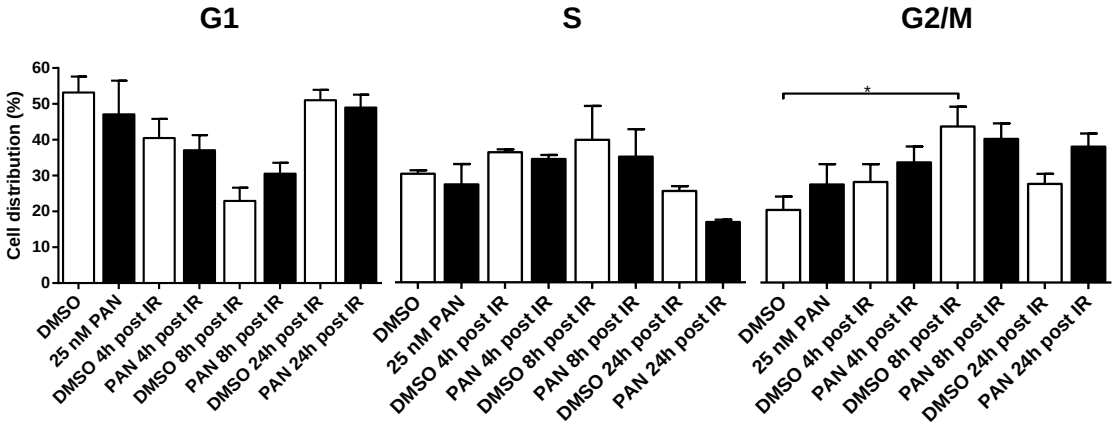


Figure 3.8. Cell cycle effects of panobinostat and irradiation in RT112 cells. RT112 cells were treated with 25 nM panobinostat (PAN) for 24 hours then dishes scraped and cells incubated in ice-cold 70% ethanol and prepared for FACS analysis. Alternatively, cells were irradiated with 5 Gy, dishes washed twice with PBS, medium changed and cell samples harvested 4, 8 or 24 hours later for FACS cell cycle analysis. Mean ± SEM of at least three experiments are presented. One-way ANOVA, Bonferroni's multiple comparisons test over DMSO control; * $p < 0.05$, ** $p < 0.01$, *** $p < 0.001$.

3.2.7 Effects of panobinostat on TP53

Due to the importance of p53 protein status for therapy outcome (see Introduction), the effects of panobinostat on p53 protein expression in *TP53* wild type (RT112) and two *TP53* mutant cell lines (CAL29 and T24) were examined. Cell lysates from RT112, CAL29 and T24 cells were subjected to western blotting for p53 at increasing concentrations of panobinostat (Figure 3.9).

In the first experiment, RT112 cells were plated, treated with panobinostat or DMSO for 24 h and cell pellets harvested or irradiated with 5 Gy, medium changed and cells harvested at 1, 2 or 4 h post-IR (treated with 50 nM panobinostat), or harvested 8 h or 24 h post-IR (treated with 10 nM, 25 nM or 50 nM panobinostat) (Figure 3.9A). In the DMSO-treated samples, upregulation of p53 protein levels are seen in all the timepoints up to 4 h, but

panobinostat attenuated the upregulation of p53 seen at the 1, 2 and 4 hour timepoints. Attenuated upregulation in panobinostat-treated samples is also evident at 8 h and 24 h in samples treated with 25 nM and 50 nM panobinostat.

To test panobinostat's effects in *TP53* mutant cell lines, CAL29 cells were treated with DMSO or 5 nM and 10 nM panobinostat (Figure 3.9B), and T24 cells (Figure 3.9C) with DMSO, 10 nM and 25 nM panobinostat for 24 h and collected, or irradiated with 5 Gy, medium changed and cell pellets harvested 4 h or 8 h later. In both cell lines, panobinostat caused a dose-dependent downregulation of p53 protein expression and in CAL29 irradiated samples panobinostat abrogated the p53 upregulation seen in control cells.

These results indicated that the *TP53* cell status does not alter the downregulation of p53 caused by panobinostat.

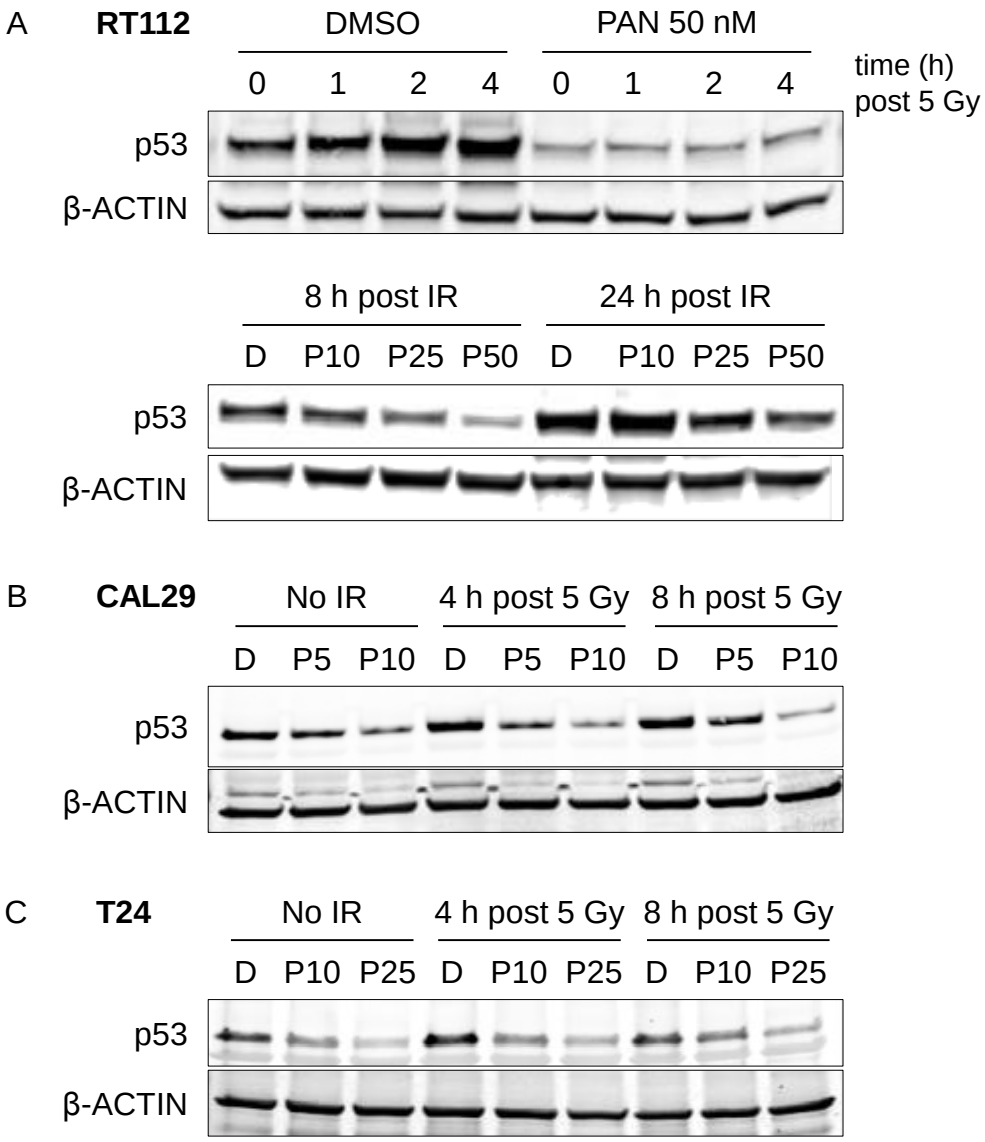


Figure 3.9. Panobinostat downregulates levels of p53 protein in a dose-dependent manner.
Western blots of cells treated with DMSO (D) or 5 nM, 10 nM, 25 nM or 50 nM panobinostat (P or PAN) for 24 h. Dishes were then harvested or irradiated with 5 Gy, medium changed and cell pellets harvested at timepoints indicated. A) RT112 B) CAL29 and C) T24 bladder cancer cell lines.

3.2.8 Transcription of TP53 after panobinostat treatment

As panobinostat caused a decrease in p53 protein levels, effects on *TP53* transcription were also studied in order to determine if panobinostat was influencing this directly. RT112 and CAL29 cells were treated with DMSO or panobinostat for 24 h, at doses of 10 nM or 25 nM panobinostat for RT112 cells and 5 nM and 10 nM panobinostat for CAL29 cells. mRNA was then extracted or samples were further irradiated with 5 Gy, medium changed and mRNAs harvested 4 hours later.

Panobinostat caused a significant decrease in *TP53* gene expression in a dose-dependent manner in unirradiated and irradiated samples in both RT112 (Figure 3.10A and B) and CAL29 (Figure 3.10C and D) cells.

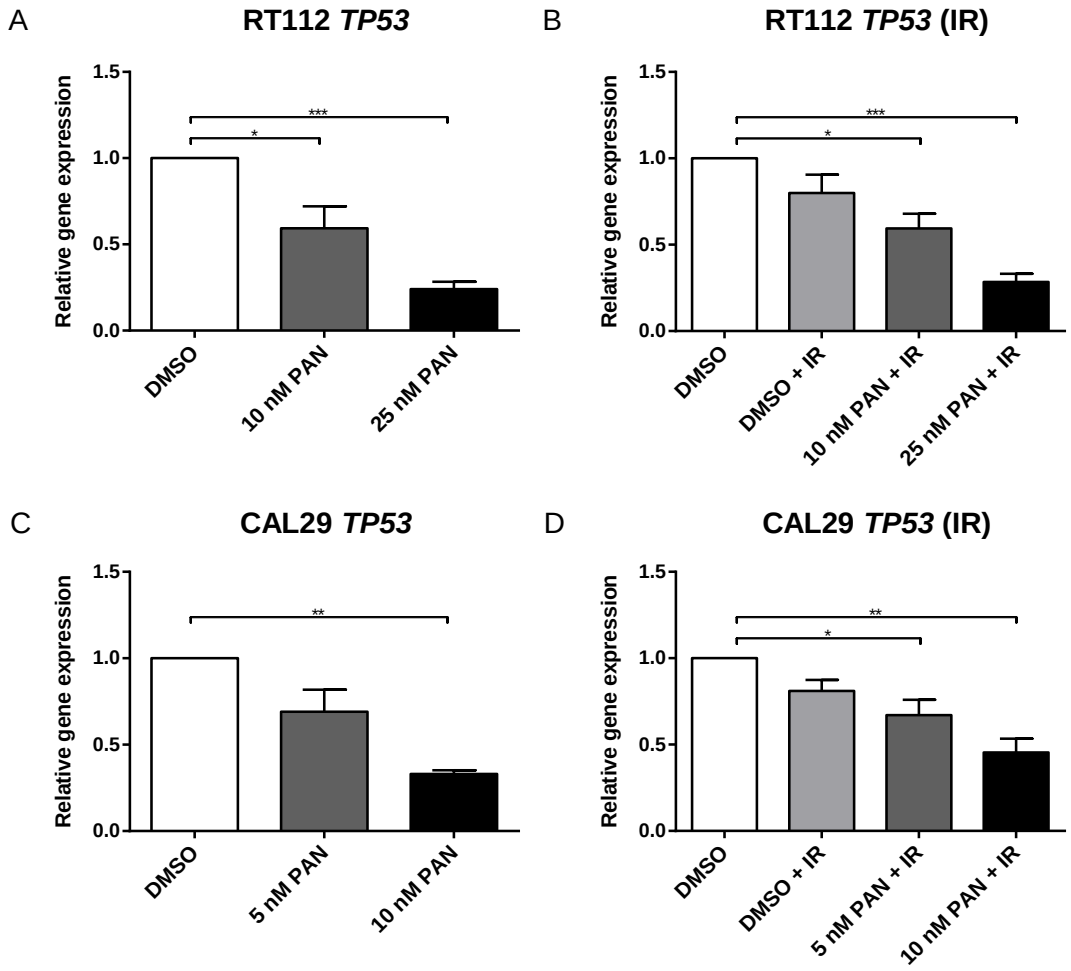


Figure 3.10. Transcription of *TP53* after panobinostat treatment alone or in combination with 5 Gy irradiation.
mRNA expression levels were measured by qPCR for *TP53* in RT112 (A and B) and CAL29 (C and D). The expression levels for each cell were normalised against those of *GAPDH* and the expression levels compared to the DMSO treated sample, set as 1. Values are displayed as the mean and SEM of three independent experiments. One-way ANOVA, Bonferroni's multiple comparisons test over DMSO control; * $p < 0.05$, ** $p < 0.01$, *** $p < 0.001$.

3.2.9 TP53 alternative promoter and panobinostat

Panobinostat can epigenetically influence gene expression. A recent report has described its role in downregulation of aromatase gene expression (aromatase converts androgens to oestrogens), through the selective downregulation of the aromatase gene promoters I.3 and II which are expressed in breast cancer tissue (Chen *et al*, 2010). In contrast, the selective gene induction of *TAp63* by the HDAC inhibitors panobinostat and the HDAC inhibitor trichostatin A has been reported (Sayan *et al*, 2010).

Despite the *TP53* gene being studied extensively for decades, alternative promoters within the *TP53* gene and alternative p53 protein variants have only recently been discovered. Bourdon *et al* (2005) have also established several roles for the p53 variants and investigated their tissue-specific expression. For example, the p53β variant helps full-length p53 with targeted gene expression, while ∆133p53 expresses dominant-negative effects towards some of p53's actions.

Since panobinostat was able to downregulate p53 protein levels in a dose-dependent manner, we hypothesised that panobinostat could modulate the expression of the *TP53* P2 promoter (see Figure 3.11), to promote the transcription of ∆133p53 variants, resulting in a dominant-negative effect towards the full length p53 protein.

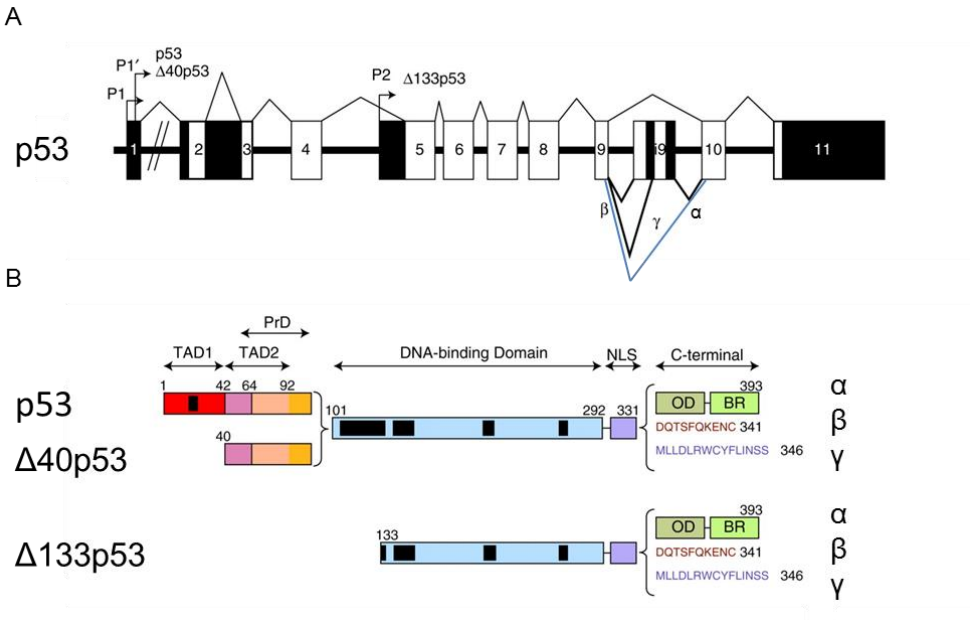


Figure 3.11. *TP53* gene ∆133p53 variants.
A) Structure of the *TP53* gene. Three alternative promoters P1, P1' and P2 and three alternative spilicing sites (α, β and γ) are shown. Transcripts from promoter P1 or P1' have a preserved N-terminal domain, whereas transcripts encoded from the P2 promoter are missing the N-terminal domain and part of the DNA-binding domain. B) Protein domains of the p53, Δ40p53 and Δ133p53 variants. Adapted from Khoury and Bourdon (2010).

RT112 cells were treated with DMSO or 10 nM or 25 nM panobinostat (Figure 3.12A), collected or irradiated with 5 Gy, medium changed and cell pellets harvested 4 h or 8 h later. In these experiments an anti-p53 antibody was used that can detect the full length p53 and also Δ133p53α, β or γ variants, if they are present in a sufficient quantity in cells. This antibody, named DO-12, was a kind gift from Professor Vojtesek, Masaryk Memorial Cancer Institute (Vojtesek *et al*, 1995).

Panobinostat caused a dose dependent downregulation of the p53 protein in RT112 cells and in the irradiated samples there was attenuation of the upregulation of p53 seen in control samples (Figure 3.12A). Δ133p53α variant was also faintly detected, and was downregulated in panobinostat treated samples. Therefore, the hypothesis that panobinostat treatment might favour expression of p53 variants from the alternative promoter appears not to be feasible.

To further determine the effects of panobinostat on p53 variants at the gene transcriptional level, transcription from the second promoter P2 in the *TP53* gene was studied in RT112 cells, treated with DMSO or 50 nM panobinostat for 24 h (Figure 3.12B and C). mRNAs were harvested after 24 h drug or vehicle treatment, or irradiated with 5 Gy after the 24 h drug incubation, medium changed and mRNAs collected 4 h later. Nested RT-PCR was performed, and products run on an agarose gel (Figure 3.12C) for subsequent quantification by densitometry. Transcription of the Δ133p53α variant was reduced in the panobinostat-treated sample, but not significantly, whereas the reduction of transcription in the irradiated and panobinostat-treated sample was significant, compared with the DMSO treated sample. Transcription of Δ133p53β was almost significantly reduced in the panobinostat-only treated sample. In the case of Δ133p53γ, no significant patterns were observed.

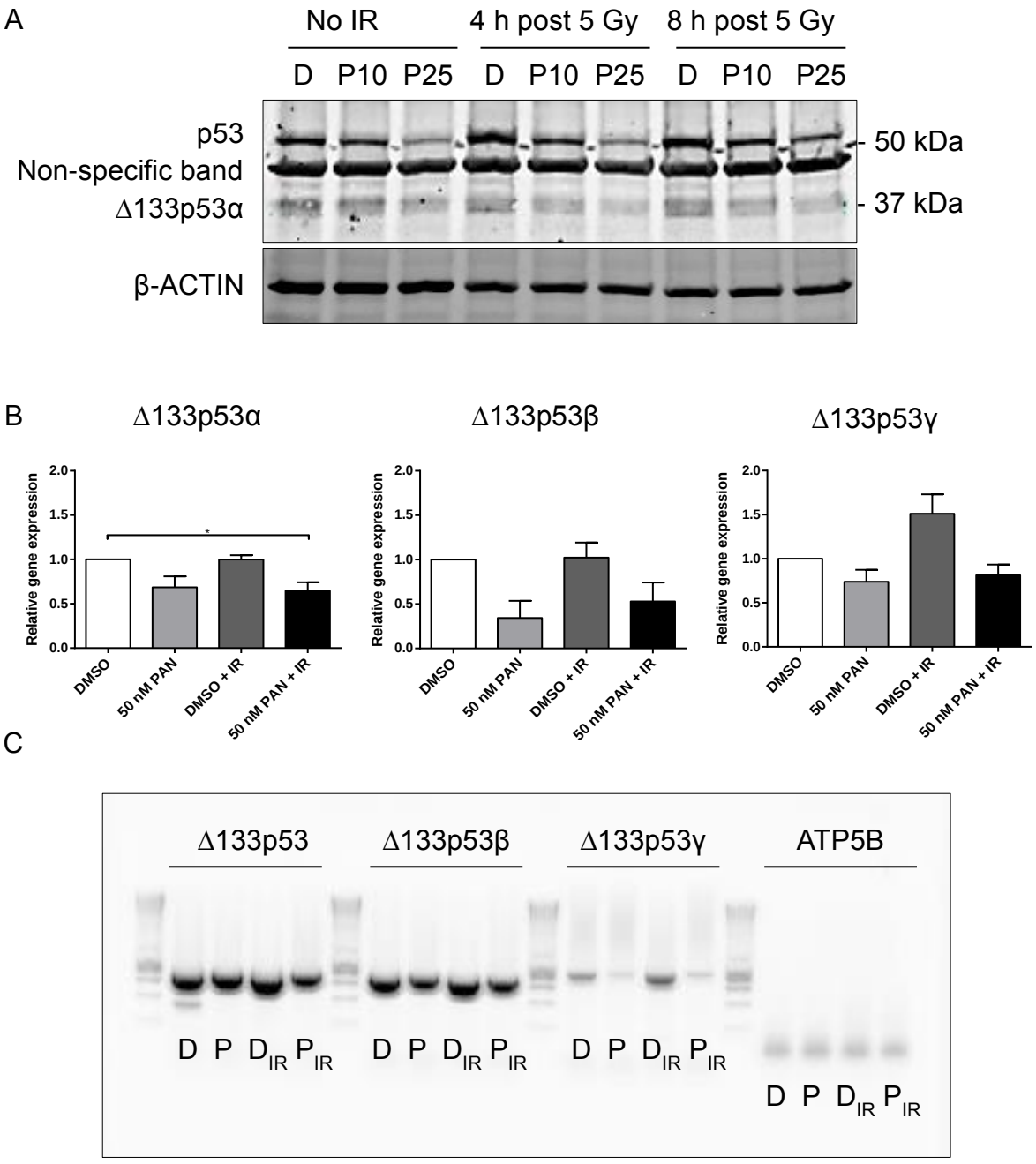


Figure 3.12. Panobinostat downregulates levels of p53 protein and Δ133p53 in a dose-dependent manner.
A) Western blot showing RT112 cells treated with DMSO (D) or 10 nM and 25 nM panobinostat. Dishes were either harvested or irradiated with 5 Gy, medium changed and cell pellets harvested at timepoints indicated. For the detection of Δ133p53α, β or γ, RT112 cells were treated with DMSO or 50 nM panobinostat for 24 h and mRNAs harvested or samples were subsequently irradiated with 5 Gy, medium changed and mRNAs harvested 4 h later. The nested RT-PCR was performed and products run on an agarose gel (C) and quantified (B) and mRNA expression levels normalised against those of ATP5B and compared to the DMSO treated sample, set as 1. The bars represent the mean and SEM of three independent experiments. One-way ANOVA, Bonferroni's multiple comparisons test over DMSO control; * $p < 0.05$, ** $p < 0.01$, *** $p < 0.001$.

3.3 Discussion

The experiments discussed in this chapter were performed to establish the cytotoxicity of panobinostat, and to determine its abilities to acetylate histone lysine residues, radiosensitise bladder cancer cells and alter the levels of wild-type and mutant p53 proteins.

3.3.1 Cytotoxicity of panobinostat

Using clonogenic assays with 24 hour drug incubation, panobinostat was found to work in the low nanomolar range in all three bladder cancer cell lines, with IC_{50} doses of 10 nM (CAL29), 27 nM (RT112) and 35 nM (T24). This is the first report of panobinostat's action in any bladder cancer cell line, and the cytotoxicity values are consistent with those from other reports over a broad range of malignancies, e.g. renal cancer cells (Cha *et al*, 2009), lung cancer cells (Crisanti *et al*, 2009), lymphoblastic leukaemia (Scuto *et al*, 2008) (see Introduction).

While in other studies the MTS and MTT metabolic assays were used to determine lethality, here, the clonogenic assay, the gold standard method was used. The results of all studies, including the presented one, highlight panobinostat as one of the most potent HDAC inhibitor developed. Interestingly, mocetinostat, an HDAC class-I specific inhibitor, also has efficacy in bladder cancer cells but in the micromolar range, i.e. significantly less potent than panobinostat. One possible explanation for panobinostat's greater potency is that it can inhibit all HDACs, whereas mocetinostat only inhibits class I HDACs. However, another pan-HDAC inhibitor, SAHA, also kills bladder cancer cells in a micromolar range (data not shown), suggesting the inhibition of all HDACs is not the key factor and perhaps panobinostat's effects on other, non-histone proteins, could be a major factor determining its cytotoxicity. Another fact that needs to be taken into account when comparing effects of different drugs is efficacy, determined by drug chemical structure. Some drugs will have

better affinity for their target(s) than others, whilst drug half-life is another variable. It is therefore difficult to directly compare effects of different HDAC inhibitors.

According to the data from clinical trials, the described cytotoxic concentrations of panobinostat seen in bladder cancer cell lines can be achieved and also safely surpassed in the plasma of patients treated with panobinostat. Crucially, these concentrations are relatively well tolerated by patients (Giles *et al*, 2006; Atadja, 2009). Given that a drug should be given to patients in as low a dose as possible, while still being effective, panobinostat was used in concentrations below the IC_{50} dose in this study (reasons for higher dose in some experiments are discussed elsewhere).

3.3.2 Acetylation of lysine residues and radiosensitising effects

In cells treated with HDAC inhibitors, acetylation of histone lysine residues is one of the most rapid, unequivocal events, making it a commonly used marker in preclinical and clinical studies using these drugs (Giles *et al*, 2006; Scuto *et al*, 2008; Folkvord *et al*, 2009). Moreover, this modification masks the positive charge of the histone lysine residues and the interaction with the DNA molecule is loosened, therefore remodelling the chromatin structure and also regulating gene expression (Camphausen & Tofilon, 2007).

In this study the effects on histone acetylation were examined in order to detect panobinostat's activity in treated cells. These rapid events could theoretically modulate chromatin structure, by making it more accessible to radiation damage and therefore enhancing the radioresponsiveness of treated cells. We therefore hypothesised that the timings of both panobinostat's acetylation induction and radiosensitising effects would coincide.

H3 lysine residues were acetylated as early as 30 minutes after panobinostat treatment, and the levels did not change over longer incubation times, even up to 24 hours. Although these observations firmly confirmed panobinostat's biological activity in the treated cells,

clonogenic assays performed after 1 h panobinostat incubation and subsequent irradiation of cells did not show any radiosensitising effects on cells, even at doses much greater than the RT112 IC_{50} dose. On the other hand, 24 hours' incubation did cause substantial radiosensitising effects in a panel of bladder cancer cells (discussed below), but the acetylation levels in RT112 cells were no higher than those detected at earlier timepoints. Contrary to our hypothesis, these findings indicate that the effects of panobinostat on histone acetylation and radiosensitisation do not correlate in a timely manner. It is possible that longer incubation times are required to achieve substantial cellular chromatin remodelling, resulting in greater cell radiosensitivity. Alternatively, the fact that the levels of acetylated histones do not change over longer durations of drug incubation speaks in favour of other factors contributing to the radiosensitising effects. These might include potential effects on the proteins involved in DNA repair or cell cycle regulation, or indeed their transcription.

In this study, radiosensitising effects of panobinostat have been shown for the first time in bladder cancer cells. Significant effects were detected at doses lower than IC_{50}, in all the bladder cell lines studied, and even the low-toxic 10 nM dose caused radiosensitisation. These observed effects are extremely promising for further testing *in vivo*, and ultimately in clinical trials, given that many bladder cancer patients are old and current therapies combined with radiotherapy are too toxic for them. On the other hand, in the CAL29 cell line, the confidence intervals were overlapping to a certain degree, and therefore higher panobinostat doses should be used to achieve significant radiosensitisation.

In previous studies, panobinostat has shown radiosensitising effects in a human lung adenocarcinoma cell line, where significant radiosensitisation was observed. The authors did not provide SER_{10} values, but have been estimated to be approximately 1.3 for 24h incubation of 25 nM panobinostat from their published graphs (Storch *et al*, 2010). Geng *et al* (2006), treated human large cell lung cancer cells with 50 nM panobinostat to achieve significant radiosensitising effects. Again, SERs were not described by the authors and have been estimated as 1.3 after 1 h incubation and 1.45 after 18-hour incubation.

Radiosensitising effects of panobinostat were also reported in prostate cancer cell lines (Xiao *et al*, 2013), but not in normal prostate epithelial cells. High panobinostat doses were used (starting from 2.5 μM). Estimations of SER_{10} values were in the range of 1.3-1.5. Panobinostat significantly radiosensitised laryngeal carcinoma and breast carcinoma cell lines. The SER_{10} for 18 h incubation at 100 nM panobinostat is estimated for breast carcinoma cell line to be 1.5 (Kim *et al*, 2009). These SER_{10}-values are comparable to those obtained in bladder cancer cells and presented in this thesis.

To determine if the radiosensitising effects of panobinostat could be attributed to class-specific HDAC inhibition, mocetinostat which inhibits the class I HDACs, and MC1568, which is a class II specific agent, were tested. Inhibition of class I HDAC enzymes resulted in some radiosensitisation, but to a lesser extent than panobinostat. One way to interpret these data is to attribute all the effects to panobinostat's better efficacy, correlating with greater effects, when compared to mocetinostat. On the other hand, these results could demonstrate a connection between class I HDAC enzymes and radiosensitising effects, but also indicate, that inhibition of class II HDACs contributes to panobinostat's effect. Unfortunately, this class II inhibition could not be tested, due to MC1568's poor solubility in the medium used and its resulting low cytotoxicity achievable in clonogenic assay. Low cytoxicity in a clonogenic assay was also confirmed in another study on pancreatic cancer cells (Wang *et al*, 2012). There were no broad alternative class II specific inhibitors commercially available. Tubacin, a drug specifically inhibiting HDAC6 could be tested. Furthermore, the HDAC8-specific inhibitor PCI-34051 could be used in order to determine the effect on the class I HDAC, which is not modulated by the class I inhibitor mocetinostat. From this, a logical subsequent step could be the siRNA knockdown of *HDAC* genes from class II and testing for the effects of panobinostat in this setting.

3.3.3 Effects on the cell cycle

The effects of panobinostat on cell cycle distribution were also tested. In RT112 cells, G2/M phase arrest was detected in a dose-dependent manner. This observation could explain the radiosensitising effects caused by panobinostat, since cells are the most sensitive in G2/M phase (Pawlik & Keyomarsi, 2004). However, these effects were not observed at 10 nM, when cells are also well radiosensitised. Furthermore, even at 25 nM this effect was barely statistically significant. Radiosensitisation could therefore rather be due to a suppressive effect on DNA repair, resulting in unrepaired cells, leading to cell death. These effects will be further presented and discussed in the second results chapter.

In order to determine whether cell death occurs by apoptosis, one option is to look for a sub-G1 peak in FACS cell analysis (Kajstura *et al*, 2007). In this study, RT112 FACS cell cycle analysis did not reveal any sub-G1 peaks, either with drug alone or in combination with IR, even at doses of panobinostat well exceeding the IC_{50}. The predominant mode of cell death resulting from IR is mitotic catastrophe (Surova and Zhivotovsky, 2013). The only cell cycle arrest observed in irradiated or panobinostat-treated and irradiated cells, was a G2/M arrest, with the peak at 8 h post-IR in DMSO and panobinostat-treated samples that had resolved 24 h post IR. This perhaps suggests that DNA damage checkpoints are aberrant and the damage in panobinostat-treated and irradiated cells was not resolved before the cells entered mitosis, resulting in mitotic catastrophe several cell cycles later. To confirm this, Annexin V apoptosis assay should be used to fully exclude apoptosis as a mode of cell death in panobinostat or in combined panobinostat and irradiation treatment.

3.3.4 Effects on p53 protein

TP53 is mutant in approximately 50% of high grade muscle invasive bladder cancers, contributing to genetic instability and having important roles in tumour recurrence and prognosis. *TP53* mutations can also result in less favourable outcomes following chemo-

and radiotherapy in bladder cancer patients (Wu, 2005). When the *TP53* gene is mutated this leads to changes in p53 protein and the function of the wild-type is generally lost. Furthermore, the mutated protein can gain some undesirable functions, such as cell proliferation and survival and promotion of invasion and metastasis (Muller & Vousden, 2013). Therefore, an important question in bladder cancer cell lines was whether panobinostat had any effects on wild-type or mutant p53 protein and whether this influenced the radiosensitising effects of panobinostat.

Interestingly, panobinostat radiosensitised all cell lines, regardless of *TP53* status (RT112 is wild-type, but CAL29 and T24 are p53 mutant) and downregulated both types of p53 protein in a dose-dependent manner. Wild-type p53 can be an important contributor to cell death following irradiation while mutant p53 can theoretically have the opposite effect, resulting in survival of cells with a more generally unstable and aggressive phenotype. Panobinostat causes protein downregulation in a dose-dependent manner and also a robust radiosensitisation of bladder cancer cells regardless of their p53 status. This could therefore mean that the p53 protein does not have a key role in these effects and thus a patient's *TP53* status will not influence their response to panobinostat treatment.

The influence of a cell's *TP53* status on radiosensitivity is unclear. We have shown that RT112 (*TP53* wild-type) and T24 (*TP53* mutant) cells have similar intrinsic radiosensitivity, which is consistent with a previous report (Moneef *et al*, 2003). The CAL29 (*TP53* mutant) cell line proved to be the most sensitive to radiation.

Another remaining important question is what effects panobinostat has on p53 protein in normal, non-transformed cells? Disregulation of p53 protein pathways in those cells could have detrimental effects on healthy tissues and result in the development of therapy-related malignancies. To date, this has not been demonstrated in any other cell line or been seen to be an issue in current clinical trials, but this question needs to be addressed in mice xenograft experiments, before entering into bladder cancer clinical trials.

Others have shown that downregulation of HDAC8 leads to a dose-dependent decrease of both wild type and mutant p53, and also decreased transcription of the *TP53* gene (Yan *et al*, 2013). Since *TP53* transcription in RT112 and CAL29 cells was reduced in a panobinostat dose-dependent manner with similar effects after irradiation, this could be mediated via panobinostat's downregulation of HDAC8. The first logical future step to confirm this, would be to test the HDAC8-specific inhibitor PCI-34051, to see if it causes similar effects on the p53 protein, followed by siRNA knockdown of *HDAC8* gene.
It is also possible, that the decrease in p53 protein levels directly causes transcriptional repression of *TP53* gene, since p53 also serves as a transcription factor for the *TP53* gene transcription (Deffie *et al*, 1993). This observation could further be tested by chromatin immunoprecipitation (ChIP) assay, looking into binding of transcription factors to the *TP53* gene promoter area to detect impaired or reduced binding of transcription factors.

To further examine the mechanism underlying the p53 downregulation seen with panobinostat treatment, we hypothesised that panobinostat could cause transcriptional upregulation of ∆133p53α, β and γ variants, reported to have dominant negative effects on the full length p53 protein and *TP53* gene expression (Bourdon *et al*, 2005; Khoury & Bourdon, 2010).

Unfortunately, the hypothesis was shown to be incorrect. Semi-quantitative RT-PCR revealed downregulated amounts of all the delta variants transcripts in the RT112 cells, after panobinostat treatment and also attenuated transcription post-irradiation. In contrast, in a DMSO treated sample, the ∆133p53β variant showed an increase post-irradiation. Western blotting was consistent with this finding, with reduction of a band at approximately 37 kDa, which was previously identified as ∆133p53α. ∆133p53β and γ could not be detected by western blot, probably due to extremely low amounts present in the cell.

CHAPTER 4: EXPLOITING "SYNTHETIC LETHALITY" IN BLADDER CANCER CELLS

4.1 Introduction

Cancer treatments are delivered to patients with the aim of killing cancer cells while affecting the normal (non-cancerous) cells as little as possible. Targeted radiotherapy is one important modality, often combined with radiosensitising agents. These are used to sensitise tumours to radiotherapy, but they often sensitise normal tissues as well, frequently to limits of tolerance (Harrington *et al*, 2011; Mladenov *et al*, 2013).

It is therefore important to identify cancer-specific therapeutic targets, so that treatment results in tumour cell, but not normal cell, death. This preferential cancer cell targeting can be achieved through "synthetic lethality". This is similar to the phenomenon in genetics. Here the term "synthetic lethality" relates to two genes, where a cell can survive when either one or the other is mutated, but cannot survive if both are mutated (Kaelin, 2005). To put this in the context of the DNA repair pathways involved in repair of IR-induced DSB, it is generally accepted that they are repaired mainly by HR or NHEJ (Hunt *et al*, 2013; Mladenov *et al*, 2013). Therefore, if one of these could be identified as deficient in a tumour, then therapeutically targeting the proficient one with a radiosensitising agent would increase the therapeutic ratio. The targeting of the functional pathway would leave unrepaired DSB, resulting in tumour cell kill, but the normal cells would still have one proficient pathway to repair the DSB, so they would survive. A successful demonstration of this phenomenon was the targeting of BRCA1 and BRCA 2 deficient cancer cells with inhibitors of the PARP1 protein, which is also involved in DSB MMEJ repair pathway (Bryant *et al*, 2005; Farmer *et al*, 2005; McCabe *et al*, 2006).

In bladder cancer, a similar exploitation of the "synthetic lethality" concept was hypothesised. High grade muscle invasive bladder tumours display a high proportion of deletions and point mutations, indicative of inaccurate/deficient DSB repair leading to

genetic instability (Florl & Schulz, 2008). Pucci *et al* shown reduced Ku70/Ku80–DNA binding in high grade breast and bladder tumours, without differences in the protein levels between tumours and normal tissues (Pucci *et al*, 2001). Moreover, Bentley *et al* established that cell free extracts from high grade bladder tumours form inaccurate joins using linearised plasmid DNA in an *in vitro* NHEJ/MMEJ assay, which is not dependent on functional Ku80, DNA-PK or XRCC4 proteins, whereas extracts from normal human urothelial cells showed accurate joining (Bentley *et al*, 2004). This finding was indicative of the tumours' inability to join DSB ends using classical NHEJ, and their preferential use of a highly aberrant DSB repair pathway, MMEJ. Furthermore, in a larger panel of non-muscle-invasive and muscle-invasive bladder cancers it was the high grade muscle-invasive tumours that demonstrated the MMEJ phenotype along with reduced Ku80-DNA binding (Bentley *et al*, 2009). Therefore agents targeting HR may exploit "synthetic lethality" in muscle-invasive bladder cancer.

In this chapter, experiments testing "synthetic lethality" in bladder cancer cells are presented. To test this potentially clinically-applicable concept, RT112-derived cells deficient in Ku80 (C13) or RAD51 (795J) proteins were used (cell lines were generated by Dr. Boling Qiao, Leeds Institute of Molecular Medicine, Leeds, UK). The cell lines were initially tested with the tyrosine kinase small molecule inhibitor imatinib (Figure 4.1) (Russell *et al*, 2003; Choudhury *et al*, 2009), demonstrating that this agent acted via the HR pathway in bladder cancer cells (Qiao *et al*, 2013). This cell model was then used in further experiments on panobinostat to determine whether this agent also acted on HR and hence could be used to exploit "synthetic lethality".

4.2 Results

4.2.1 Effects of imatinib on RT112 cell proliferation

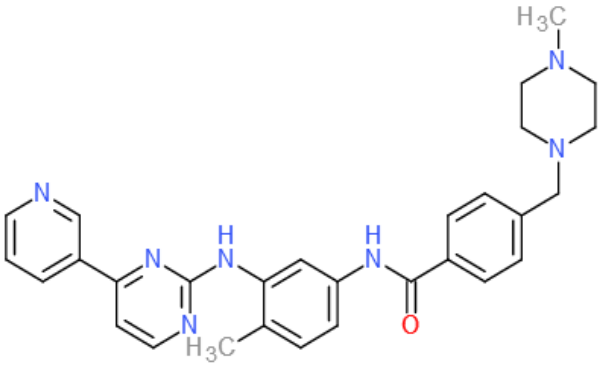
Before radiosensitisation of Ku80KD and RAD51KD cells could be evaluated, the growth-inhibitory activity of imatinib in RT112 cells was tested. A 14 day drug incubation was used for the clonogenic assay. Imatinib was found to kill RT112 cells in the micromolar range (μM). As shown in Figure 4.2A, the half maximal inhibitory concentration for the drug (IC_{50}) was 8 μM.

4.2.2 Imatinib's effects on HR and radiosensitisation of Ku80KD cells

The hypothesis that imatinib targets HR and hence would radiosensitise Ku80KD cells more than RAD51KD cells was tested (Figure 4.1). A 24 hour cell incubation was used before irradiation and subsequent cell replating and 14 day imatinib incubation.

Radiosensitising clonogenic assays were performed at two doses, namely a low, nontoxic dose 3 μM (IC_{10}), and a high, 6 μM dose (IC_{40}) (see cytotoxicity curve, Figure 4.2A). In Figure 4.2C, at low dose, significant radiosensitising effects on Ku80KD cells can be seen, with an SER_{10} (sensitisation enhancement ratio at 10% cell survival) of 1.27 (P=0.03). In the other two cell lines, imatinib did not radiosensitise (RAD51KD) or the effects was not significant (RT112, SER_{10}=1.07, P=0.051). At high 6 μM doses, the SER_{10} for Ku80KD cells increased to 1.69 (P=0.03). The other two cell lines were also radiosensitised, with $SERs_{10}$ of 1.34 in RT112 (P=0.03) and 1.11 in the RAD51KD cells (P=0.03) (Figure 4.2B and C). Non-silencing control (NSC), a non-specific siRNA expressing-cell line, was also used in these experiments and behaved as the RT112 parental cell line (data not shown). Results showed that Ku80KD cells were radiosensitised more than the RT112 and RAD51KD cell lines, suggesting that a major mechanism for imatinib radiosensitisation is via the HR pathway (see Discussion).

A



B

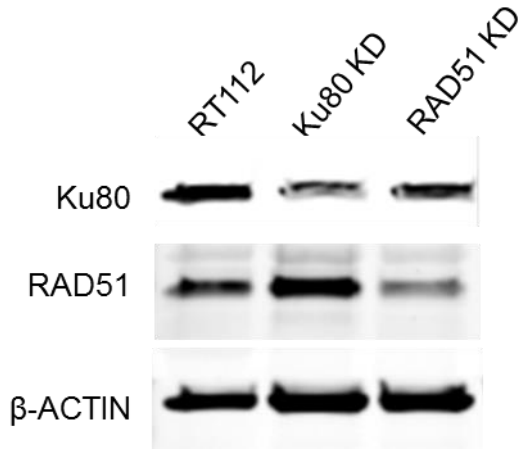
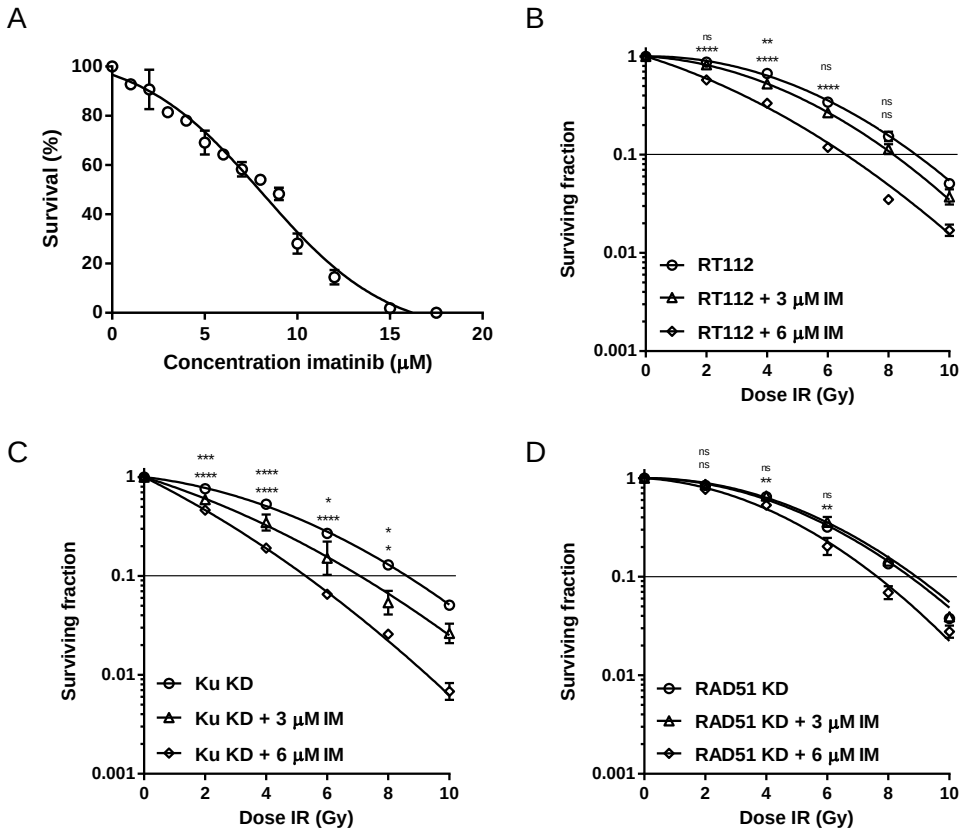


Figure 4.1. Chemical structure of imatinib and cells depleted for RAD51 and Ku80. A) Chemical structure of imatinib. B) Western blot showing RT112 and cells depleted for Ku80 or RAD51.



E

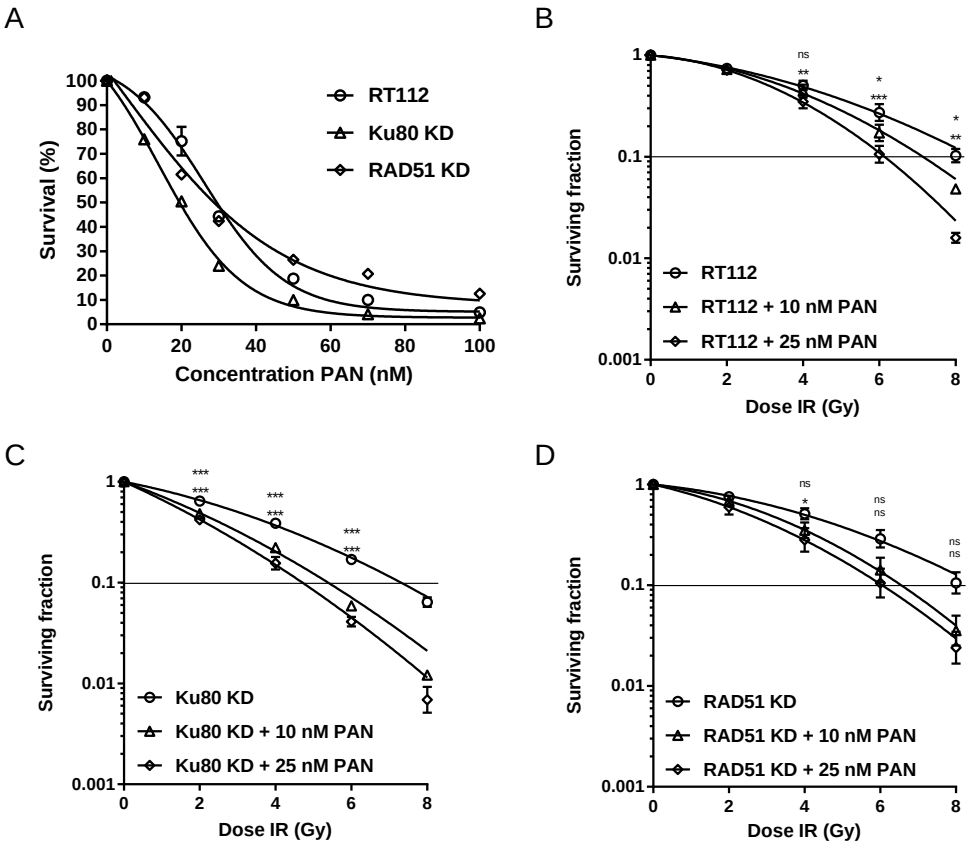
Cell line	SER_{10}	
	3 μM IM	6 μM IM
RT112	1.07	1.34
Ku KD	1.27	1.69
RAD51 KD	1.00	1.11

Figure 4.2. Cytotoxicity and "synthetic lethality" in bladder cancer and imatinib. A) Clonogenic assay was used to determine imatinib's cytotoxicity in RT112 cells (IC_{50} = 8 μM). B) Clonogenic assays combining irradiation and fixed doses of drug in RT112. C) Ku80KD and (D) RAD51KD cells. E) Table of sensitisation enhancement ratios at 10% survival (SER_{10}) is presented. Error bars represent mean survival of at least three independent experiments and SEM. The horizontal line in B, C and D represents 10% cell survival. Experiments in this figure were performed together with Dr. Martin Kerr (Gray Institute for Radiation Oncology and Biology, Oxford). Two-way ANOVA, Bonferroni's multiple comparisons test over DMSO control; * $p < 0.05$, ** $p < 0.01$, *** $p < 0.001$, **** $p < 0.0001$; ns = non-significant; upper row low drug dose, lower row high drug dose.

4.2.3 Ku80KD cells are the most sensitive to panobinostat

Once “synthetic lethality” was demonstrated with the HR-targeting agent imatinib, the inhibitory effects of the HDAC inhibitor panobinostat were tested by clonogenic assay in RT112, RAD51KD and Ku80KD cells treated for 24 hours. Panobinostat's IC_{50} was 27 nM in RT112, 25 nM in RAD51KD and most toxic in Ku80KD cells, where the value was 19 nM (Figure 4.3A).

To further test the effects of panobinostat as a radiosensitiser, knock-down cells were then treated for 24 hours at one of two doses, corresponding to non-toxic 10 nM (IC_{10}) and 25 nM (IC_{40}) levels in the parental cell line, RT112. Cells were plated and irradiated for clonogenic assays. Ku80KD cells treated with 10 nM panobinostat were significantly radiosensitised (SER_{10}=1.35, P=0.04). Effects on RAD51KD cells were also significant, but less marked (SER_{10}=1.22, P=0.04), and similarly in the parental cell line, as described in the previous Results chapter (SER_{10}=1.16, P=0.05). The higher dose of panobinostat, 25 nM (IC_{40}) radiosensitised all the cell lines tested, with the greatest effect in Ku80KD cells, SER_{10}=1.56, P=0.05. The SER_{10} value in RAD51KD cells was 1.31 (P=0.03), similar to that in RT112 (SER_{10}=1.31, P=0.01), Figures 4.2B, C and D and E. Greater radiosensitisation of Ku80KD cells would indicate that HR is preferentially targeted by panobinostat.



E

Cell line	SER_{10}	
	10 nM PAN	25 nM PAN
RT112	1.16 (IC_{10})	1.31 (IC_{40})
Ku80 KD	1.35 (IC_{20})	1.56 (IC_{60})
RAD51 KD	1.22 (IC_{40})	1.31 (IC_{40})

Figure 4.3. "Synthetic lethality'' in bladder cancer and panobinostat.
A) Clonogenic assays following 24 h treatment of RT112, Ku80KD and RAD51KD cells with increasing panobinostat (PAN) concentrations. Clonogenic assays in RT112 (B), Ku80KD (C) and RAD51KD (D) treated with increasing ionising radiation doses and 10 nM or 25 nM PAN; E) Table with the sensitisation enhancement ratios at 10% (SER_{10}) cell survival. All experiments were performed at least three times. Error bars represent the mean and SEM. Two-way ANOVA, Bonferroni's multiple comparisons test over DMSO control; * $p < 0.05$, ** $p < 0.01$, *** $p < 0.001$; ns = non-significant; upper row low drug dose, lower row high drug dose.

4.2.4 Effects of panobinostat on key HR and NHEJ proteins

Panobinostat significantly radiosensitised RT112, T24 and CAL29 bladder cancer cell lines (described in first Results chapter). Since irradiation induces DSB that can be resolved by either HR or NHEJ, the effects of panobinostat on some of the key proteins from the both pathways were investigated, both without IR and at 4 and 8 hours after 5 Gy irradiation.

In RT112 cells treated with panobinostat for 24 hours, levels of RAD51 protein were downregulated in a dose-dependent manner, from as little as 10 nM. Similarly, levels of another HR protein CtIP were also depleted in a panobinostat dose-dependent manner. The Ku70 and Ku80 proteins of the NHEJ pathway were also studied and no marked effects were detected, even at doses well beyond IC_{50}. Acetylation of histone H3K18 was upregulated with panobinostat treatment (Figure 4.4).

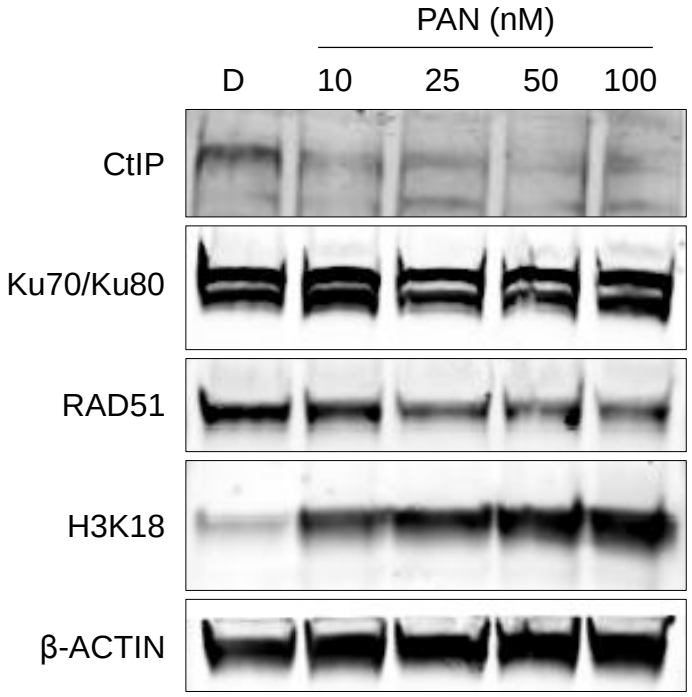


Figure 4.4. Panobinostat downregulates RAD51 and CtIP proteins.
Western blot of RT112 cells post-24 hour panobinostat (PAN) treatment in a dose-dependent manner, from 10 nM to 100 nM. Levels of the HR RAD51 and CtIP and NHEJ Ku70/80 proteins were tested. Acetylation of H3K18 was used as an indicator panobinostat's biological activity.

4.2.4.1 Effects of panobinostat on the key HR proteins post-IR

Results obtained in panobinostat-only treated cells indicated that it preferentially targeted the HR pathway proteins. In order to confirm these results in other bladder cancer cell lines and to further investigate panobinostat's effects in post-irradiation samples, RT112, CAL29 and T24 cells were first treated for 24 h with DMSO (mock control), and two doses of panobinostat, 10 nM (IC_{10}) and 25 nM (IC_{40}) in RT112, 5 nM (IC_{25}) and 10 nM (IC_{45}) in CAL29 and 10 nM (IC_{10}) and 25 nM (IC_{30}) in T24 cells. Next, cells were irradiated to 5 Gy, medium changed and cell pellets collected 4 and 8 hours later. Panobinostat's effects on protein levels were expected to be decreased at these timepoints. Levels of RAD51 protein were tested in CAL29 and T24 cells and found to be downregulated with panobinostat alone. When irradiation and panobinostat were combined, attenuation of any protein increases by IR were seen at all drug doses at both 4 and 8-hour post-IR timepoints (Figure 4.5).

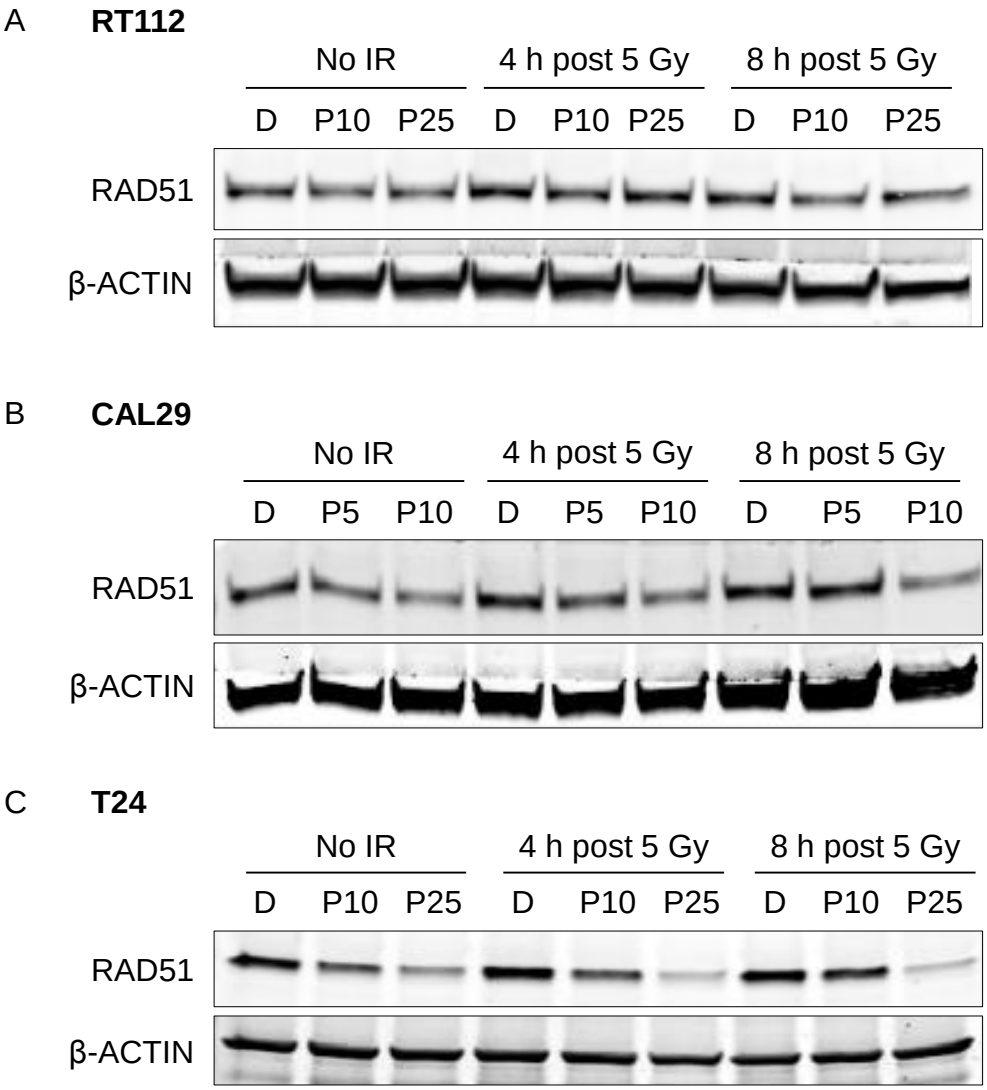


Figure 4.5. Panobinostat downregulates RAD51.
Western blots of the HR protein RAD51 protein levels in RT112 (A), CAL29 (B) and T24 (C) cells, treated with DMSO (D) or panobinostat (P) in a dose dependent manner. Next, cells were irradiated to 5 Gy, medium changed and cells harvested 4 and 8 hours later.

The RAD51 results led us to test another crucial HR protein, CtIP. Expression levels were tested in RT112, CAL29 and T24 cells. Panobinostat decreased CtIP levels in RT112 and CAL29 cells in a dose-dependent manner. This was not the case in T24 cells. Marked protein attenuation at 4 and 8 hours post 5 Gy was observed in RT112 and CAL29 cells, whereas in T24 cells this was only seen at the higher dose of 25 nM (Figure 4.6).

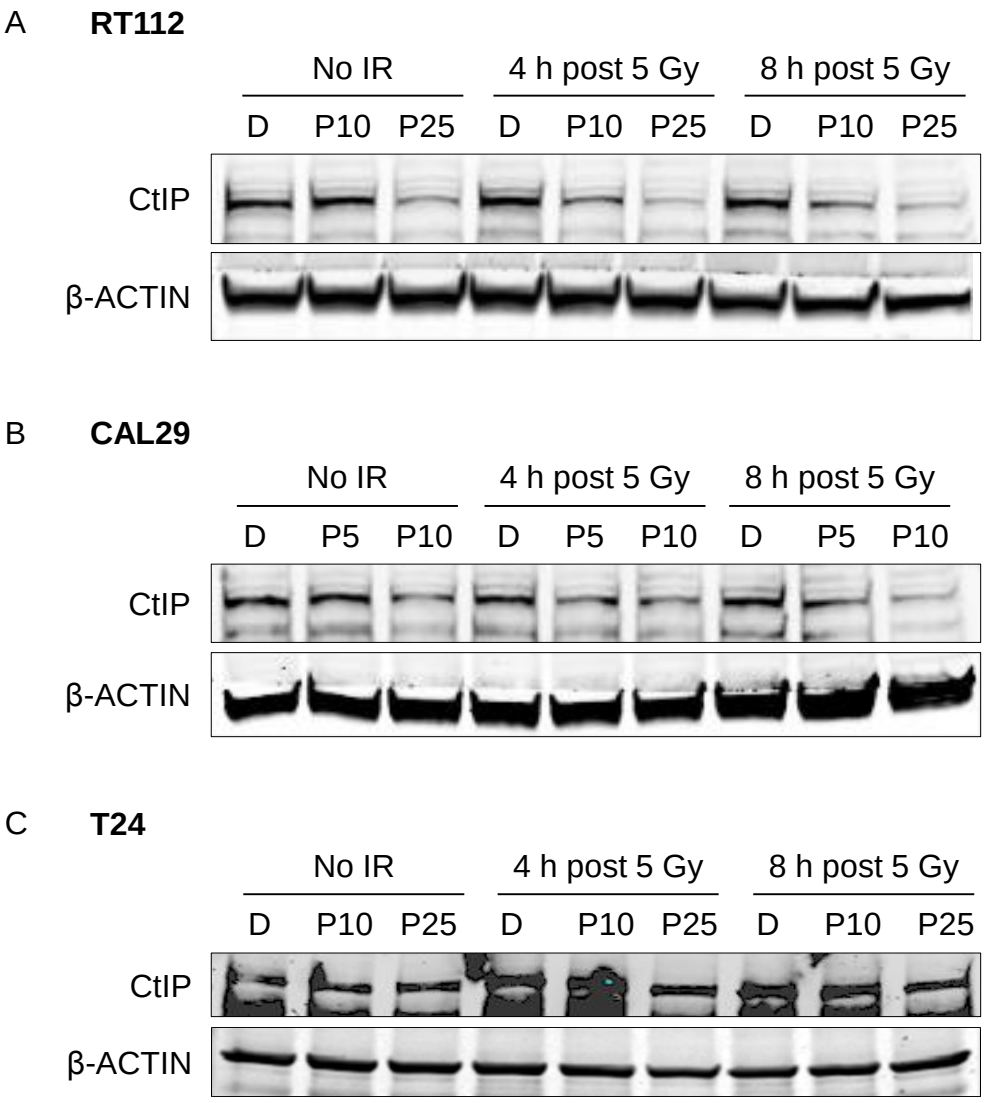


Figure 4.6. Panobinostat attenuates upregulation of CtIP protein.
Western blots representing effects of panobinostat (P) on the HR protein CtIP in RT112 (A), CAL29 (B) and T24 (C) cells. Cells were also irradiated with 5 Gy, medium changed and cells harvested 4 and 8 hours later.

4.2.4.2 Effects of panobinostat on NHEJ proteins post-irradiation

No effects on NHEJ Ku70/80 proteins were seen in cells treated solely with panobinostat (Figure 4.4), however the possibility remained that the levels could be affected where panobinostat and irradiation were combined. Therefore, protein levels of Ku70/80 were measured in RT112, CAL29 and T24 cells treated with 24 hours of panobinostat and then irradiated with 5 Gy. In the case of RT112, another key NHEJ protein, DNA-PK was also tested, to further verify the effects on the NHEJ proteins.

Panobinostat treatment alone or in combination with irradiation did not result in any marked change in the levels of the Ku70/80 proteins or DNA-PK (in the case of RT112 cells) (Figure 4.7).

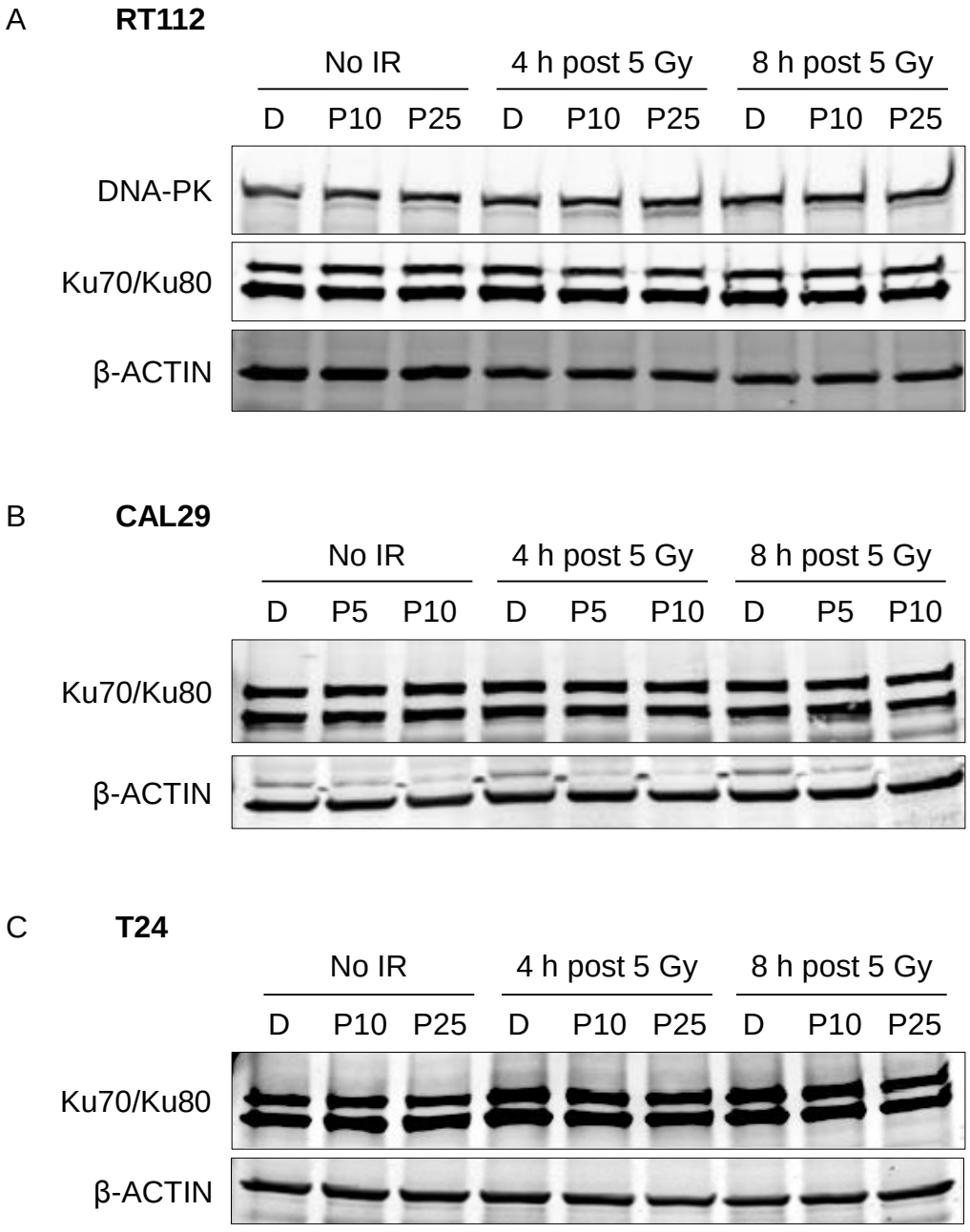


Figure 4.7. Panobinostat does not cause any marked effects on NHEJ protein levels.
A) Western blot represent RT112 (A), CAL29 (B) and T24 (C) cells, treated for 24 h with 5 (P5), 10 (P10) and 25 nM (P25) panobinostat and a mock control, DMSO (D). Cells were also irradiated with 5 Gy, medium changed and cells harvested 4 and 8 hours later.

4.2.5 Effects on NHEJ and HR proteins in RAD51KD and Ku80KD cells

Cells use d for the “synthetic lethality” experiments and depleted for RAD51 or Ku80 proteins were also tested for panobinostat’s effects on RAD51 and Ku70/80 proteins, to see if panobinostat consistently showed similar effects on the HR and NHEJ proteins to those presented above. These western blots confirmed reduced levels of either RAD51 or Ku80 proteins in RAD51KD and Ku80KD cells, compared to the parental cell line, RT112 (Figure 4.8). RAD51 levels were reduced post-irradiation by panobinostat treatment in all cell lines. Consistent with previous results, panobinostat did not change Ku70/80 levels in any treated cell line. Acetylation of histone H3K18 was used as a marker for panobinostat’s biological activity.

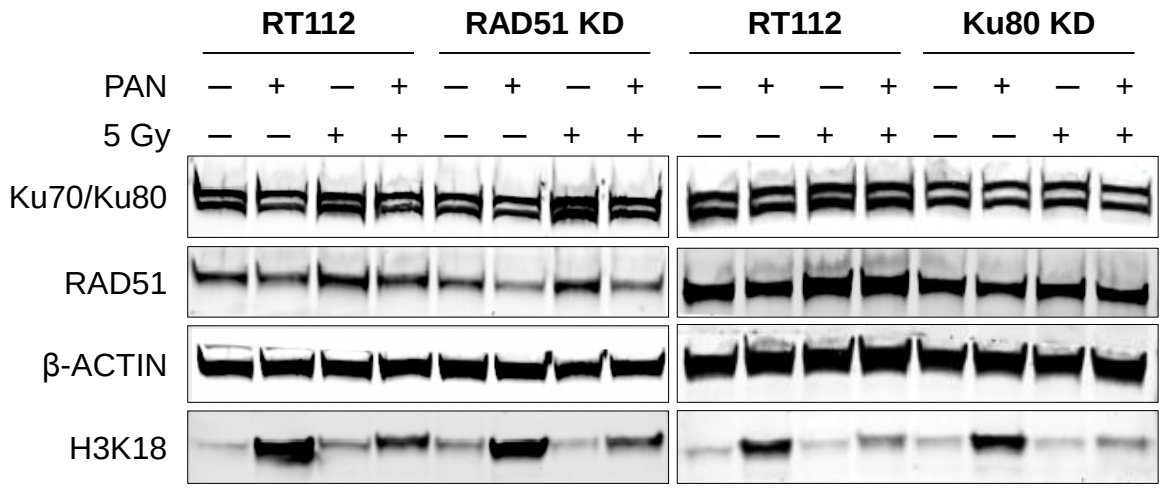


Figure 4.8. Effects of panobinostat on the major HR and NHEJ proteins in cells depleted for RAD51 or Ku80.
Western blots showing 25 nM panobinostat-treated (PAN) RT112, RAD51KD and Ku80KD. Cells were harvested immediately or 4 h after 5 Gy irradiation with the medium changed.

4.2.6 Panobinostat and transcriptional regulation of RAD51 and CtIP genes

To determine whether panobinostat's downregulation of RAD51 and CtIP protein levels is due to transcriptional repression of the *RAD51* and *CtIP* genes, rather than post-transcriptional or post-translational effects*, mRNA* levels were measured in RT112 and CAL29 cells, by the qPCR method. No significant effects were observed in *RAD51* gene expression in RT112, following panobinostat alone or panobinostat plus IR. In CAL29 cells at the lower 5 nM dose no effects were observed, but a significant (P=0.02) downregulation was detected at the higher, 10nM dose (Figure 4.9). A significant, 30% downregulation of *CtIP* gene expression was observed in RT112 cells at 25 nM treatment without irradiation (P=0.01) (Figure 4.10A). No significant patterns were observed in RT112 samples collected 4 h post 5 Gy, but a significant upregulation of the *CtIP* gene in CAL29 cells was seen at 10 nM (P=0.04) (Figure 4.10D).

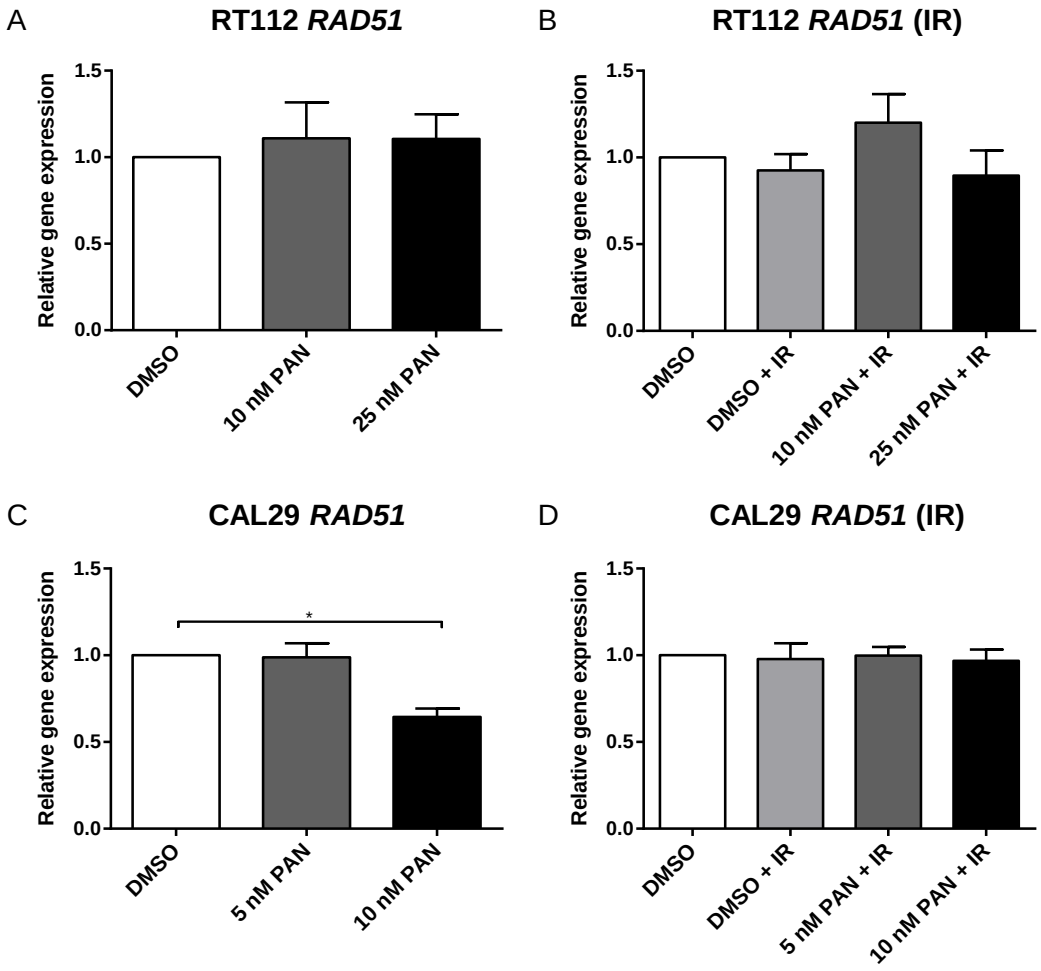


Figure 4.9. *RAD51* gene expression after panobinostat treatment.
mRNA expression of the *RAD51* gene after panobinostat treatment was measured by qPCR. RT112 (A) and CAL29 cells (C) were treated at doses of panobinostat indicated. RT112 (B) and CAL29 (D) were also irradiated with 5 Gy, medium changed and mRNAs harvested 4 hours later. Error bars represent the mean and SEM of three independent experiments. One-way ANOVA, Bonferroni's multiple comparisons test over DMSO control; * $p < 0.05$, ** $p < 0.01$, *** $p < 0.001$.

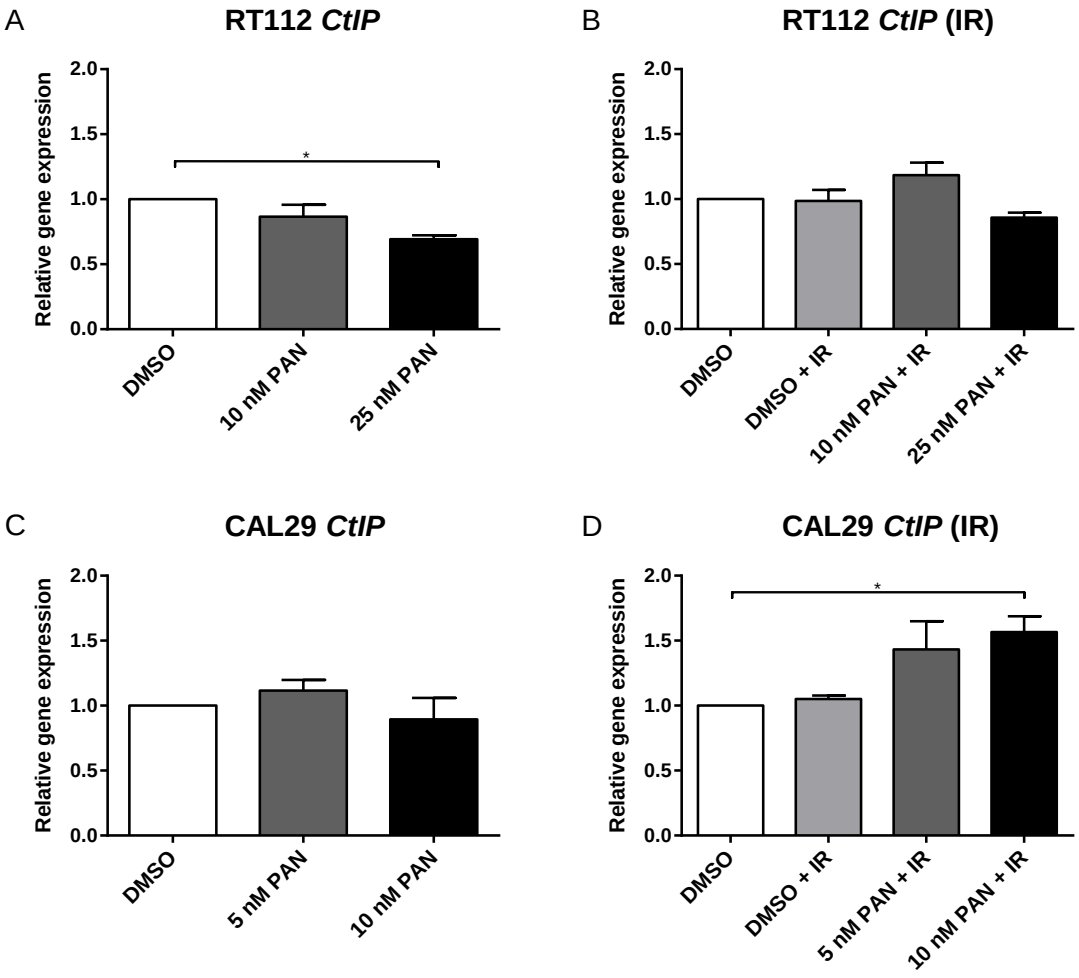


Figure 4.10. Expression of *CtIP* in RT112 and CAL29 cells after panobinostat treatment.
qPCR expression of *CtIP* gene after 24 h treatment of RT112 (A) and CAL29 (D) cells with two doses of panobinostat. RT112 (B) and CAL29 (D) were also treated with panobinostat for 24 h, irradiated with 5 Gy, medium changed and mRNAs harvested 4 h. Error bars represent the mean and SEM of three independent experiments. One-way ANOVA, Bonferroni's multiple comparisons test over DMSO control; * $p < 0.05$, ** $p < 0.01$, *** $p < 0.001$.

4.3 Discussion

In our lab, RAD51 and Ku80 have been stably knocked down using shRNAi technology in an RT112 parental cell line in order to examine synthetic lethality of radiosensitisers in a bladder cancer model. The Ku80 and RAD51 cells used in Chapter 4 experiments were chosen from a broad panel of cell lines, with different levels of depletions of Ku80 or RAD51 proteins. Cell lines were selected with moderate/minor levels of depletions, to mimic real tumours that are only impaired and not depleted of proteins in either DSB repair pathway (termed Ku80KD or RAD51KD in this thesis). The first agent tested was imatinib, previously established to be targeting homologous recombination (Choudhury *et al*, 2009), with the hypothesis that it would radiosensitise cells impaired in NHEJ pathway function (here represented by Ku80KD) more than cells impaired in HR (RAD51KD). Indeed, imatinib effectively radiosensitised the Ku80KD cells, and less so parental RT112 cells at both IC_{10} and IC_{40} doses, while RAD51KD cells were not sensitised at all at the lower dose (IC_{10}). At higher doses (IC_{40}) the effect on the Ku80KD cells was even greater, with a limited effect observed in RAD51KD cells and RT112 cells, reported in Qiao *et al* (2013).

These results are consistent with our hypothesis and confirmed the synthetic lethality phenomenon in bladder cancer cells. This may be due to the fact that Ku80KD cells have to rely heavily on the HR pathway to repair DNA DSB caused by ionising radiation. When imatinib targets HR, the tumour cells have both pathways impaired so unrepaired DSB damage accumulates, resulting in greater cell kill. In contrast, RAD51KD cells already have HR impairment and the addition of an HR-targeting agent therefore does not cause much additional cell kill.

Having established this cell system, panobinostat was then tested in order to establish which pathway is panobinostat's major target. Without panobinostat, Ku80KD cells are intrinsically more radiosensitive, whereas RAD51KD and RT112 cells have similar radiosensitivities. This finding may reflect the fact that the HR pathway is the less

important IR damage repair pathway in higher eukaryotes, since NHEJ is active throughout the cell cycle, but HR is only active in S/G2 phase (Rothkamm *et al*, 2003). Even at the lower 10 nM dose panobinostat was a more efficient radiosensitiser in Ku80KD cells, compared to the RAD51KD or RT112 cells. This observation may be due to the greater cytotoxicity of panobinostat (IC_{10} = 5 nM in Ku80KD, compared to 10 nM in RT112 cells) in Ku80KD cells and consequential greater cell death in clonogenic assay, compared with the RT112 cell line. In terms of the SER, this was greater for the Ku80KD cells at the 10 nM dose (IC_{20}) compared with RT112 cells at 25 nM (IC_{40}), at 1.35 and 1.31, respectively. This indicates that it is not only the drug's cellular cytotoxicity but some other mechanisms which are contributing to the greater radiosensitisation. In terms of the synthetic lethality concept, the impact of the drug on the HR pathway could be causing additional radiosensitisation in Ku80KD cells, but not in the other two.

There are some shortcomings of the stable-KD models used in this thesis. For example, Ku80 is a very abundant protein, and modest downregulation may only have limited effects. Since cells with only moderate KD were used for both the Ku80KD model and the RAD51 KD model, it is therefore important for the future panobinostat work to test bladder cancer cells with a higher level of Ku80 or RAD51 KD. Alternative models can also be exploited, for example a transient siRNA RAD51 KD system or an inducible shRNA system. This could also be approached using cell lines that are known to be defective for a component of either the NHEJ or HR pathways.

Investigation of panobinostat's effects on the key NHEJ and HR proteins by western blotting proved to be consistent with the radiosensitising effects observed by clonogenic assay and the hypothesis of synthetic lethality. Panobinostat caused a dose-dependent downregulation of the key HR proteins, RAD51 and CtIP, even at 10 nM doses in all of the studied cell lines, whereas no effects on the levels of Ku70/80 proteins could be observed, even at doses well beyond the IC_{50} dose in RT112 cells.

To examine this phenomenon further, cell lines were also irradiated after panobinostat treatment and samples collected several hours later. The levels of RAD51 proteins were

attenuated in all the post-irradiation samples. Similarly, attenuation of CtIP levels was observed. In contrast, protein levels of a key NHEJ protein, DNA-PK, were unchanged post-panobinostat treatment, with or without irradiation. Moreover, the levels of Ku70/80 proteins over the three studied bladder cancer cell lines were unchanged in a similar treatment protocol. These observations are supportive of the HR pathway being targeted in panobinostat-treated bladder cancer cell lines and the effects on HR contributing to the radiosensitisation. Indeed, one other report has shown radiosensitisation of multiple myeloma cells by low dose SAHA, through blocking the RAD51 response to irradiation (Chen *et al*, 2012). Furthermore, the CtIP protein is essential for efficient HR (Sartori *et al*, 2007), and cells from patients with a *CtIP* gene mutation, producing inefficient truncated CtIP protein, are hypersensitive to DNA damage (Qvist *et al*, 2011).

A significant downregulation of CtIP gene expression was observed in RT112 cells at 25 nM panobinostat treatment without irradiation, but no significant patterns were observed in irradiated samples. However, a significant upregulation of the CtIP gene was seen post-irradiation in CAL29 cells, even after treatment with panobinostat, suggesting that effects on CtIP are cell line dependent and that gene transcription is not the only factor that can influence CtIP protein levels. RAD51 gene transcription was also studied, with no significant effects on gene transcription seen in RT112 or CAL29 cells post-irradiation. These results imply that some other mechanism, possibly post-transcriptional, plays a role in the marked downregulation of RAD51 protein that was observed.

However, while almost no radiosensitising effects were observed in imatinib-treated RAD51KD cells, panobinostat did cause radiosensitisation of RAD51KD cells, to a similar extent to that seen in RT112 cells. Some effects on the NHEJ pathway could therefore be expected. Perhaps this observation indicates that while the effects of panobinostat cannot be observed in terms of protein level changes, there may be a post-translational modification of the protein, such as acetylation, which downregulates protein function. Indeed, Rosato *et al* have shown that the HDAC inhibitor dacinostat causes Ku70 protein acetylation, resulting in impaired Ku-DNA binding and also an impaired Ku70-Ku80 interaction (Rosato *et al*, 2008).

In the thesis 30% RAD51 KD was used, which is a level that might be insufficient to achieve an HR deficiency phenotype. For example, Quiros *et al* (2011) have reported on various levels of RAD51 KD in combination with IR, and found that the KD to 30% in glioma cells only slightly increases radiosensitivity of those cells, with radiosensitivity increasing slightly with greater amounts of KD. Similarly, in the RAD51 KD cell lines, chemosensitisation with various agents can be achieved, which is something that was not observed with panobinostat (the IC_{50} dose was similar to parental RT112 cell line). Furthermore, Short *et al* (2011) have also confirmed this observation in glioma cells, with RAD51 KD levels inversely correlating with radiosensitivity and also chemosensitivity to temozolomide. Also, Ko *et al* (2008) found RAD51 KD to make lung cancer cells sensitive to gefitinib.

The reasons why some of the phenomena were not observed in the thesis study might be a relatively moderate KD level. It is also a difficulty to maintain constitutive RAD51 downregulation in a stable state for longer periods, since cells that escape RAD51 depletion can outgrow the depleted cells. It is therefore crucial for the future, to test panobinostat also in cells, with greater RAD51 KD and in transient KD models (discussed elsewhere). The issues addressed above make it difficult to interpret the results of experiments performed to understand the mode of action of panobinostat. Other assays should be used to test if such RAD51 depletion causes any major functional impairment of the HR pathway.

Therefore, to more comprehensively examine panobinostat's effects on the HR and NHEJ pathways, several other approaches need to be taken. A reporter assay could be established in bladder cancer cells, testing for the efficiency of HR and NHEJ using the I-SceI based assay used in the lab of Vera Gorbunova (Mao *et al*, 2008). Also, we have a NHEJ/MMEJ plasmid-based assay established in our lab, to test cell free extracts from cells treated with panobinostat. This could determine whether the NHEJ pathway in treated samples is intact or whether panobinostat is driving cells to use the less accurate MMEJ pathway.

Acetylation of proteins could be examined by immunoprecipitating lysed cells using an antibody against the protein of interest, and immunoblotting the membrane with a suitable anti-acetyl antibody. Furthermore, changes in protein-DNA interactions could be studied using the electrophoretic mobility shift assay (EMSA). Panobinostat's effect on the HR or NHEJ pathways could also be tested using an immunofluorescent foci assay, in order to detect potential disruptions in pathway events.

In conclusion, muscle invasive bladder tumours are deficient in NHEJ pathway function, and they all show a MMEJ phenotype in the *in vitro* NHEJ assay, with impaired Ku-DNA binding and aberrant *TP53* function (Bentley *et al*, 2004, 2009). An agent which targets the HR pathway would be a good therapy for these types of tumours. Panobinostat proved to be an efficient radiosensitiser in bladder cancer cells. It was shown to target the HR pathway more in bladder cancer cells and, therefore, the "synthetic lethality" phenomenon could be exploited in muscle invasive bladder tumours. This potential novel therapeutic approach will need to be tested in mouse xenografts, to confirm panobinostat's "synthetic lethal" action towards the bladder cancer cell lines. If successful, the work could be taken forward to early phase clinical trials in bladder cancer patients.

CHAPTER 5: PANOBINOSTAT AND DNA DAMAGE: EFFECTS UPSTREAM OF NHEJ AND HR PATHWAYS

5.1 Introduction

The MRN complex plays a key role in the multiple steps involved in DNA DSB detection, signalling and repair. The complex plays a role as a sensor and recruiter to DSB sites, whereby the NBS1 protein brings the ATM protein to the DSB sites. ATM then self-phosphorylates and becomes active (Berkovich *et al*, 2007; Lee & Paull, 2007). Activated pATM then phosphorylates H2AX histones (γH2AX). γH2AX regulates DSB repair by attracting repair factors and more MRN complex molecules to the damage site and once the break is repaired it becomes dephosphorylated (Iijima *et al*, 2008; Rupnik *et al*, 2008). H2AX can also be phosphorylated by the ATR protein, involved in ssDNA signalling, and also DNA-PK, involved in the NHEJ pathway.

The MRN complex also has an important function in DSB end stabilisation via MRE11, and via an endonuclease activity, facilitated by the CtIP protein, it directs DNA end resection, leading to formation of a 3'-overhang, which is a crucial step before the search for homologous sequence can be initiated (Williams *et al*, 2010; Polo & Jackson, 2011). This step determines whether the HR pathway is used for DSB repair, but this process can later convert end joining to MMEJ, if HR is abrogated (Mladenov *et al*, 2013).

The aim of the experiments presented in this chapter was to examine the effects of panobinostat on DNA DSB signalling events upstream of DSB repair by HR or NHEJ, where the MRE11/NBS1/RAD50 complex is central to those signalling events. Effects of panobinostat on the proteins of the MRN complex and their gene expression were therefore studied. γH2AX foci were studied by using confocal microscopy as a tool to study DSB induction and repair (dynamics over time) after cells were exposed to irradiation, panobinostat or a combination of both. Expression of the *HDAC1-11* genes were tested in the bladder cancer cell lines used in this thesis, and also in normal human

urothelial cells (NHU), to determine the levels of HDAC mRNA present in the cells and to detect potential panobinostat effects on *HDAC* expression.

5.2 Results

5.2.1 Panobinostat and effects on the MRE11/RAD50/NBS1 complex

As the MRN complex has important roles both upstream in DSB signalling and downstream in DSB repair, the effects of panobinostat on the MRN complex were tested using 24 h panobinostat of doses up to 100 nM. Downregulation of NBS1 protein expression in RT112 cells was observed on western blot at 25 nM and above. Similarly, effects on MRE11 could be detected, but at doses as low as 10 nM. Acetylation of histone H3K18 expression, which was markedly increased at 10 nM and higher doses, was used to confirm the action of panobinostat. In order to see if panobinostat also has any effects on DSB formation, changes in γH2AX expression were tested. The expression levels were upregulated in a panobinostat dose-dependent manner, with some increase in H2AX phosphorylation detected already at 10 nM and marked upregulation at 25 nM and beyond (Figure 5.1A).

Effects on RAD50 protein expression were also tested in RT112 cells, and neither 10 nM nor 25 nM panobinostat had any observable effect. Furthermore, cells were also irradiated with 5 Gy, the medium changed and cell pellets harvested 4 and 8 hours later, with no effect at either timepoint on the levels of RAD50 protein (Figure 5.1B); see later for same experiments for MRE11 and NBS1 (Figure 5.5).

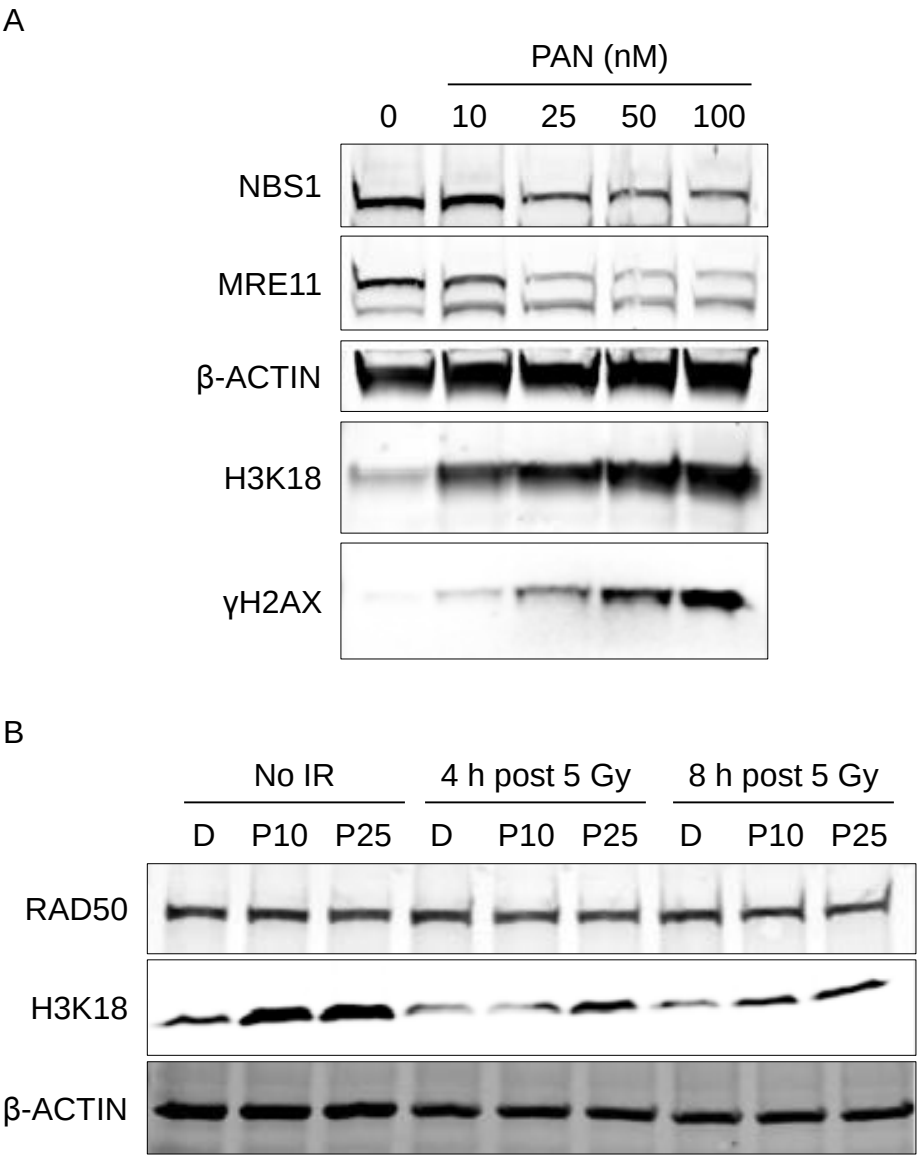


Figure 5.1. Panobinostat causes downregulation of MRE11 and NBS1 proteins in a dose-dependent manner.
A) Western blot of expression from RT112 cells treated with DMSO (D) or panobinostat (PAN or P) for 24 h. Acetylation of histone H3K18 was used to mark panobinostat's activity. Levels of phosphorylated H2AX (γH2AX) as a marker of DSB were also tested. B) RT112 lysates were blotted for RAD50 protein expression, cells were treated with panobinostat (PAN) or DMSO (D) for 24 h and harvested, or irradiated with 5 Gy, medium changed and harvested 4 and 8 h later.

5.2.2 Panobinostat increases the amount of γH2AX in cells

Western blots were used to determine the overall amounts of γH2AX in cells. As the levels were found to increase in a panobinostat dose-dependent manner (Figure 5.1A), this was further tested in RT112 cells treated with either DMSO or panobinostat plus irradiation (5 Gy). One, 2 and 4 hours-post irradiation, an upregulated γH2AX signal was observed in both the DMSO and panobinostat-treated samples, with a stronger effect in the panobinostat treated samples (Figure 5.2A).

In a subsequent experiment, RT112 cells were treated with DMSO or panobinostat (dose range 10 nM, 25 nM and 50 nM), as per the previous experiment and harvested at 8 h or 24 h post-IR. Compared to the DMSO samples, panobinostat samples still displayed elevated γH2AX at 8 h but by 24 h the γH2AX signal for the 25 nM and 50 nM samples was much lower than at 8 h (Figure 5.2B).

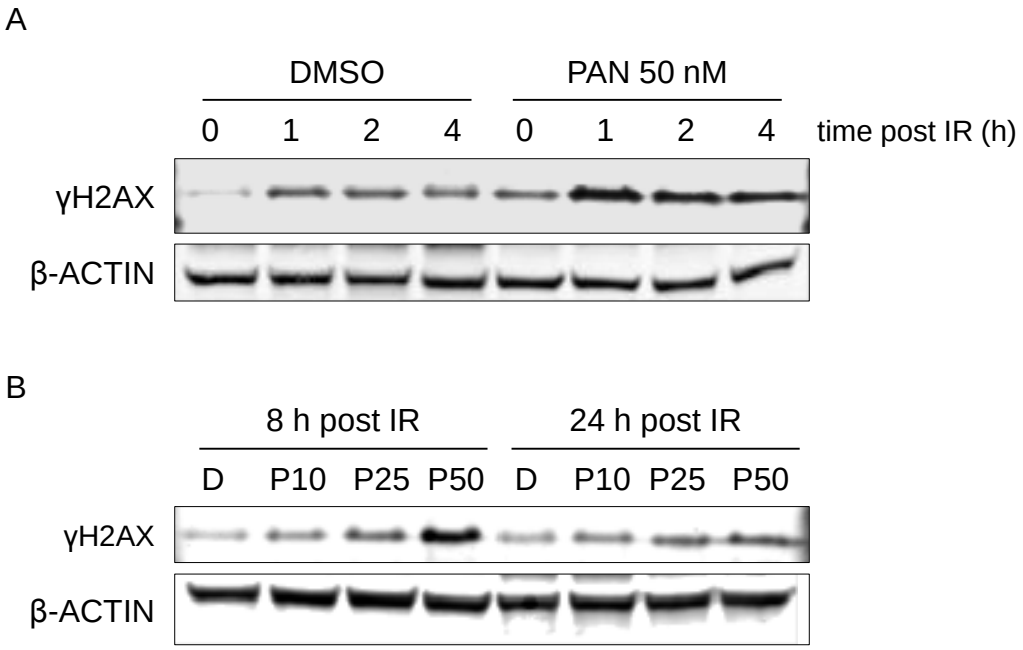


Figure 5.2. Induction of γH2AX after panobinostat treatment and irradiation.
A) Western blot showing induction of γH2AX at 1, 2 and 4 hours post-5 Gy irradiation in DMSO (D) and panobinostat (P) treated samples for 24 hours. Medium was removed, cells washed twice with PBS and harvested at timepoints indicated. B) Cells were prepared in the same way as in (A), but were treated with panobinostat and harvested at 8 and 24 hours post-5 Gy irradiation.

5.2.3 Panobinostat induces an increase in γH2AX foci

Since the amount of γH2AX signal was upregulated in panobinostat samples, γH2AX foci formation in RT112 cells was also tested also using confocal microscopy. A significant increase in the number of γH2AX foci per cell with panobinostat treatment, over a dose range up to 50 nM for 24 h, was detected, compared with the DMSO control. The number of cells with higher numbers of foci per cell increased over the dose range and the proportion of γH2AX negative cells fell (the cut-off number for an individual cell to be positive was 6 foci or more) (Figure 5.3).

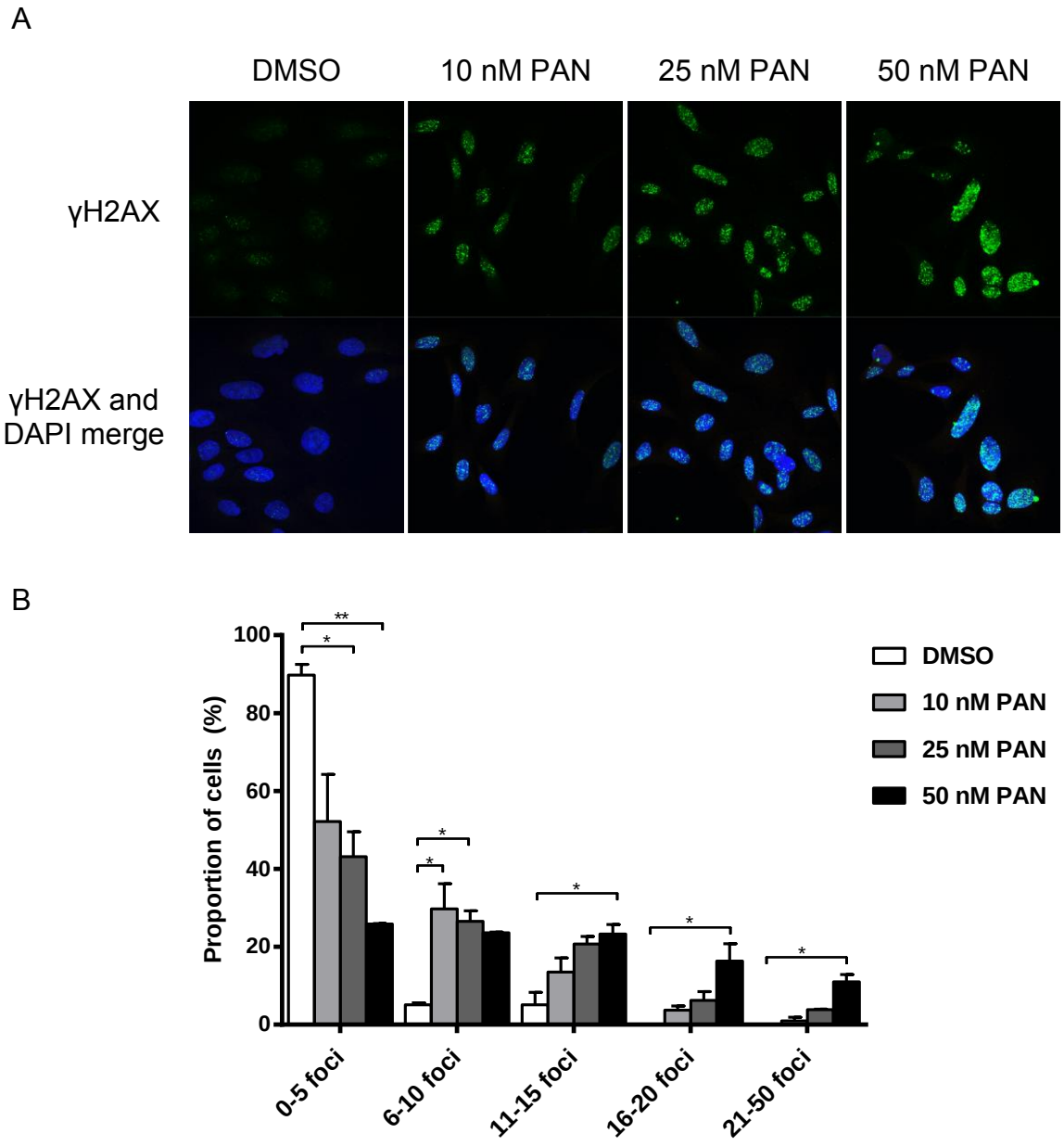


Figure 5.3. Panobinostat causes an increase in γH2AX foci in a dose-dependent manner.
A) Confocal microscopy images of RT112 cells treated with DMSO as a vehicle control or increasing concentrations of panobinostat (PAN) for 24 h. Slides were stained with DAPI and monoclonal anti-γH2AX antibody. B) Quantification of slides based on the number of foci per cell. Seventy to 100 cells were analysed per sample. Mean and SEM of two experiments are presented. One-way ANOVA, Bonferroni's multiple comparisons test over DMSO control; * $p < 0.05$, ** $p < 0.01$, *** $p < 0.001$.

5.2.4 Panobinostat delays γH2AX foci repair post-irradiation

To study the time course of repair of γH2AX foci following drug treatment, cells were first treated with DMSO or panobinostat for 24 h and then irradiated with 5 Gy. The medium was removed and cells washed twice with PBS and fresh medium added. The slides were processed for immunofluorescence microscopy 0.5, 1, 4, 24 and 48 hours later.

A rapid induction of the γH2AX signal in cells was observed as early as 0.5 h post-irradiation in both panobinostat- and DMSO-treated samples. Similarly, at the 1 h timepoint, signal was strongly present in all cells (Figure 5.4A). Quantification of cells positive for γH2AX foci (6 foci or more) revealed that at both timepoints all cells (100%) were positive in both cases (Figure 5.4B). At the 4 h timepoint, signal was still strongly present in panobinostat-treated cells, but less so in the DMSO samples. Quantification of foci showed 97% of cells treated with panobinostat to be γH2AX positive, but only 65% in the DMSO treated samples. This decrease in γH2AX positive cells indicates some repair. At the 24 and 48 h timepoints, more foci were still unresolved in panobinostat-treated samples. The levels were slightly lower than the level of the unirradiated panobinostat samples at 48 h, probably reflecting the fact panobinostat had been washed off the cells 48 hours previously. In the DMSO sample, foci levels had returned to the level of the unirradiated sample (Figure 5.4B). Therefore, a repair delay was detected in panobinostat treated samples at 4 hours.

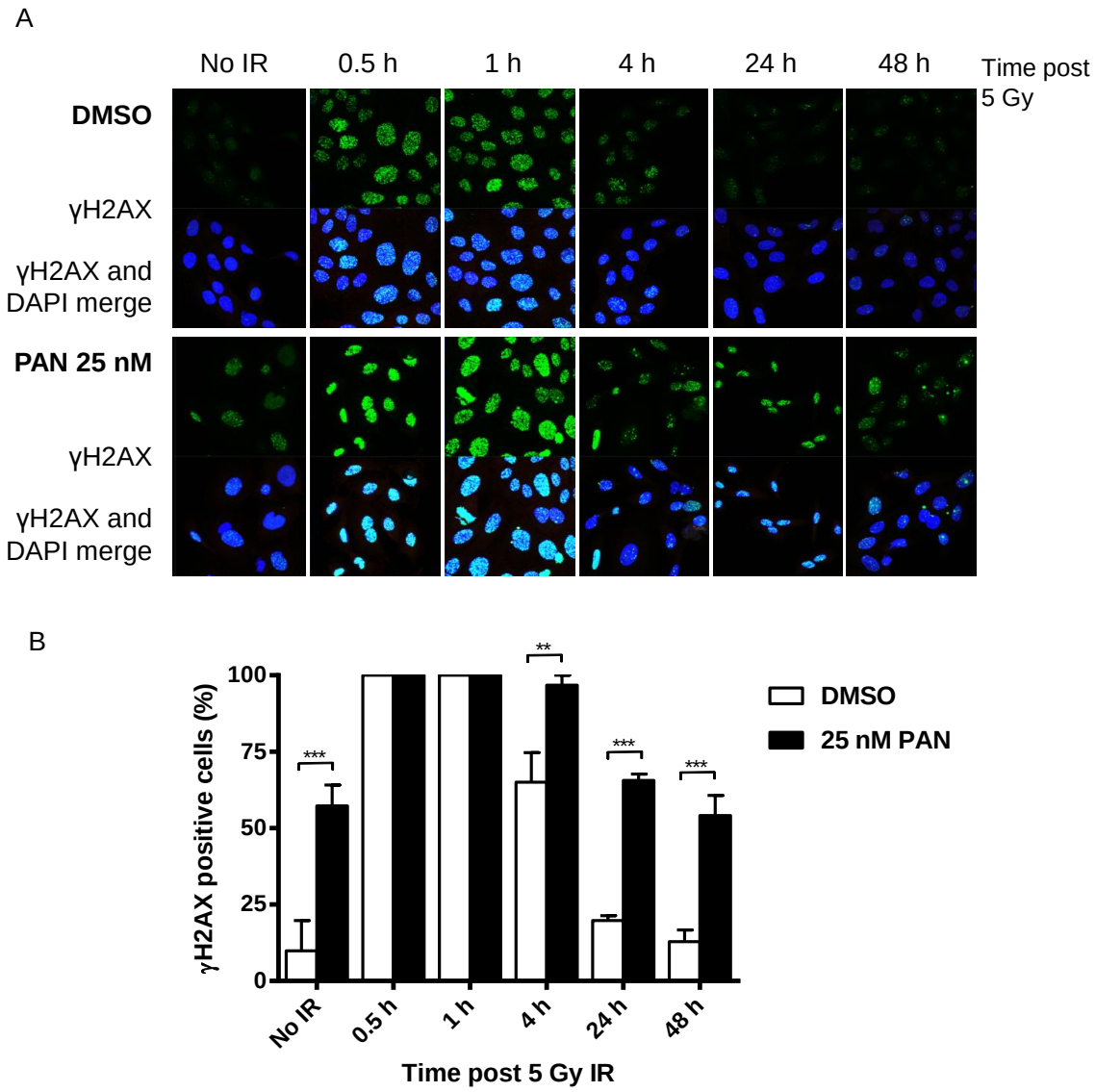


Figure 5.4. Panobinostat causes post-irradiation γH2AX foci resolution delay.
A) RT112 cells were treated with 25 nM panobinostat for 24 h and either harvested or irradiated with 5 Gy, medium removed, cells washed twice with PBS and then harvested at 0.5, 1, 4, 24 or 48 h timepoints. B) Quantification of foci number from (A) with bars representing mean of γH2AX cells positive (6 foci or more) from two independent experiments. Error bars represent SEM. Seventy to 100 cells were counted per slide. Two-way ANOVA, Bonferroni's multiple comparisons test over DMSO control; * $p < 0.05$, ** $p < 0.01$, *** $p < 0.001$.

5.2.5 Effects of panobinostat on NBS1 and MRE11

Panobinostat caused downregulation of the MRE11 and NBS1 proteins in a dose-dependent manner (Figure 5.1) and also γH2AX foci repair delay in RT112 cells. In order to test if panobinostat also causes a decrease in MRE11 and NBS1 following ionising radiation, RT112 and T24 cells were either treated with 10 nM or 25 nM panobinostat and CAL29 with 5 nM or 10 nM panobinostat for 24 h prior to processing, or cells were treated and subsequently irradiated with 5 Gy, prior to collection 4 and 8 hours later.
In RT112 cells, MRE11 and NBS1 protein levels in the DMSO treated samples did not increase after irradiation, whereas MRE11 protein levels in CAL29 did increase slightly at 8 h post-IR. In T24 cells, a slight increase in MRE11 and NBS1 was detected in irradiated DMSO control samples.

In panobinostat-treated RT112 lysates, some reduction in MRE11 and NBS1 protein expression levels at 4 h and 8 h timepoints were seen (Figure 5.5A). In CAL29 cells treated with only panobinostat, a decrease in NBS1 protein was detected at the 10 nM dose (IC_{50} dose) and similarly at 4 and 8 hours post irradiation, whereas convincing downregulatory effects on the MRE11 protein were observed-post irradiation, at the 8 hour timepoint (Figure 5.5B).

In T24 cells both NBS1 and MRE11 proteins levels slightly decreased upon panobinostat treatment at 10 nM (IC_{10}) and 25 nM (IC_{30}) doses, with similar effects post-drug/IR in combination (Figure 5.5C).

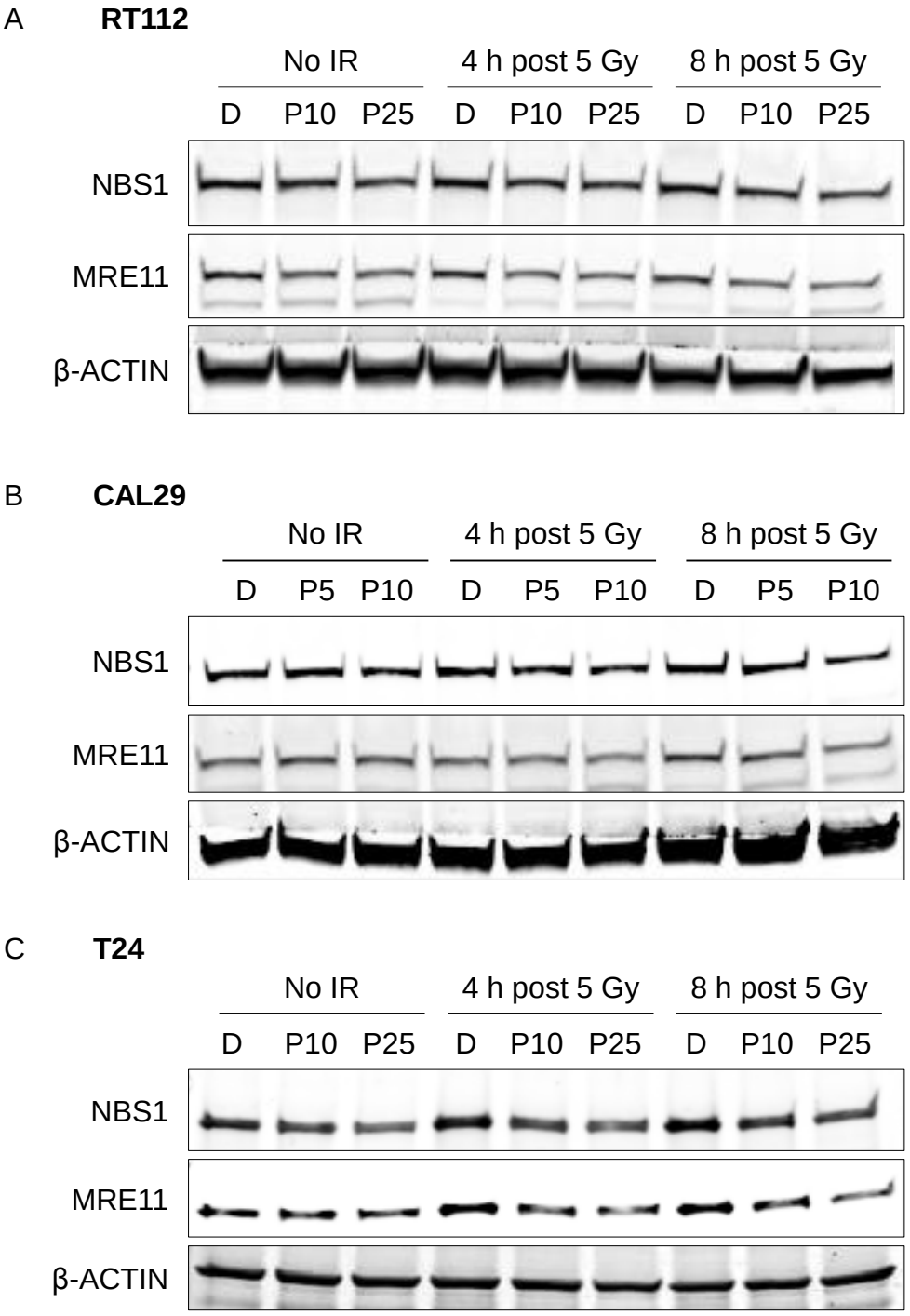


Figure 5.5. Effects of panobinostat on MRE11 and NBS1 protein expression in bladder cancer cells.
Western blot showing expression of MRE11 and NBS1 in RT112 (A), CAL29 (B) and T24 cells (C). Cells were treated with DMSO (D), panobinostat (P) and harvested, or then irradiated (5 Gy), medium removed, plated twice washed with PBS and harvested as indicated.

In order to exclude the effects of DMSO over time on the MRN complex levels in the bladder cancer cells shown in Figures 5.1 and 5.5, a control experiment was performed. Here cells were treated with DMSO for 24 h, medium removed and cells harvested as indicated. The MRN protein levels were constant over the timepoints used (Figure 5.6).

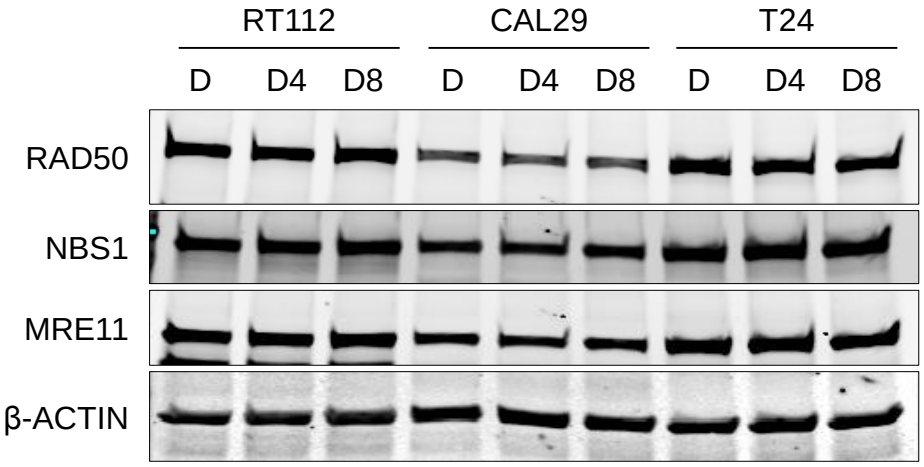


Figure 5.6. Control western blot for MRN complex in cells, treated with DMSO. RT112, CAL29 and T24 cells were treated with DMSO for 24 h, and medium changed. Cells were harvested 0, 4 or 8 hours later.

5.2.6 Panobinostat and transcription of MRE11/NBS1/RAD50 genes

Since panobinostat treatment caused some effects on MRE11 and NBS1 protein levels, the effects on *MRE11/RAD50/NBS1* complex gene transcription were also evaluated in RT112 and CAL29 cells. Cells were treated with panobinostat for 24 h and either mRNA harvested, or the cells were irradiated (5 Gy), the medium removed, dishes washed as per protocol, fresh medium added and RNA harvested 4 h later.

No significant change was detected in *MRE11* gene expression with panobinostat treatment alone or in combination with irradiation in either cell line (Figure 5.7).
In RT112 cells, *RAD50* expression was upregulated by 22% by 10 nM panobinostat and by 12% for the combination of panobinostat and irradiation. In CAL29 cells, the same dose (but higher IC dose) increased *RAD50* expression by 26% and in the irradiated samples by 48% (Figure 5.7). In contrast, *NBS1* gene expression was downregulated in

RT112 by 32% by 10 nM and by 52% by 25 nM. In the RT112 sample treated with 25 nM panobinostat + IR, *NBS1* expression was decreased by 25%. The effects were less marked in CAL29 cells, with the only significant downregulation being in the 5 nM drug sample with *NBS1* downregulated by 18%.

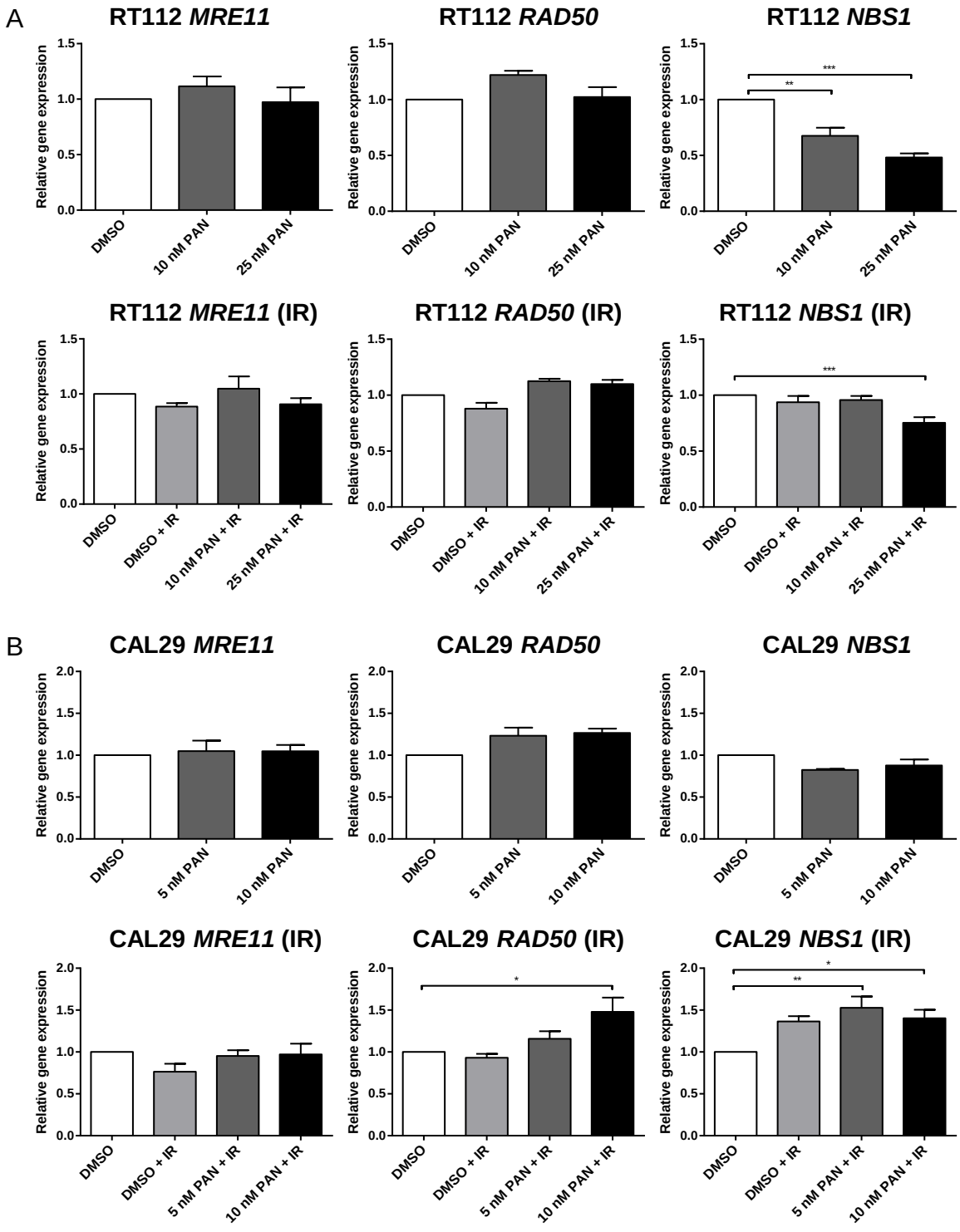


Figure 5.7. Transcription of *MRE11/RAD50/NBS1* genes after panobinostat alone or in combination with 5 Gy irradiation.
mRNA expression levels were measured by qPCR for *MRE11, RAD50* and *NBS1* in RT112 (A) and CAL29 (B) cells. The expression levels for each cell were normalised against those of GAPDH and the expression levels compared to the DMSO treated sample. The bars represent mean and SEM of three independent experiments. One-way ANOVA, Bonferroni's multiple comparisons test over DMSO control; * $p < 0.05$, ** $p < 0.01$, *** $p < 0.001$.

5.2.7 Modulation of HDAC gene transcription by panobinostat

Panobinostat is an established pan-HDAC inhibitor. HDAC inhibitors are known to affect gene transcription (see HDAC inhibitors and effects on gene transcription). We were therefore interested to know whether panobinostat causes any effects on the transcription of HDACs. In this thesis only effects on HDAC transcription were tested, but the analysis of HDAC protein levels should also be undertaken. In order to determine panobinostat's effects on *HDAC* gene expression, transcription of all 11 *HDAC* genes was assessed in untreated (DMSO) and panobinostat-treated RT112, CAL29 and T24 bladder cancer cell lines and in one normal human urothelial (NHU) cell line. The dose of 50 nM was used, just above the IC_{50} value in all the studied cell lines. Since the IC_{50} for NHU cells could not be established by clonogenic assay (NHU do not form colonies without feeder cells), the 50 nM concentration was used as a clinically achievable and relevant dose.

First, expression of the *HDAC1-11* genes in the untreated (DMSO) samples was measured and calibrated to GAPDH expression, for direct comparison among all the cell lines. In Figure 5.8, the *HDAC* expression profile is represented for each cell line. Among the cell lines, *HDAC1* and *HDAC2* were the most highly expressed (up to one order of magnitude higher than next highest, *HDAC3*) and *HDAC5* and *HDAC11* were the lowest expressors, although there was some variation among the cell lines, e.g. high *HDAC9* in CAL29 cells.

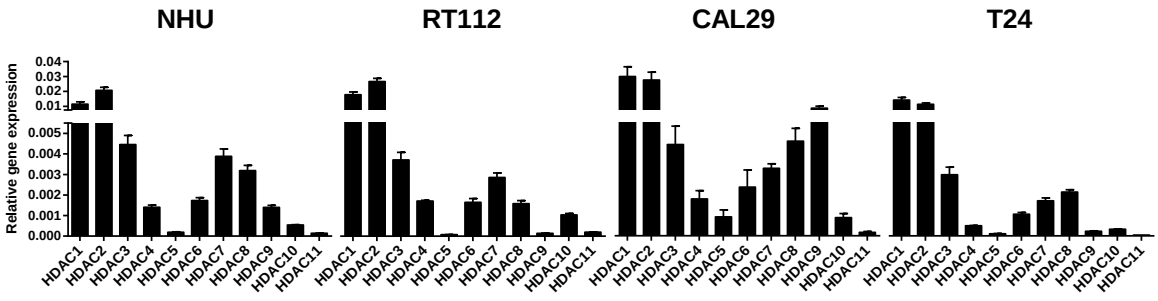


Figure 5.8. *HDAC* expression in normal human urothelial (NHU) and RT112, CAL29 and T24 bladder cancer cell lines.
qPCR was performed in control (DMSO treated) cells. Relative gene expressions were normalised and calibrated to GAPDH levels. Error bars represent SEM of three independent experiments.

The data from the Figure 5.8 was also represented for each *HDAC* with the four cell lines separately to allow for ease of comparisons (Figure 5.9). *HDAC1* was upregulated in RT112 and CAL29 cancer cells compared with NHU cells, but the results were barely significant. Generally, the lowest expression values for all *HDAC* genes were detected in T24 cancer cells. These results show that the expression of *HDAC* genes varied among all the cell lines and did not indicate any consistent pattern of up- or downregulation between NHU and tumour cell lines.

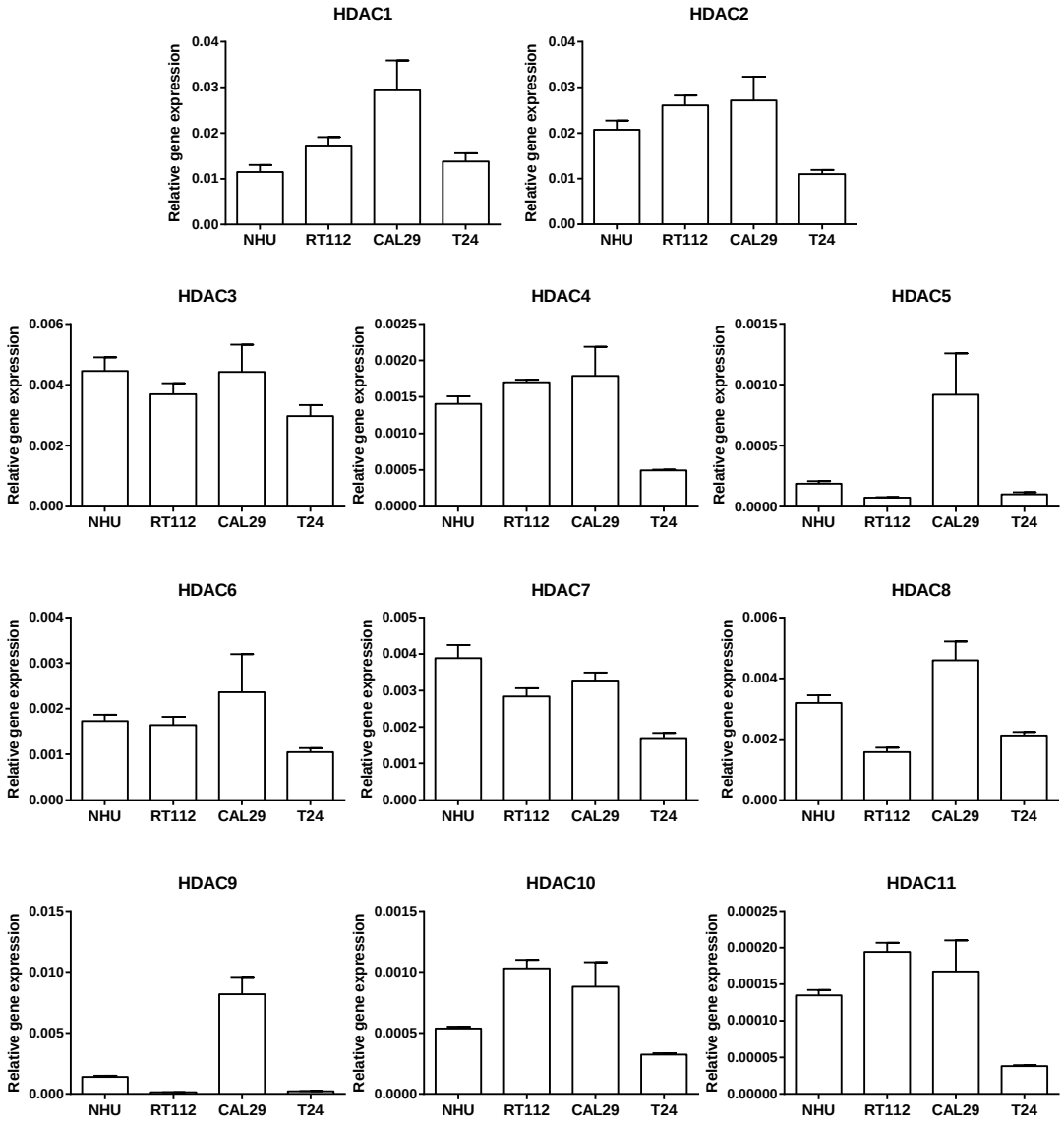


Figure 5.9. Comparisons of *HDAC* gene expressions between the cell lines.
qPCR gene expression of *HDACs 1-11* in DMSO treated normal human urothelial (NHU) cells, RT112, CAL29 and T24 bladder cancer cells. Relative gene expression levels were normalised and calibrated to GAPDH expression levels. Error bars represent SEM of three independent experiments.

Effects of panobinostat on *HDAC1-11* expression were also determined and compared to the DMSO control cells, as shown in Figure 5.10. Panobinostat did not show a consistent pattern of effects on *HDAC* gene expression. Panobinostat caused downregulation of some *HDACs*, but also caused upregulated expression of other *HDAC* genes. These effects were also present in the NHU cell line. The most notable effects of panobinostat on the HDAC gene expression were as follows:

HDAC2, *HDAC7* and *HDAC10* were downregulated in all cell lines, with the most notable and highly significant downregulation in *HDAC7* expression. The effect was much more potent in RT112, CAL29 and T24 cancer cells, where the expression reductions were 14-, 27- and 22-fold, respectively, compared to the untreated cancer cells, whereas in the NHU cells, the *HDAC7* expression reduction was only 1.5-fold in the panobinostat-treated sample.

Marked upregulation of *HDAC5* was detected in all treated cancer cells and the NHU's, but the baseline expression levels of *HDAC5* in studied cells were very low.

The expression of the remaining HDAC's was variable. In T24 cells there was a general downregulation of all the remaining *HDACs*, while there was upregulation in both RT112 and CAL29 of *HDACs 1*, *3*, *4* and *11*, upregulation in RT112 but downregulation in CAL29 of *HDAC6* and *9*, and downregulation in RT112 but upregulation in CAL29 of *HDAC8* (not all effects statistically significant).

Due to the complexity and amount of the data to be represented, panobinostat results were also represented as a fold change, compared to the expression of the untreated NHU for each *HDAC* (set as 0 change) on the $\log_2$ scale (Figure 5.11).

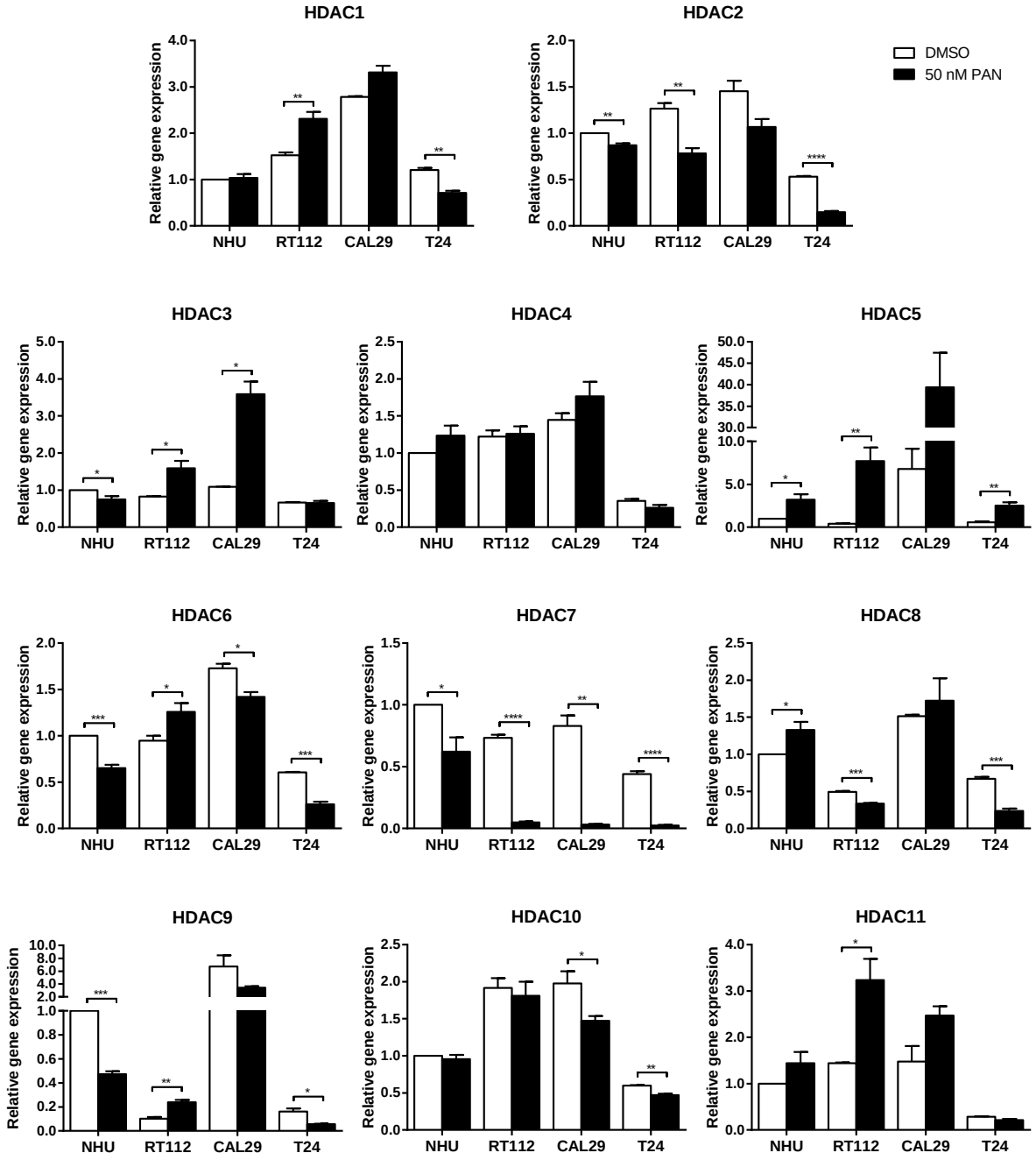


Figure 5.10. Expression of 11 *HDAC* genes with or without panobinostat treatment. qPCR expression of *HDACs 1-11* in untreated or 50 nM panobinostat-treated normal human urothelial cells (NHU), RT112, CAL29 and T24 bladder cancer cells. Relative gene expression was normalised to *GAPDH* from untreated NHU cells (set as 1). Error bars represent SEM of three independent experiments. Two-tailed t-test over DMSO control; * $p < 0.05$, ** $p < 0.01$, *** $p < 0.001$, **** $p < 0.0001$.

Figure 5.11 shows a heterogeneous pattern of *HDAC* expression over all the cell lines, with panobinostat causing decreased and also increased expression of different *HDAC*

genes. The most notable result, consistent in all the cancer cells, but with minimal effect in NHU cells, is the expression of *HDAC7.*

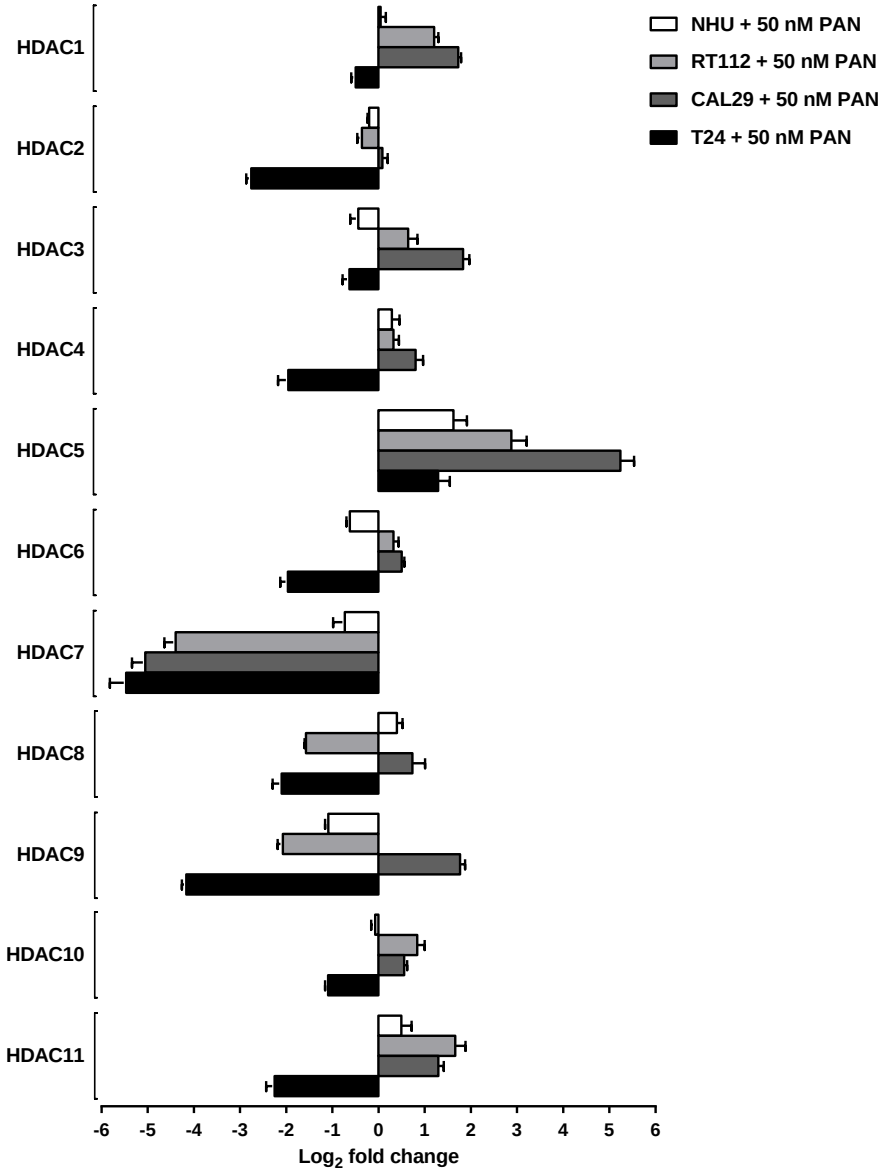


Figure 5.11. Effects of panobinostat on *HDAC* gene expression.
qPCR expression of *HDACs 1-11* in panobinostat-treated normal human urothelial cells (NHU), RT112, CAL29 and T24 bladder cancer cells. Relative gene expression was normalised to *GAPDH* from untreated NHU cells (set as 0) on the $\log_2$ scale. Error bars represent SEM of three independent experiments.

5.3 Discussion

The experiments in this chapter were carried out in order to further investigate the effects of panobinostat upstream of the HR and NHEJ repair pathways and also the effects which could explain the radiosensitisation of bladder cancer cells by panobinostat. To date, bladder cancer cells have not been studied in combined low-dose HDAC inhibitor-irradiation treatments, and only recently the radiosensitising effects of “low dose” panobinostat have been reported in prostate carcinoma cells (the authors in this study used panobinostat in the micromolar range, which is very inconsistent with other reports of panobinostat use, see Discussion of the first Results chapter) (Xiao *et al*, 2013).

In terms of the MRN complex, panobinostat’s effects on any of the proteins of the MRN complex have not yet been described in the literature. However, several reports have described the effects of HDAC inhibitors on the levels of MRE11 and RAD50 proteins, whereas NBS1 protein downregulation upon treatment with these inhibitors has not yet been described in the literature. Vorinostat downregulated MRE11 and RAD50 levels in prostate and non-small cell lung carcinoma cells, an effect limited to the cancer cells, as it was not seen in normal human foreskin fibroblasts (Lee *et al*, 2010). Furthermore, dacinostat treatment had downregulatory effects on RAD50 protein levels in leukaemia cells (Rosato *et al*, 2008) and vorinostat in melanoma cells, alone or 4 h post-irradiation (Munshi *et al*, 2006).

Panobinostat caused some decrease in two proteins of the MRN complex, NBS1 and MRE11 in a dose-dependent manner in RT112 cells, but RAD50 protein levels appeared unchanged. Whereas both MRE11 and NBS1 were downregulated in T24 bladder cancer cells, only NBS1 was downregulated in CAL29 cells. Effects were also tested 4 and 8 h after 5 Gy irradiation in all cell lines. Interestingly, the levels of MRE11 and NBS1 were not upregulated in the RT112 cell lysates treated with IR alone. However, decreased levels of MRE11 and NBS1 were observed at those two timepoints, in drug/IR treated samples. In the T24 cells, the levels of MRE11 and NBS1 in the irradiated samples did increase

slightly, but the levels of the proteins were abrogated in panobinostat-treated samples compared with the DMSO-treated samples.

The MRN complex has a crucial role in the initiation of DSB detection and also in the recruitment of the ATM protein to sites of DSB, resulting in the phosphorylation of the H2AX histone, to become γH2AX. Furthermore, the MRN complex is also involved in DSB end-resection and the binding of DNA ends together (Rupnik *et al*, 2010). It also serves as a platform for other repair proteins that get recruited to the DSB sites.

Although protein levels of the MRN complex components were downregulated by panobinostat, induction of γH2AX in panobinostat-only treated cells was detected, indicating that MRN complex function "upstream" of this event may be functional despite panobinostat treatment. This implies that the MRN complex has two major roles, both upstream of DSB repair, the signalling function (intact here), and also a "downstream" nuclease component (this function will be discussed below). Consistent with this, previous reports have stated that the nuclease function of the MRN complex is not essential for the signalling of DSB, but only for the DSB repair (Williams *et al*, 2008; Rupnik *et al*, 2010). Another explanation for this functional induction of H2AX histones is the fact that they can also be phosphorylated by two other kinases, the ATR and also DNA-PK. DNA-PK was also tested in panobinostat treatment experiments and the levels did not change, as shown in the previous Results chapter. The effects on the ATR kinase should be studied to fully test this hypothesis.

It has been determined that NBS1 is needed for MRE11's nuclease activities (Paull & Gellert, 1999). Since the levels of NBS1 were reduced after panobinostat treatment, this could possibly impair MRE11 nuclease function. Furthermore, Desai-Mehta *et al* (2001) established that interactions between MRE11 and NBS1 are important for cell survival post-IR. In the present study, panobinostat reduced survival in bladder cancer cells after panobinostat/IR in combination. Reductions in NBS1 and MRE11 protein levels were also observed. Decreased protein levels could lead to impaired MRE11-NBS1 interactions, or perhaps panobinostat can cause some post-translational modifications of these two

proteins, resulting in lower protein-protein interactions and hence decreased post-IR survival. Trujillo *et al* (1998) have observed that only a fraction of MRE11/RAD50 complexes interact with NBS1, or is NBS1 substoichoimetric with regards to the other two proteins. Panobinostat could therefore change the stoichiometric balance between the MRN complex proteins by reducing the levels of NBS1 and MRE11, leading to impaired MRN complex function.

The next question is why panobinostat causes γH2AX induction in bladder cancer cells? Changes in γH2AX foci number measured by confocal microscopy or the intensity of western blot signal are accepted methods of studying the dynamics of post-irradiation DNA DSB damage and repair mechanisms (Bonner *et al*, 2008). This marker is well established for studying cells post-IR, but has also been reported for use as a DNA DSB marker with SAHA drug-only treatment (Lee *et al*, 2010; Mah *et al*, 2010).

In the present study, treatment of RT112 bladder cancer cells with panobinostat for 24 h caused a dose-dependent increase in the number of γH2AX foci positive and a drop in γH2AX-negative cells. The effect was seen at low, non-toxic doses and became significant at higher doses. In other reports, small cell lung carcinoma cells treated for 20 h with panobinostat showed a modest increase in the number of γH2AX foci (Geng *et al*, 2006). The HDAC inhibitors SAHA, FK228 and apicidin significantly induced the number of foci in ovarian cancer cells, and the effects correlated with the cytotoxicity of the drug towards the cancer cells (Wilson *et al*, 2011). Lee *et al* tested DNA DSB induction after exposure of prostate cancer, non-small cell lung cancer and normal human fibroblast cell lines to vorinostat for 24 h with replating into HDAC inhibitor-free medium for an additional 48 h. Interestingly, the γH2AX levels quickly dropped in the normal human cells, whereas they persisted in the cancer cells, as confirmed by western blot and also immunofluorescence microscopy (Lee *et al*, 2010).

The present finding of γH2AX induction using panobinostat could imply direct damage to the DNA and induction of DSB by the drug itself, as previously reported for the HDAC inhibitors TSA, apicidin and NaB in leukemia cells (Gaymes *et al*, 2006). Another

explanation could be an indirect mechanism through generation of reactive oxidative species, as described in SAHA-treated SV40-transformed human fibroblasts (Ungerstedt *et al*, 2005) and leukaemia cells treated with the pan-HDAC inhibitor dacinostat (LAQ-824) at minimally toxic doses, leading to DSB DNA damage and γH2AX foci induction (Rosato *et al*, 2008).

Effects of panobinostat on γH2AX foci resolution post-5 Gy were also presented. Irradiation without drug treatment caused enough DSB breaks per cell (approximately 20-40 DSB are created per Gy), for all the cells to be counted as γH2AX positive at 0.5 and 1h timepoints, with similar effects in panobinostat-treated cells. At 4 hours post irradiation, 25 nM panobinostat treated cells showed a significant delay in the repair of γH2AX foci, whereas in DMSO control cells repair was clearly underway. At 24 and 48 hour timepoints there was still a greater proportion of unrepaired foci in the panobinostat-treated cells. This delay in γH2AX resolution in the panobinostat-treated bladder cancer cells indicates impairment of DSB repair, possibly due to panobinostat's effects on the MRN complex protein levels, resulting in impairment of the "downstream" component of the complex function.

In other reports, panobinostat treatment of lung cancer cells for 18 h with 3 Gy irradiation prolonged the duration of γH2AX foci for another 24 hours (Geng *et al*, 2006) and similar effects have been shown for dacinostat in lung adenocarcinoma and large cell carcinoma (Cuneo *et al*, 2007). Breast cancer cells treated with vorinostat for 16 h and then 2 Gy irradiation experienced delayed repair, with significant delay in foci repair up to 48 hours later (Baschnagel *et al*, 2009). It is interesting to note that these residual or persistent γH2AX foci can mark cells with damage that will prove lethal to the cells (Banáth *et al*, 2010; Mah *et al*, 2010; Bourton *et al*, 2011).

The γH2AX foci assay used in our study has some limitations, for example indiscriminate detection of ssDNA and stalled replication forks (Löbrich *et al*, 2010). In order to further confirm the nature of the γH2AX foci, other assays, such as the neutral comet assay

(Singh *et al*, 1988) or pulsed-field electrophoresis could be performed (Schwartz & Cantor, 1984; Turney *et al*, 2012).

In order to examine further why the MRE11 and NBS1 protein levels are downregulated with panobinostat treatment, transcription of the *MRE11, RAD50 and NBS1* genes was studied. *MRE11* transcription levels were not significantly affected either by drug alone or drug + IR. *RAD50* transcription was slightly upregulated in RT112 cells and attenuated in the irradiated sample. In CAL29, RAD50 levels were upregulated in a dose-dependent manner in post-IR samples. With panobinostat only treatment, *NBS1* was significantly repressed in RT112 cells but only slightly in CAL29 cells (the overall trend was not significant). Post-IR a downregulatory pattern could be seen in RT112, but there was upregulation of transcription in CAL29 cells.

Transcription of the *MRE11* gene therefore cannot explain the downregulation of MRE11 protein seen, but rather indicates that this effect is regulated at the post-transcriptional level. This could be further tested using the cycloheximide (CHX) assay. The NBS1 protein level decrease seen in panobinostat-treated cells could be, at least for RT112, attributed to the decreased transcription of *NBS1*. A similar effect on *NBS1* transcription was observed in dacinostat-treated leukemia cells (Rosato *et al*, 2008), but they did not compare mRNA and protein levels. Similar downregulatory effects on *NBS1* transcription were also seen with TSA-treated squamous carcinoma cells (Zhang *et al*, 2007).

The effects of panobinostat on the expression of all 11 *HDAC* genes were studied, having not yet been described in the literature. This study revealed differences in HDAC expression patterns over three different bladder cancer cell lines. *HDAC1* and *HDAC2* expression is notably higher than all the other HDACs in all the cell lines tested, whereas the levels of *HDAC5* and *HDAC11* were extremely low in all the cell lines. Levels of gene transcription do not necessarily correlate with protein levels, so the protein levels of all the HDAC's and the effects of panobinostat treatment need to be tested.

Strikingly, transcription of *HDAC7* was virtually totally eliminated in all the three cancer cell lines, with a much milder effect in the NHU cell line. Dokmanovic *et al* have found similar cancer cell-specific HDAC7 protein downregulation by vorinostat and correlation to growth arrest (Dokmanovic *et al*, 2007). To further determine the potential role of HDAC7 in panobinostat's effects on radiosensitisation, the HDAC7 protein levels should also be tested and the gene inhibited with the shRNA technology.

To confirm our findings and also to test for other potential effects of panobinostat on gene expression, it would also be informative to perform microarray analysis to assess global changes in gene expression induced in UC cells by panobinostat.

Two distinct mechanisms can therefore be proposed. The effects of panobinostat on NBS1 protein levels could be transcriptional, while the effects on MRE11 may be post-transcriptional. These could be the targeting of protein stability perhaps through direct acetylation of this protein. This should be further tested by co-immunoprecipitation experiments, described in the second Results chapter discussion. Although this is less likely in the case of NBS1, since the protein was shown not to be acetylated by HDAC inhibitors (Yuan *et al*, 2007), this should be further tested. Another possible mechanism for further investigation is the MRE11-NBS1 interaction which may be weakened or disrupted after panobinostat treatment.

To conclude, panobinostat may only target some of the activities of the MRN complex, with possible normal DSB damage recognition and γH2AX foci induction. However, when panobinostat reduces the absolute amounts of MRE11 and NBS1 proteins available, there may be insufficient protein to further potentiate the repair signal and to effectively complete the downstream DSB repair. Also, panobinostat appears to regulate NBS1 and MRE11 by two distinct mechanisms, perhaps by inhibiting MRE11 protein stability and gene transcription in the case of NBS1. Furthermore, it will be important to test the role of HDAC7 in these effects.

CHAPTER 6: GENERAL DISCUSSION AND FUTURE PLANS

6.1 General discussion

In this thesis, the HDAC inhibitor panobinostat was studied as a radiosensitiser in bladder cancer cell lines and was found to exert cytotoxic and robust radiosensitising effects in the low nanomolar range. For these effects to happen, bladder cancer cells had to be incubated for 24 hours, even though the biological activity of panobinostat (acetylated histone lysine residues) was observed already at very short incubation times. This is an important finding for future clinical biomarker development and dose scheduling of the drug, as currently, acetylated lysine residues in the chromatin of the tumour biopsy (Ree *et al*, 2010), or from leucocytes collected from patients' blood are considered the key indicators of biological activity of HDAC inhibitors (Rigby *et al*, 2012). It is possible that longer incubation times are required for panobinostat to achieve substantial cellular chromatin remodelling, resulting in greater cellular radiosensitivity or for the drug to affect the proteins involved in DNA repair.

An important factor determining outcome following therapy is the tumour's *TP53* status, mutant in more than 50% of high grade muscle invasive tumours, and determining less favourable outcomes after chemo- and radiotherapy (Wu, 2005). Two important observations from this study were the downregulation of p53 protein levels was seen in a panobinostat dose-dependent manner and also that *TP53* status did not have any influence on the radiosensitising effects of panobinostat treatment. On the other hand, these effects on the p53 protein will have to be carefully examined in the future mouse xenograft models and clinical trials, in order to investigate potential dangerous cytotoxic effects in the normal tissue through p53 protein downregulation.

In order to further test the radiosensitising effects of panobinostat, and to establish if panobinostat acts preferentially through the NHEJ or HR DNA DSB repair pathways, our

"synthetic lethality" cell system was used. Panobinostat was a more efficient radiosensitiser in Ku80KD cells, compared to the RAD51KD or RT112 cells. This observation indicated that the effects on the HR pathway are the predominant mode of action for panobinostat. This was tested further, and confirmed with panobinostat's dose-dependent downregulation of key HR proteins. On the other hand, no effects on the levels of selected key NHEJ proteins could be observed. This fact is important from the clinical perspective, since muscle invasive bladder cancers were reported to have an inefficient NHEJ pathway (Bentley *et al*, 2004), and therefore targeting the proficient HR repair pathway could make the difference in terms of effects on cancerous versus noncancerous tissue.

HDAC inhibitors have been shown to both upregulate and downregulate gene expression. In order to test if panobinostat causes these effects at the transcriptional level, gene transcription was also studied. No effects were observed in *RAD51* gene transcription with panobinostat alone or in combination with irradiation, indicating that the effects of panobinostat are post-transcriptional. These effects, such as acetylation of proteins, are likely to be another important mechanism of action for panobinostat.

To test if panobinostat also affects the MRN complex, upstream of the HR repair pathway, the protein levels upon panobinostat treatment were determined and also γH2AX foci induction, which is influenced by the function of the MRN complex. Normal DSB damage recognition and γH2AX foci induction was observed despite panobinostat treatment but with delayed foci repair. Therefore, when panobinostat reduces the absolute amounts of MRE11 and NBS1 proteins available, there may be sufficient protein to potentiate the repair signal, but insufficient to effectively complete the downstream DSB repair. On the other hand, the effects of panobinostat and mocetinostat on radiosensitisation and on the protein levels of some proteins were minor, it would also be beneficial for the future, to compare effects of panobinostat with another HDAC inhibitor.

6.2 Future Plans

These results give evidence for panobinostat acting as a radiosensitising agent in bladder cancer cells, so the next major step is to taking this forward to test the radiosensitising effects of panobinostat (determined as tumour growth delay) in a Balb/C nude mouse xenograft model and to determine the effects on normal tissue.

Geng *et al* (2006) have reported panobinostat to be an efficient radiosensitiser in a lung cancer model in mouse xenografts, with low toxicity towards non-cancerous cells.
In the proposed study, *in vivo* experiments could be done in RT112 and Ku80KD cell line xenografts, to confirm panobinostat's "synthetic lethal" action towards the bladder cancer cell lines. Furthermore, toxicity towards normal tissues should also be tested. The Gray Institute has acquired a small animal microirradiator (SARRP, Xstrahl), that could be used in this proposed study.

The results of this study would be of very important clinical translational value, since low toxic agents in combination with radiotherapy are needed for bladder cancer patients, even more so since HDAC inhibitors have already been tested in early clinical trials in combination with radiotherapy, with good tolerability. The first such study was the PRAVO study, testing combination of vorinostat and radiotherapy for the pelvis in gastrointestinal malignancies with 30 Gy in 10 fractions over two weeks (Ree *et al*, 2010), and the recent review based on the experience from the PRAVO study gives important principles for the conduct of the future early clinical studies (Ree & Hollywood, 2013).

Currently, there are only two clinical trials testing the combination of panobinostat and radiotherapy. The first trial, a phase I study in prostate, oesophageal and head and neck cancer has been completed and results are awaited, and the phase II is currently ongoing (http://clinicaltrials.gov; NCT00670553). Another phase I trial, is studying the combination of panobinostat and stereotactic radiation for the treatment of gliomas (NCT01324635).

In the next few years critical reports on the clinical tolerability of the combination of panobinostat and radiotherapy will be published. If the proposed panobinostat xenograft study in bladder cancer yields favourable results, hopefully panobinostat will become a novel treatment for muscle invasive bladder cancer, given that many bladder cancer patients are old and current therapies combined with radiotherapy are too toxic for them.

REFERENCES

Aben KK, Witjes A, Schoenberg MP, Hulsberger Van de Kaa C (2002) Familial aggregation of urothelial cell carcinoma. *Int J Cancer* **98**: 274–278.

Adimoolam S, Sirisawad M, Chen J, Thiemann P, Ford JM, Buggy JJ (2007) HDAC inhibitor PCI-24781 decreases RAD51 expression and inhibits homologous recombination. *Proc Natl Acad Sci U S A* **104**: 19482–19487.

Allfrey VG, Faulkner R, Mirsky AE (1964) Acetylation and methylation of histones and their possible role in the regulation of RNA synthesis. *Proc Natl Acad Sci U S A* **51**: 786–794.

Atadja P (2009) Development of the pan-DAC inhibitor panobinostat (LBH589): successes and challenges. *Cancer Lett* **280**: 233–241.

Babjuk M, Burger M, Zigeuner R, Shariat SF, van Rhijn BWG, Compérat E, Sylvester RJ, Kaasinen E, Böhle A, Palou Redorta J, Rouprêt M (2013) EAU Guidelines on Non-Muscle-invasive Urothelial Carcinoma of the Bladder: Update 2013. *Eur Urol* 1–15.

Babjuk M, Oosterlinck W, Sylvester R, Kaasinen E, Böhle A, Palou-Redorta J, Rouprêt M (2011) EAU guidelines on non-muscle-invasive urothelial carcinoma of the bladder, the 2011 update. *Eur Urol* **59**: 997–1008.

Bakkar AA, Wallerand H, Radvanyi F, Lahaye J, Pissard S, Lecerf L, Chopin DK, Gil S, Medina D De (2003) FGFR3 and TP53 Gene Mutations Define Two Distinct Pathways in Urothelial Cell Carcinoma of the Bladder. *Cancer Res* **63**: 8108–8112.

Banáth JP, Klokov D, MacPhail SH, Banuelos CA, Olive PL (2010) Residual gammaH2AX foci as an indication of lethal DNA lesions. *BMC Cancer* **10**: 4.

Barneda-Zahonero B, Parra M (2012) Histone deacetylases and cancer. *Mol Oncol* **6**: 579–589.

Bartkova J, Tommiska J, Oplustilova L, Aaltonen K, Tamminen A, Heikkinen T, Mistrik M, Aittomäki K, Blomqvist C, Heikkilä P, Lukas J, Nevanlinna H, Bartek J (2008) Aberrations of the MRE11-RAD50-NBS1 DNA damage sensor complex in human breast cancer: MRE11 as a candidate familial cancer-predisposing gene. *Mol Oncol* **2**: 296–316.

Baschnagel A, Russo A, Burgan WE, Carter D, Beam K, Palmieri D, Steeg PS, Tofilon P, Camphausen K (2009) Vorinostat enhances the radiosensitivity of a breast cancer brain metastatic cell line grown in vitro and as intracranial xenografts. *Mol Cancer Ther* **8**: 1589–1595.

Baumann M, Saunders Michele I, Joiner MC (2002) Modified fractionation. In Basic Clinical Radiobiology, G.G. Steel, ed. (London: Arnold), pp. 147–157.

Bentley J, Diggle CP, Harnden P, Knowles MA, Kiltie AE (2004) DNA double strand break repair in human bladder cancer is error prone and involves microhomology-associated end-joining. *Nucleic Acids Res* **32**: 5249–5259.

Bentley J, L'Hote C, Platt F, Hurst CD, Lowery J, Taylor C, Sak SC, Harnden P, Knowles MA, Kiltie AE (2009) Papillary and Muscle Invasive Bladder Tumors with Distinct Genomic Stability Profiles Have Different DNA Repair Fidelity and KU DNA-Binding Activities. *Genes Chromosomes Cancer* **321**: 310–321.

Berkovich E, Monnat RJ, Kastan MB (2007) Roles of ATM and NBS1 in chromatin structure modulation and DNA double-strand break repair. *Nat Cell Biol* **9**: 683–690.

Blattmann C, Oertel S, Ehemann V, Thiemann M, Huber PE, Bischof M, Witt O, Deubzer HE, Kulozik AE, Debus J, Weber K-J (2010) Enhancement of radiation response in osteosarcoma and rhabdomyosarcoma cell lines by histone deacetylase inhibition. *Int J Radiat Oncol Biol Phys* **78**: 237–245.

Bonner WM, Redon CE, Dickey JS, Nakamura AJ, Sedelnikova OA, Solier S, Pommier Y (2008) γ H2AX and cancer. *Nat Rev Cancer* **8**: 957–967.

Bourdon J-C, Fernandes K, Murray-Zmijewski F, Liu G, Diot A, Xirodimas DP, Saville MK, Lane DP (2005) P53 Isoforms Can Regulate P53 Transcriptional Activity. *Genes Dev* **19**: 2122–2137.

Bourton EC, Plowman PN, Smith D, Arlett CF, Parris CN (2011) Prolonged expression of the γ-H2AX DNA repair biomarker correlates with excess acute and chronic toxicity from radiotherapy treatment. *Int J Cancer* **129**: 2928–2934.

Bratland A, Dueland S, Hollywood D, Flatmark K, Ree AH (2011) Gastrointestinal toxicity of vorinostat: reanalysis of phase 1 study results with emphasis on dose-volume effects of pelvic radiotherapy. *Radiat Oncol* **6**: 33.

Brausi M, Collette L, Kurth K, Meijden AP Van Der, Oosterlinck W, Witjes JA, Newling D, Bouf C, Sylvester RJ (2002) European Urology Variability in the Recurrence Rate at First Follow-up Cystoscopy after TUR in Stage Ta T1 Transitional Cell Carcinoma of the Bladder: A Combined Analysis of Seven EORTC Studies. *Eur Urol* **41**: 523–531.

British Uro-oncology Group (BUG) and British Association of Urological Surgeons (BAUS) Section of Oncology and Action on Bladder Cancer (ABC) (2013) MDT (Multi-Disciplinary Team) Guidance for Managing Bladder Cancer.

Brown T, Slack R, Rushton L (2012) Occupational cancer in Britain. Urinary tract cancers: bladder and kidney. *Br J Cancer* **107 Suppl**: S76–84.

Bryant HE, Schultz N, Thomas HD, Parker KM, Flower D, Lopez E, Kyle S, Meuth M, Curtin NJ, Helleday T (2005) Specific killing of BRCA2-deficient tumours with inhibitors of poly(ADP-ribose) polymerase. *Nature* **434**: 913–917.

Bubenik J, Baresova M, Viklicky V, Jakoubkova J, Sainerova H, Donner J (1973) Established cell line of urinary bladder carcinoma (T24) containing tumour-specific antigen. *Int J Cancer* **11**: 765–773.

Buckley MT, Yoon J, Yee H, Chiriboga L, Liebes L, Ara G, Qian X, Bajorin DF, Sun T-T, Wu X-R, Osman I (2007) The histone deacetylase inhibitor belinostat (PXD101) suppresses bladder cancer cell growth in vitro and in vivo. *J Transl Med* **5**: 49.

Budman DR, Tai J, Calabro A, John V (2011) The histone deacetylase inhibitor panobinostat demonstrates marked synergy with conventional chemotherapeutic agents in human ovarian cancer cell lines. *Invest New Drugs* **29**: 1224–1229.

Buis J, Stoneham T, Spehalski E, Ferguson DO (2012) Mre11 regulates CtIP-dependent double-strand break repair by interaction with CDK2. *Nat Struct Mol Biol* **19**: 246–252.

Buisson R, Dion-Côté A-M, Coulombe Y, Launay H, Cai H, Stasiak AZ, Stasiak A, Xia B, Masson J-Y (2010) Cooperation of breast cancer proteins PALB2 and piccolo BRCA2 in stimulating homologous recombination. *Nat Struct Mol Biol* **17**: 1247–1254.

Bunting SF, Callén E, Wong N, Chen H-T, Polato F, Gunn A, Bothmer A, Feldhahn N, Fernandez-Capetillo O, Cao L, Xu X, Deng C-X, Finkel T, Nussenzweig M, Stark JM, Nussenzweig A (2010) 53BP1 inhibits homologous recombination in Brca1-deficient cells by blocking resection of DNA breaks. *Cell* **141**: 243–254.

Burger M, Catto JWF, Dalbagni G, Grossman HB, Herr H, Karakiewicz P, Kassouf W, Kiemeney L a, La Vecchia C, Shariat S, Lotan Y (2013) Epidemiology and risk factors of urothelial bladder cancer. *Eur Urol* **63**: 234–241.

Camphausen K, Burgan W, Cerra M, Oswald KA, Trepel JB, Lee M-J, Tofilon PJ (2004a) Enhanced Radiation-Induced Cell Killing and Prolongation of H2AX Foci Expression by the Histone Deacetylase Inhibitor MS-275. *Cancer Res* **64**: 316–321.

Camphausen K, Cerna D, Scott T, Sproull M, Burgan WE, Cerra M a, Fine H, Tofilon PJ (2005) Enhancement of in vitro and in vivo tumor cell radiosensitivity by valproic acid. *Int J Cancer* **114**: 380–386.

Camphausen K, Scott T, Sproull M, Tofilon PJ (2004b) Enhancement of xenograft tumor radiosensitivity by the histone deacetylase inhibitor MS-275 and correlation with histone hyperacetylation. *Clin Cancer Res* **10**: 6066–6071.

Camphausen K, Tofilon PJ (2007) Inhibition of histone deacetylation: a strategy for tumor radiosensitization. *J Clin Oncol* **25**: 4051–4056.

Candelaria M, Cetina L, Perez-Cardenas E, de la Cruz-Hernandez E, González-Fierro A, Trejo-Becerril C, Taja-Chayeb L, Chanona J, Arias D, Duenas-Gonzalez A (2010) Epigenetic therapy and cisplatin chemoradiation in FIGO stage IIIB cervical cancer. *Eur J Gynaecol Oncol* **31**: 386–391.

Carney JP, Maser RS, Olivares H, Davis EM, Le Beau M, Yates JR, Hays L, Morgan WF, Petrini JH (1998) The hMre11/hRad50 protein complex and Nijmegen breakage syndrome: linkage of double-strand break repair to the cellular DNA damage response. *Cell* **93**: 477–486.

Catalano MG, Pugliese M, Gargantini E, Grange C, Bussolati B, Asioli S, Bosco O, Poli R, Compagnone A, Bandino A, Mainini F, Fortunati N, Boccuzzi G (2012) Cytotoxic activity of the histone deacetylase inhibitor panobinostat (LBH589) in anaplastic thyroid cancer in vitro and in vivo. *Int J cancer* **130**: 694–704.

Cattan N, Rochet N, Mazeau C, Zanghellini E, Mari B, Chauzy C, Stora de Novion H, Amiel J, Lagrange JL, Rossi B, Gioanni J (2001) Establishment of two new human bladder carcinoma cell lines, CAL 29 and CAL 185. Comparative study of cell scattering and

epithelial to mesenchyme transition induced by growth factors. *Br J Cancer* **85**: 1412–1417.

Cha T-L, Chuang M-J, Wu S-T, Sun G-H, Chang S-Y, Yu D-S, Huang S-M, Huan SK-H, Cheng T-C, Chen T-T, Fan P-L, Hsiao P-W (2009) Dual degradation of aurora A and B kinases by the histone deacetylase inhibitor LBH589 induces G2-M arrest and apoptosis of renal cancer cells. *Clin Cancer Res* **15**: 840–850.

Chalasani V, Chin JL, Izawa JI (2009) Histologic variants of urothelial bladder cancer and nonurothelial histology in bladder cancer. *Can Urol Assoc J* **3**: S193–8.

Chan DW, Chen BP, Prithivirajsingh S, Kurimasa A, Story MD, Qin J, Chen DJ (2002) Autophosphorylation of the DNA-dependent protein kinase catalytic subunit is required for rejoining of DNA double-strand breaks. *Genes Dev* **16**: 2333–2338.

Chapman JR, Barral P, Vannier J-B, Borel V, Steger M, Tomas-Loba A, Sartori A a, Adams IR, Batista FD, Boulton SJ (2013) RIF1 is essential for 53BP1-dependent nonhomologous end joining and suppression of DNA double-strand break resection. *Mol Cell* **49**: 858–871.

Chen CL, Sung J, Cohen M, Chowdhury WH, Sachs MD, Li Y, Lakshmanan Y, Yung BYM, Lupold SE, Rodriguez R (2006) Valproic acid inhibits invasiveness in bladder cancer but not in prostate cancer cells. *J Pharmacol Exp Ther* **319**: 533–542.

Chen L, Nievera CJ, Lee AY-L, Wu X (2008) Cell cycle-dependent complex formation of BRCA1.CtIP.MRN is important for DNA double-strand break repair. *J Biol Chem* **283**: 7713–7720.

Chen S, Ye J, Kijima I, Evans D (2010) The HDAC inhibitor LBH589 (panobinostat) is an inhibitory modulator of aromatase gene expression. *Proc Natl Acad Sci U S A* **107**: 11032–11037.

Chen X, Wong P, Radany EH, Stark JM, Laulier C, Wong JYC (2012) Suberoylanilide hydroxamic acid as a radiosensitizer through modulation of RAD51 protein and inhibition of homology-directed repair in multiple myeloma. *Mol Cancer Res* **10**: 1052–1064.

Cheng Q, Barboule N, Frit P, Gomez D, Bombarde O, Couderc B, Ren G-S, Salles B, Calsou P (2011) Ku counteracts mobilization of PARP1 and MRN in chromatin damaged with DNA double-strand breaks. *Nucleic Acids Res* **39**: 9605–9619.

Chinnaiyan P, Cerna D, Burgan WE, Beam K, Williams ES, Camphausen K, Tofilon PJ (2008) Postradiation sensitization of the histone deacetylase inhibitor valproic acid. *Clin Cancer Res* **14**: 5410–5415.

Chinnaiyan P, Vallabhaneni G, Armstrong E, Huang S-M, Harari PM (2005) Modulation of radiation response by histone deacetylase inhibition. *Int J Radiat Oncol Biol Phys* **62**: 223–229.

Chou T-C (2010) Drug combination studies and their synergy quantification using the Chou-Talalay method. *Cancer Res* **70**: 440–446.

Choudhury A, Swindell R, Logue JP, Elliott PA, Livsey JE, Wise M, Symonds P, Wylie JP, Ramani V, Sangar V, Lyons J, Bottomley I, McCaul D, Clarke NW, Kiltie AE, Cowan RA

(2011) Phase II study of conformal hypofractionated radiotherapy with concurrent gemcitabine in muscle-invasive bladder cancer. *J Clin Oncol* **29**: 733–738.

Choudhury A, Zhao H, Jalali F, Al Rashid S, Ran J, Supiot S, Kiltie AE, Bristow RG (2009) Targeting homologous recombination using imatinib results in enhanced tumor cell chemosensitivity and radiosensitivity. *Mol Cancer Ther* **8**: 203–213.

Choueiri TK, Raghavan D (2008) Chemotherapy for muscle-invasive bladder cancer treated with definitive radiotherapy: persisting uncertainties. *Nat Clin Pract Oncol* **5**: 444–454.

Clayton AL, Hazzalin C a, Mahadevan LC (2006) Enhanced histone acetylation and transcription: a dynamic perspective. *Mol Cell* **23**: 289–296.

Cody J, Nabi G, Dublin N, McClinton S, Neal D, Pickard R, Yong S (2012) Urinary diversion and bladder reconstruction/replacement using intestinal segments for intractable incontinence or following cystectomy. *Cochrane Database Syst Rev* **2**: CD003306.

Cooper MJ, Haluschak JJ, Johnson D, Schwartz S, Morrison LJ, Lippa M, Hatzivassiliou G, Tan J (1994) p53 mutations in bladder carcinoma cell lines. *Oncol Res* **6**: 569–579.

Cosgrove MS, Boeke JD, Wolberger C (2004) Regulated nucleosome mobility and the histone code. *Nat Struct Mol Biol* **11**: 1037–1043.

Cosgrove MS, Wolberger C (2005) How does the histone code work? *Biochem Cell Biol* **83**: 468–476.

Crisanti MC, Wallace AF, Kapoor V, Vandermeers F, Dowling ML, Pereira LP, Coleman K, Campling BG, Fridlender ZG, Kao GD, Albelda SM (2009) The HDAC inhibitor panobinostat (LBH589) inhibits mesothelioma and lung cancer cells in vitro and in vivo with particular efficacy for small cell lung cancer. *Mol Cancer Ther* **8**: 2221–2231.

Cuneo KC, Fu A, Osusky K, Huamani J, Hallahan DE, Geng L (2007) Histone deacetylase inhibitor NVP-LAQ824 sensitizes human nonsmall cell lung cancer to the cytotoxic effects of ionizing radiation. *Anticancer Drugs* **18**: 793–800.

Dash A, Galsky MD, Vickers AJ, Serio AM, Koppie TM, Dalbagni G, Bochner BH (2006) Impact of renal impairment on eligibility for adjuvant cisplatin-based chemotherapy in patients with urothelial carcinoma of the bladder. *Cancer* **107**: 506–513.

Deffie A, Wu H, Reinke V, Lozano G (1993) The Tumor Suppressor p53 Regulates Its Own Transcription. *Moiecular Cell Biol* **13**: 3415–3423.

Deorukhkar A, Shentu S, Park HC, Diagaradjane P, Puduvalli V, Aggarwal B, Guha S, Krishnan S (2010) Inhibition of radiation-induced DNA repair and prosurvival pathways contributes to vorinostat-mediated radiosensitization of pancreatic cancer cells. *Pancreas* **39**: 1277–1283.

Desai-Mehta A, Cerosaletti KM, Concannon P (2001) Distinct Functional Domains of Nibrin Mediate Mre11 Binding, Focus Formation, and Nuclear Localization. *Mol Cell Biol* **21**: 2184–2191.

Dickinson M, Johnstone RW, Prince HM (2010) Histone deacetylase inhibitors: potential targets responsible for their anti-cancer effect. *Invest New Drugs* **28 Suppl 1**: S3–20.

Dokmanovic M, Perez G, Xu W, Ngo L, Clarke C, Parmigiani RB, Marks PA (2007) Histone deacetylase inhibitors selectively suppress expression of HDAC7. *Mol Cancer Ther* **6**: 2525–2534.

Douglas BG, Fowler JF (1976) The Effect of Multiple Small Doses of X Rays on Skin Reactions the Mouse and a Basic Interpretation. *Radiat Res* **66**: 401–426.

Duong V, Bret C, Altucci L, Mai A, Duraffourd C, Loubersac J, Harmand PO, Bonnet S, Valente S, Maudelonde T, Cavailles V, Boulle N (2008) Specific activity of class II histone deacetylases in human breast cancer cells. *Mol Cancer Res* **6**: 1908–1919.

Duvic M, Talpur R, Ni X, Zhang C, Hazarika P, Kelly C, Chiao JH, Reilly JF, Ricker JL, Richon VM, Frankel SR (2007) Phase 2 trial of oral vorinostat (suberoylanilide hydroxamic acid, SAHA) for refractory cutaneous T-cell lymphoma (CTCL). *Blood* **109**: 31–39.

Edwards A, Li J, Atadja P, Bhalla K, Haura EB (2007) Effect of the histone deacetylase inhibitor LBH589 against epidermal growth factor receptor-dependent human lung cancer cells. *Mol Cancer Ther* **6**: 2515–2524.

Efstathiou JA, Spiegel DY, Shipley WU, Heney NM, Kaufman DS, Niemierko A, Coen JJ, Skowronski RY, Paly JJ, McGovern FJ, Zietman AL (2012) Long-term outcomes of selective bladder preservation by combined-modality therapy for invasive bladder cancer: the MGH experience. *Eur Urol* **61**: 705–711.

Falck J, Coates J, Jackson SP (2005) Conserved modes of recruitment of ATM, ATR and DNA-PKcs to sites of DNA damage. *Nature* **434**: 605–611.

Falck J, Forment J V, Coates J, Mistrik M, Lukas J, Bartek J, Jackson SP (2012) CDK targeting of NBS1 promotes DNA-end resection, replication restart and homologous recombination. *EMBO Rep* **13**: 561–568.

Farmer H, McCabe N, Lord CJ, Tutt ANJ, Johnson DA, Richardson TB, Santarosa M, Dillon KJ, Hickson I, Knights C, Martin NMB, Jackson SP, Smith GCM, Ashworth A (2005) Targeting the DNA repair defect in BRCA mutant cells as a therapeutic strategy. *Nature* **434**: 917–921.

Fattah F, Lee EH, Weisensel N, Wang Y, Lichter N, Hendrickson EA (2010) Ku regulates the non-homologous end joining pathway choice of DNA double-strand break repair in human somatic cells. *PLoS Genet* **6**: e1000855.

Flatmark K, Nome R V, Folkvord S, Bratland A, Rasmussen H, Ellefsen MS, Fodstad Ø, Ree AH (2006) Radiosensitization of colorectal carcinoma cell lines by histone deacetylase inhibition. *Radiat Oncol* **1**: 25.

Florl AR, Schulz WA (2008) Chromosomal instability in bladder cancer. *Arch Toxicol* **82**: 173–182.

Flygare J, Benson F, Hellgren D (1996) Expression of the human RAD51 gene during the cell cycle in primary human peripheral blood lymphocytes. *Biochim Biophys Acta* **1312**: 231–236.

Folkvord S, Ree AH, Furre T, Halvorsen T, Flatmark K (2009) Radiosensitization by SAHA in experimental colorectal carcinoma models-in vivo effects and relevance of histone acetylation status. *Int J Radiat Oncol Biol Phys* **74**: 546–552.

Franken NAP, Rodermond HM, Stap J, Haveman J, van Bree C (2006) Clonogenic assay of cells in vitro. *Nat Protoc* **1**: 2315–2319.

Freedman ND, Silverman DT, Hollenbeck AR, Schatzkin A, Abnet CC (2011) Association between smoking and risk of bladder cancer among men and women. *JAMA* **306**: 737–745.

Fukuda T, Sumiyoshi T, Takahashi M, Kataoka T, Asahara T, Inui H, Watatani M, Yasutomi M, Kamada N, Miyagawa K (2001) Alterations of the double-strand break repair gene MRE11 in cancer. *Cancer Res* **61**: 23–26.

Gakis G, Stenzl A (2010) Ileal Neobladder and Its Variants. *Eur Urol Suppl* **9**: 745–753.

Gaymes TJ, Padua RA, Pla M, Orr S, Omidvar N, Chomienne C, Mufti GJ, Rassool F V (2006) Histone deacetylase inhibitors (HDI) cause DNA damage in leukemia cells: a mechanism for leukemia-specific HDI-dependent apoptosis? *Mol Cancer Res* **4**: 563–573.

Geng L, Cuneo KC, Fu A, Tu T, Atadja PW, Hallahan DE (2006) Histone deacetylase (HDAC) inhibitor LBH589 increases duration of gamma-H2AX foci and confines HDAC4 to the cytoplasm in irradiated non-small cell lung cancer. *Cancer Res* **66**: 11298–11304.

Van Gent DC, van der Burg M (2007) Non-homologous end-joining, a sticky affair. *Oncogene* **26**: 7731–7740.

Ghoneim MA, El-Mekresh MM, El-Baz MA, El-Attar IA, Ashamallah A (1997) Radical cystectomy for carcinoma of the bladder: critical evaluation of the results in 1,026 cases. *J Urol* **158**: 393–399.

Giannini G, Ristori E, Cerignoli F, Rinaldi C, Zani M, Viel A, Ottini L, Crescenzi M, Martinotti S, Bignami M, Frati L, Screpanti I, Gulino A (2002) Human MRE11 is inactivated in mismatch repair-deficient cancers. *EMBO Rep* **3**: 248–254.

Giles F, Fischer T, Cortes J, Garcia-Manero G, Beck J, Ravandi F, Masson E, Rae P, Laird G, Sharma S, Kantarjian H, Dugan M, Albitar M, Bhalla K (2006) A phase I study of intravenous LBH589, a novel cinnamic hydroxamic acid analogue histone deacetylase inhibitor, in patients with refractory hematologic malignancies. *Clin Cancer Res* **12**: 4628–4635.

Glaser KB, Staver MJ, Waring JF, Stender J, Ulrich RG, Davidsen SK (2003) Gene Expression Profiling of Multiple Histone Deacetylase (HDAC) Inhibitors: Defining a Common Gene Set Produced by HDAC Inhibition in T24 and MDA Carcinoma Cell Lines. *Mol Cancer Ther* **2**: 151–163.

Glozak M a, Seto E (2007) Histone deacetylases and cancer. *Oncogene* **26**: 5420–5432.

Goebell PJ, Knowles MA (2010) Bladder cancer or bladder cancers? Genetically distinct malignant conditions of the urothelium. *Urol Oncol* **28**: 409–428.

Gouda I, Mokhtar N, Bilal D, El-Bolkainy T, El-Bolkainy NM (2007) Bilharziasis and bladder cancer: a time trend analysis of 9843 patients. *J Egypt Natl Canc Inst* **19**: 158–162.

Griffiths T (2013) Current perspectives in bladder cancer management. *Int J Clin Pract* **2006**: 435–448.

Grignon DJ (2009) The current classification of urothelial neoplasms. *Mod Pathol* **22 Suppl 2**: S60–69.

Groselj B, Sharma NL, Hamdy FC, Kerr M, Kiltie AE (2013) Histone deacetylase inhibitors as radiosensitisers: effects on DNA damage signalling and repair. *Br J Cancer* **108**: 748–754.

Harrington K, Jankowska P, Hingorani M (2007) Molecular biology for the radiation oncologist: the 5Rs of radiobiology meet the hallmarks of cancer. *Clin Oncol* **19**: 561–571.

Harrington KJ, Billingham LJ, Brunner TB, Burnet NG, Chan CS, Hoskin P, Mackay RI, Maughan TS, Macdougall J, McKenna WG, Nutting CM, Oliver A, Plummer R, Stratford IJ, Illidge T (2011) Guidelines for preclinical and early phase clinical assessment of novel radiosensitisers. *Br J Cancer* **105**: 628–639.

Hasegawa H, Yamada Y, Tsukasaki K, Mori N, Tsuruda K, Sasaki D, Usui T, Osaka A, Atogami S, Ishikawa C, Machijima Y, Sawada S, Hayashi T, Miyazaki Y, Kamihira S (2011) LBH589, a deacetylase inhibitor, induces apoptosis in adult T-cell leukemia/lymphoma cells via activation of a novel RAIDD-caspase-2 pathway. *Leukemia* **25**: 575–587.

Hebbes TR, Thorne AW, Crane-Robinson C (1988) A direct link between core histone acetylation and transcriptionally active chromatin. *EMBO J* **7**: 1395–1402.

Heney NM, Kaufman DS, Shipley WU (2009) Surgery: selective bladder-preserving therapy for muscle-invasive cancer. *Nat Rev Clin Oncol* **6**: 193–194.

Herr HW, Donat SM (2008) Quality control in transurethral resection of bladder tumours. *BJU Int* **102**: 1242–1246.

Hiel J, Weemaes C, Van den Huevel L, Van Engelen B (2000) Nijmegen breakage syndrome. *Arch Dis Child* **82**: 400–406.

Höglund M (2012) The bladder cancer genome; chromosomal changes as prognostic makers, opportunities, and obstacles. *Urol Oncol* **30**: 533–540.

Hopfner K-P, Craig L, Moncalian G, Zinkel RA, Usui T, Owen BAL, Karcher A, Henderson B, Bodmer J-L, McMurray CT, Carney JP, Petrini JHJ, Tainer JA (2002) The Rad50 zinc-hook is a structure joining Mre11 complexes in DNA recombination and repair. *Nature* **418**: 562–566.

Hopfner KP, Karcher A, Craig L, Woo TT, Carney JP, Tainer JA (2001) Structural biochemistry and interaction architecture of the DNA double-strand break repair Mre11 nuclease and Rad50-ATPase. *Cell* **105**: 473–485.

Hoskin PJ, Rojas AM, Bentzen SM, Saunders MI (2010) Radiotherapy with concurrent carbogen and nicotinamide in bladder carcinoma. *J Clin Oncol* **28**: 4912–4918.

Huddart RA, Hall E, Lewis R, Birtle A (2010) Life and death of spare (selective bladder preservation against radical excision): reflections on why the spare trial closed. *BJU Int* **106**: 753–755.

Hunt CR, Ramnarain D, Horikoshi N, Iyengar P, Pandita RK, Shay JW, Pandita TK (2013) Histone modifications and DNA double-strand break repair after exposure to ionizing radiations. *Radiat Res* **179**: 383–392.

Iijima K, Ohara M, Seki R, Tauchi H (2008) Dancing on Damaged Chromatin: Functions of ATM and the RAD50/MRE11/NBS1 Complex in Cellular Responses to DNA Damage. *J Radiat Res* **49**: 451–464.

Jakob B, Splinter J, Conrad S, Voss K-O, Zink D, Durante M, Löbrich M, Taucher-Scholz G (2011) DNA double-strand breaks in heterochromatin elicit fast repair protein recruitment, histone H2AX phosphorylation and relocation to euchromatin. *Nucleic Acids Res* **39**: 6489–6499.

James ND, Hussain SA, Hall E, Jenkins P, Tremlett J, Rawlings C, Crundwell M, Sizer B, Sreenivasan T, Hendron C, Lewis R, Waters R, Huddart RA (2012) Radiotherapy with or without chemotherapy in muscle-invasive bladder cancer. *N Engl J Med* **366**: 1477–1488.

Jenuwein T, Allis CD (2001) Translating the histone code. *Science (80-)* **293**: 1074–1080.

Jonathan EC, Bernhard EJ, McKenna WG (1999) How does radiation kill cells? *Curr Opin Chem Biol* **3**: 77–83.

Junker K, van Oers JMM, Zwarthoff EC, Kania I, Schubert J, Hartmann A (2008) Fibroblast Growth Factor Receptor 3 Mutations in Bladder Tumors Correlate with Low Frequency of Chromosome Alterations. *Neoplasia* **10**: 1–7.

Junqueira-Neto S, Vieira FQ, Montezuma D, Costa NR, Antunes L, Baptista T, Oliveira AI, Graça I, Rodrigues A, Magalhães JS, Oliveira J, Henrique R, Jerónimo C (2013) Phenotypic impact of deregulated expression of class I histone deacetylases in urothelial cell carcinoma of the bladder. *Mol Carcinog* 1–9.

Kachhap SK, Rosmus N, Collis SJ, Kortenhorst MSQ, Wissing MD, Hedayati M, Shabbeer S, Mendonca J, Deangelis J, Marchionni L, Lin J, Hoti N, Nortier JWR, DeWeese TL, Hammers H, Carducci MA (2010) Downregulation of Homologous Recombination DNA Repair Genes by HDAC Inhibition in Prostate Cancer Is Mediated through the E2F1 Transcription Factor. *PLoS One* **5**: e11208.

Kaelin WG (2005) The concept of synthetic lethality in the context of anticancer therapy. *Nat Rev Cancer* **5**: 689–698.

Kajstura M, Halicka HD, Pryjma J, Darzynkiewicz Z (2007) Discontinuous Fragmentation of Nuclear DNA During Apoptosis Revealed by Discrete “Sub-G 1” Peaks on DNA Content Histograms. *Cytometry* **71**: 125–131.

Kamrava M, Citrin D, Sproull M, Lita E, Smith S, Crouse N, Cooley-Zgela T, Fine H, Camphausen K (2008) Acute toxicity in a phase II clinical trial of valproic acid in

combination with temodar and radiation therapy in patients with glioblastoma multiforme. *Int J Radiat Oncol* **72**: S211.

Karagiannis TC, Kn H, El-Osta A (2005) The histone deacetylase inhibitor, Trichostatin A, enhances radiation sensitivity and accumulation of gammaH2A.X. *Cancer Biol Ther* **4**: 787–793.

Kastan MB, Bartek J (2004) Cell-cycle checkpoints and cancer. *Nature* **432**: 316–323.

Kawabata T, Nishida K, Takasugi K, Ogawa H, Sada K, Kadota Y, Inagaki J, Hirohata S, Ninomiya Y, Makino H (2010) Increased activity and expression of histone deacetylase 1 in relation to tumor necrosis factor-alpha in synovial tissue of rheumatoid arthritis. *Arthritis Res Ther* **12**: R133.

Khanna KK, Jackson SP (2001) DNA double-strand breaks: signaling, repair and the cancer connection. *Nat Genet* **27**: 247–254.

Khoury MP, Bourdon J-C (2010) The isoforms of the p53 protein. *Cold Spring Harb Perspect Biol* **2**: a000927.

Kim IA, Kim JH, Shin JH, Kim IH, Kim JS, Wu H-G, Chie EK, Kim YH, Kim B-K, Hong S, Park SW, Ha SW, Park C Il (2005) A histone deacetylase inhibitor, trichostatin A, enhances radiosensitivity by abrogating G2/M arrest in human carcinoma cells. *Cancer Res Treat* **37**: 122–128.

Kim IA, No M, Lee JM, Shin JH, Oh JS, Choi EJ, Kim IH, Atadja P, Bernhard EJ (2009) Epigenetic modulation of radiation response in human cancer cells with activated EGFR or HER-2 signaling: potential role of histone deacetylase 6. *Radiother Oncol* **92**: 125–132.

Kim JH, Shin JH, Kim IH (2004) Susceptibility and radiosensitization of human glioblastoma cells to trichostatin A, a histone deacetylase inhibitor. *Int J Radiat Oncol Biol Phys* **59**: 1174–1180.

Kim SP, Shah ND, Weight CJ, Thompson RH, Wang JK, Karnes RJ, Han LC, Ziegenfuss JY, Frank I, Tollefson MK, Boorjian S a (2013a) Population-based trends in urinary diversion among patients undergoing radical cystectomy for bladder cancer. *BJU Int* **112**: 478–484.

Kim YJ, Greer CB, Cecchini KR, Harris LN, Tuck DP, Kim TH (2013b) HDAC inhibitors induce transcriptional repression of high copy number genes in breast cancer through elongation blockade. *Oncogene* **32**: 2828–2835.

Knowles MA (2006) Molecular subtypes of bladder cancer: Jekyll and Hyde or chalk and cheese? *Carcinogenesis* **27**: 361–373.

Knowles MA (2008) Molecular pathogenesis of bladder cancer. *Int J Clin Oncol* **13**: 287–297.

Ko J-C, Hong J-H, Wang L-H, Cheng C-M, Ciou S-C, Lin S-T, Jheng M-Y, Lin Y-W (2008) Role of repair protein Rad51 in regulating the response to gefitinib in human non-small cell lung cancer cells. *Mol Cancer Ther* **7**: 3632–3641.

Konety BR, Allareddy V, Herr H (2006) Complications after radical cystectomy: analysis of population-based data. *Urology* **68**: 58–64.

Konsoula Z, Cao H, Velena A, Jung M (2011) Adamantanyl-histone deacetylase inhibitor H6CAHA exhibits favorable pharmacokinetics and augments prostate cancer radiation sensitivity. *Int J Radiat Oncol Biol Phys* **79**: 1541–1548.

Kortenhorst MSQ, Zahurak M, Shabbeer S, Kachhap S, Galloway N, Parmigiani G, Verheul HMW, Carducci M a (2008) A multiple-loop, double-cube microarray design applied to prostate cancer cell lines with variable sensitivity to histone deacetylase inhibitors. *Clin Cancer Res* **14**: 6886–6894.

Kotian S, Liyanarachchi S, Zelent A, Parvin JD (2011) Histone deacetylases 9 and 10 are required for homologous recombination. *J Biol Chem* **286**: 7722–7726.

Kotwal S, Choudhury A, Johnston C, Paul AB, Whelan P, Kiltie AE (2008) Similar treatment outcomes for radical cystectomy and radical radiotherapy in invasive bladder cancer treated at a United Kingdom specialist treatment center. *Int J Radiat Oncol Biol Phys* **70**: 456–463.

Kragelj B, Zaletel-Kragelj L, Sedmak B, Cufer T, Cervek J (2005) Phase II study of radiochemotherapy with vinblastine in invasive bladder cancer. *Radiother Oncol* **75**: 44–47.

Kuo LJ, Yang L-X (2008) Gamma-H2AX - a novel biomarker for DNA double-strand breaks. *In Vivo (Brooklyn)* **22**: 305–310.

Lachenmayer A, Toffanin S, Cabellos L, Alsinet C, Hoshida Y, Villanueva A, Minguez B, Tsai H-W, Ward SC, Thung S, Friedman SL, Llovet JM (2012) Combination therapy for hepatocellular carcinoma: additive preclinical efficacy of the HDAC inhibitor panobinostat with sorafenib. *J Hepatol* **56**: 1343–1350.

Lamarche BJ, Orazio NI, Weitzman MD (2010) The MRN complex in double-strand break repair and telomere maintenance. *FEBS Lett* **584**: 3682–3695.

Lee J-H, Choy ML, Ngo L, Foster SS, Marks PA (2010) Histone deacetylase inhibitor induces DNA damage, which normal but not transformed cells can repair. *Proc Natl Acad Sci U S A* **107**: 14639–14644.

Lee J-H, Paull TT (2005) ATM activation by DNA double-strand breaks through the Mre11-Rad50-Nbs1 complex. *Science (80-)* **308**: 551–554.

Lee J-H, Paull TT (2007) Activation and regulation of ATM kinase activity in response to DNA double-strand breaks. *Oncogene* **26**: 7741–7748.

Li S, Ting NS, Zheng L, Chen PL, Ziv Y, Shiloh Y, Lee EY, Lee WH (2000) Functional link of BRCA1 and ataxia telangiectasia gene product in DNA damage response. *Nature* **406**: 210–215.

Liberman D, Lughezzani G, Sun M, Alasker A, Thuret R, Abdollah F, Budaus L, Widmer H, Graefen M, Montorsi F, Shariat SF, Perrotte P, Karakiewicz PI (2011) Perioperative mortality is significantly greater in septuagenarian and octogenarian patients treated with radical cystectomy for urothelial carcinoma of the bladder. *Urology* **77**: 660–666.

Livak KJ, Schmittgen TD (2001) Analysis of relative gene expression data using real-time quantitative PCR and the 2(-Delta Delta C(T)) Method. *Methods* **25**: 402–408.

Löbrich M, Shibata A, Beucher A, Fisher A, Ensminger M, Goodarzi AA, Barton O, Jeggo PA (2010) γH2AX foci analysis for monitoring DNA double-strand break repair. *Cell Cycle* **9**: 662–669.

Lomax ME, Folkes LK, O'Neill P (2013) Biological Consequences of Radiation-induced DNA Damage: Relevance to Radiotherapy. *Clin Oncol* **25**: 578–585.

Lopez-Beltran A (2008) Bladder cancer: clinical and pathological profile. *Scand J Urol Nephrol Suppl* **42**: 95–109.

Luger K, Mader AW, Richmond RK, Sargent DF, Richmond TJ (1997) Crystal structure of the nucleosome core particle at 2.8 A resolution. *Nature* **389**: 251–260.

Mah LJ, El-Osta A, Karagiannis TC (2010) gammaH2AX: a sensitive molecular marker of DNA damage and repair. *Leukemia* **24**: 679–686.

Majewski W, Tarnawski R (2009) Acute and late toxicity in radical radiotherapy for bladder cancer. *Clin Oncol* **21**: 598–609.

Malmström P-U, Sylvester RJ, Crawford DE, Friedrich M, Krege S, Rintala E, Solsona E, Di Stasi SM, Witjes JA (2009) An individual patient data meta-analysis of the long-term outcome of randomised studies comparing intravesical mitomycin C versus bacillus Calmette-Guérin for non-muscle-invasive bladder cancer. *Eur Urol* **56**: 247–256.

Mann BS, Johnson JR, Cohen MH, Justice R, Pazdur R (2007) FDA approval summary: vorinostat for treatment of advanced primary cutaneous T-cell lymphoma. *Oncologist* **12**: 1247–1252.

Manova V, Singh SK, Iliakis G (2012) Processing of DNA double strand breaks by alternative non-homologous end-joining in hyperacetylated chromatin. *Genome Integr* **3**: 4.

Mao Z, Bozzella M, Seluanov A, Gorbunova V (2008) Comparison of nonhomologous end joining and homologous recombination in human cells. *DNA Repair (Amst)* **7**: 1765–1771.

Mariappan P, Zachou A, Grigor KM (2010) Detrusor muscle in the first, apparently complete transurethral resection of bladder tumour specimen is a surrogate marker of resection quality, predicts risk of early recurrence, and is dependent on operator experience. *Eur Urol* **57**: 843–849.

Masoudi A, Elopre M, Amini E, Nagel ME, Ater JL, Gopalakrishnan V, Wolff JEA (2008) Influence of valproic acid on outcome of high-grade gliomas in children. *Anticancer Res* **28**: 2437–2442.

Masters JRW, Hepburn PJ, Walker L, Highman WJ, Trejdosiewicz LK, Povey S, Parkar M, Hill BT, Riddle PR, Franks LM (1986) Tissue Culture Model of Transitional Cell Carcinoma: Characterization of Twenty-two Human Urothelial Cell Lines. *Cancer Res* **46**: 3630–3636.

Mazzucchelli R, Cheng L, Lopez-Beltran A, Scarpelli M, Montironi R (2012) Classification and grading of noninvasive and invasive neoplasms of the urothelium. *Anal Quant Cytol Histol* **34**: 111–119.

McCabe N, Turner NC, Lord CJ, Kluzek K, Bialkowska A, Swift S, Giavara S, O'Connor MJ, Tutt AN, Zdzienicka MZ, Smith GCM, Ashworth A (2006) Deficiency in the repair of DNA damage by homologous recombination and sensitivity to poly(ADP-ribose) polymerase inhibition. *Cancer Res* **66**: 8109–8115.

McDonald MM, Swagerty D, Wetzel L (2006) Assessment of microscopic hematuria in adults. *Am Fam Physician* **73**: 1748–1754.

McVey M, Lee SE (2008) MMEJ repair of double-strand breaks (director's cut): deleted sequences and alternative endings. *Trends Genet* **24**: 529–538.

Miller KM, Tjeertes J V, Coates J, Legube G, Polo SE, Britton S, Jackson SP (2010) Human HDAC1 and HDAC2 function in the DNA-damage response to promote DNA nonhomologous end-joining. *Nat Struct Mol Biol* **17**: 1144–1151.

Minucci S, Pelicci PG (2006) Histone deacetylase inhibitors and the promise of epigenetic (and more) treatments for cancer. *Nat Rev Cancer* **6**: 38–51.

Mladenov E, Magin S, Soni A, Iliakis G (2013) DNA double-strand break repair as determinant of cellular radiosensitivity to killing and target in radiation therapy. *Front Oncol* **3**: 113.

Moneef MAL, Sherwood BT, Bowman KJ, Kockelbergh RC, Symonds RP, Steward WP, Mellon JK, Jones GDD (2003) Measurements using the alkaline comet assay predict bladder cancer cell radiosensitivity. *Br J Cancer* **89**: 2271–2276.

Montironi R, Mazzucchelli R, Scarpelli M, Lopez-Beltran A, Cheng L (2008) Morphological diagnosis of urothelial neoplasms. *J Clin Pathol* **61**: 3–10.

Morgan WF, Sowa MB (2005) Effects of ionizing radiation in nonirradiated cells. *Proc Natl Acad Sci* **102**: 14127–14128.

Mueller CM, Caporaso N, Greene MH (2008) Familial and genetic risk of transitional cell carcinoma of the urinary tract. *Urol Oncol* **26**: 451–464.

Muller PAJ, Vousden KH (2013) P53 Mutations in Cancer. *Nat Cell Biol* **15**: 2–8.

Munshi A, Hobbs M, Meyn RE (2005a) Clonogenic cell survival assay. *Methods Mol Med* **110**: 21–28.

Munshi A, Kurland JF, Nishikawa T, Tanaka T, Hobbs ML, Tucker SL, Ismail S, Stevens C, Meyn RE (2005b) Histone deacetylase inhibitors radiosensitize human melanoma cells by suppressing DNA repair activity. *Clin Cancer Res* **11**: 4912–4922.

Munshi A, Tanaka T, Hobbs ML, Tucker SL, Richon VM, Meyn RE (2006) Vorinostat, a histone deacetylase inhibitor, enhances the response of human tumor cells to ionizing radiation through prolongation of gamma-H2AX foci. *Mol Cancer Ther* **5**: 1967–1974.

Nagy L, Kao H, Chakravarti D, Lin RJ, Hassig CA, Ayer DE, Schreiber SL, Evans RM (1997) Nuclear receptor repression mediated by a complex containing SMRT, mSin3A, and histone deacetylase. *Cell* **89**: 373–380.

Nicholson S (2012) Chemotherapy for bladder cancer in patients with impaired renal function. *Nat Rev Urol* **9**: 52–57.

Niegisch G, Knievel J, Koch A, Hader C, Fischer U, Albers P, Schulz WA (2012) Changes in histone deacetylase (HDAC) expression patterns and activity of HDAC inhibitors in urothelial cancers. *Urol Oncol* **In Press**: x.doi.org/10.1016/j.urolonc.2012.06.015.

Nielsen ME, Shariat SF, Karakiewicz PI, Lotan Y, Rogers CG, Amiel GE, Bastian PJ, Vazina A, Gupta A, Lerner SP, Sagalowsky AI, Schoenberg MP, Palapattu GS (2007) Advanced age is associated with poorer bladder cancer-specific survival in patients treated with radical cystectomy. *Eur Urol* **51**: 699–706; discussion 706–8.

Nikjoo H, O'Neill P, Wilson WE, Goodhead DT (2001) Computational Approach for Determining the Spectrum of DNA Damage Induced by Ionizing Radiation. *Radiat Res* **156**: 577–583.

Noguchi H, Yamashita H, Murakami T, Hirai K, Noguchi Y, Maruta J, Yokoi T, Noguchi S (2009) Successful treatment of anaplastic thyroid carcinoma with a combination of oral valproic acid, chemotherapy, radiation and surgery. *Endocr J* **56**: 245–249.

Noon AP, Albertsen PC, Thomas F, Rosario DJ, Catto JWF (2013) Competing mortality in patients diagnosed with bladder cancer: evidence of undertreatment in the elderly and female patients. *Br J Cancer* **108**: 1534–1540.

O'Connor OJ, Maher MM (2010) CT Urography. *Am J Roentgenol* **195**: W320–4.

O'Driscoll M, Jeggo P a (2006) The role of double-strand break repair - insights from human genetics. *Nat Rev Genet* **7**: 45–54.

Ott OJ, Rödel C, Weiss C, Wittlinger M, St Krause F, Dunst J, Fietkau R, Sauer R (2009) Radiochemotherapy for bladder cancer. *Clin Oncol* **21**: 557–565.

Ozawa A, Tanji N, Kikugawa T, Sasaki T, Yanagihara Y, Miura N, Yokoyama M (2010) Inhibition of bladder tumour growth by histone deacetylase inhibitor. *BJU Int* **105**: 1181–1186.

Pacheco M, Nielsen TO (2012) Histone deacetylase 1 and 2 in mesenchymal tumors. *Mod Pathol* **25**: 222–230.

Panier S, Boulton SJ (2014) Double-strand break repair: 53BP1 comes into focus. *Nat Rev Mol Cell Biol* **15**: 7–18.

Park YB, Chae J, Kim YC, Cho Y (2011) Crystal structure of human Mre11: understanding tumorigenic mutations. *Structure* **19**: 1591–1602.

Parkin DM (2011) Cancers attributable to occupational exposures in the UK in 2010. *Br J Cancer* **105 Suppl** : S70–2.

Paull TT, Gellert M (1998) The 3’ to 5' Exonuclease Activity of Mre11 Facilitates Repair of DNA Double-Strand Breaks. *Mol Cell* **1**: 969–979.

Paull TT, Gellert M (1999) Nbs1 potentiates ATP-driven DNA unwinding and endonuclease cleavage by the Mre11/Rad50 complex. *Genes Dev* **13**: 1276–1288.

Pawlik TM, Keyomarsi K (2004) Role of cell cycle in mediating sensitivity to radiotherapy. *Int J Radiat Oncol Biol Phys* **59**: 928–942.

Pelucchi C, Bosetti C, Negri E, Malvezzi M, La Vecchia C (2006) Mechanisms of disease: The epidemiology of bladder cancer. *Nat Clin Pract Urol* **3**: 327–340.

Peserico A, Simone C (2011) Physical and functional HAT/HDAC interplay regulates protein acetylation balance. *J Biomed Biotechnol* **2011**: 371832.

Plna K, Hemminki K (2001) Familial bladder cancer in the National Swedish Family Cancer Database. *J Urol* **166**: 2129–2133.

Ploeg M, Aben KKH, Kiemeney LA (2009) The present and future burden of urinary bladder cancer in the world. *World J Urol* **27**: 289–293.

Pogo B, Allfrey V, Mirsky A (1966) RNA synthesis and histone acetylation during the course of gene activation in lymphocytes. *Proc Natl Acad Sci* 805–812.

Polo SE, Jackson SP (2011) Dynamics of DNA damage response proteins at DNA breaks: a focus on protein modifications. *Genes Dev* **25**: 409–433.

Povirk LF (2012) Processing of Damaged DNA Ends for Double-Strand Break Repair in Mammalian Cells. *ISRN Mol Biol* **2012**: 1–16.

Prince H, Bishton M (2009) Panobinostat (LBH589): a novel pan-deacetylase inhibitor with activity in T cell lymphoma. *Hematol Meet Reports* **3**: 33–38.

Prince HM, Dickinson M (2012) Romidepsin for cutaneous T-cell lymphoma. *Clin Cancer Res* **18**: 3509–3515.

Pucci S, Mazzarelli P, Rabitti C, Giai M, Gallucci M, Flammia G, Alcini a, Altomare V, Fazio VM (2001) Tumor specific modulation of KU70/80 DNA binding activity in breast and bladder human tumor biopsies. *Oncogene* **20**: 739–747.

Qiao B, Kerr M, Groselj B, Teo MTW, Knowles MA, Bristow RG, Phillips RM, Kiltie AE (2013) Imatinib radiosensitizes bladder cancer by targeting homologous recombination. *Cancer Res* **73**: 1611–1620.

Quint K, Agaimy A, Di Fazio P, Montalbano R, Steindorf C, Jung R, Hellerbrand C, Hartmann A, Sitter H, Neureiter D, Ocker M (2011) Clinical significance of histone deacetylases 1, 2, 3, and 7: HDAC2 is an independent predictor of survival in HCC. *Virchows Arch An Int J Pathol* **459**: 129–139.

Quiros S, Roos WP, Kaina B (2011) Rad51 and BRCA2 - New molecular targets for sensitizing glioma cells to alkylating anticancer drugs. *PLoS One* **6**: e27183.

Qvist P, Huertas P, Jimeno S, Nyegaard M, Hassan MJ, Jackson SP, Børglum AD (2011) CtIP Mutations Cause Seckel and Jawad Syndromes. *PLoS Genet* **7**: e1002310.

Rassool F V, Tomkinson AE (2010) Targeting abnormal DNA double strand break repair in cancer. *Cell Mol Life Sci C* **67**: 3699–3710.

Ree AH, Dueland S, Folkvord S, Hole KH, Seierstad T, Johansen M, Abrahamsen TW, Flatmark K (2010) Vorinostat, a histone deacetylase inhibitor, combined with pelvic palliative radiotherapy for gastrointestinal carcinoma: the Pelvic Radiation and Vorinostat (PRAVO) phase 1 study. *Lancet Oncol* **11**: 459–464.

Ree AH, Hollywood D (2013) Design and conduct of early-phase radiotherapy trials with targeted therapeutics: Lessons from the PRAVO experience. *Radiother Oncol* **108**: 3–16.

Rigby L, Muscat A, Ashley D, Algar E (2012) Methods for the analysis of histone H3 and H4 acetylation in blood. *Epigenetics* **7**: 875–882.

Rodel C, Grabenbauer GC, Kuhn R, Papadopolous T, Dunst J, Meyer M, Schrott KM, Sauer R (2002) Combined-Modality Treatment and Selective Organ Preservation in Invasive Bladder Cancer: Long-Term Results. *J Clin Oncol* **20**: 3061–3071.

Rogakou EP, Boon C, Redon C, Bonner WM (1999) Megabase Chromatin Domains Involved in DNA Double-Strand Breaks In Vivo. *J Cell Biol* **146**: 905–915.

Ropero S, Esteller M (2007) The role of histone deacetylases (HDACs) in human cancer. *Mol Oncol* **1**: 19–25.

Rosato RR, Almenara JA, Maggio SC, Coe S, Atadja P, Dent P, Grant S (2008) Role of histone deacetylase inhibitor-induced reactive oxygen species and DNA damage in LAQ-824/fludarabine antileukemic interactions. *Mol Cancer Ther* **7**: 3285–3297.

Rothkamm K, Krüger I, Thompson LH, Lobrich M (2003) Pathways of DNA double-strand break repair during the mammalian cell cycle. *Mol Cell Biol* **23**: 5706–5715.

Rupnik A, Grenon M, Lowndes N (2008) The MRN complex. *Curr Biol* **18**: R455–7.

Rupnik A, Lowndes NF, Grenon M (2010) MRN and the race to the break. *Chromosoma* **119**: 115–135.

Russell JS, Brady K, Burgan WE, Cerra MA, Oswald KA, Camphausen K, Tofilon PJ (2003) Gleevec-Mediated Inhibition of Rad51 Expression and Enhancement of Tumor Cell Radiosensitivity. *Cancer Res* **63**: 7377–7383.

Samartzis N, Imesch P, Dedes KJ, Samartzis EP, Fedier A, Fink D, Caduff R, Fehr MK (2011) Expression pattern of class I histone deacetylases in vulvar intraepithelial neoplasia and vulvar cancer: a tissue microarray study. *BMC Cancer* **11**: 463.

Sangar VK, Ragavan N, Matanhelia SS, Watson MW, Blades RA (2005) The economic consequences of prostate and bladder cancer in the UK. *BJU Int* **95**: 59–63.

Sartori AA, Lukas C, Coates J, Mistrik M, Fu S, Bartek J, Baer R, Lukas J, Jackson SP (2007) Human CtIP promotes DNA end resection. *Nature* **450**: 509–514.

Sayan BS, Yang AL, Conforti F, Bernardini S, Tucci P, Vasa-Nicotera M, Knight RA, Melino G (2010) Induction of TAp63 by histone deacetylase inhibitors. *Biochem Biophys Res Commun* **391**: 1748–1751.

Schwartz DC, Cantor CR (1984) Separation of yeast chromosome-sized DNAs by pulsed field gradient gel electrophoresis. *Cell* **37**: 67–75.

Scuto A, Kirschbaum M, Kowolik C, Kretzner L, Juhasz A, Atadja P, Pullarkat V, Bhatia R, Forman S, Yen Y, Jove R (2008) The novel histone deacetylase inhibitor, LBH589, induces expression of DNA damage response genes and apoptosis in Ph- acute lymphoblastic leukemia cells. *Blood* **111**: 5093–5100.

Sexton WJ, Wiegand LR, Correa JJ, Politis C, Dickinson SI, Kang LC (2010) Bladder cancer: a review of non-muscle invasive disease. *Cancer Control* **17**: 256–268.

Shao Z, Davis AJ, Fattah KR, So S, Sun J, Lee K-J, Harrison L, Yang J, Chen DJ (2012) Persistently bound Ku at DNA ends attenuates DNA end resection and homologous recombination. *DNA Repair (Amst)* **11**: 310–316.

Sharma N, Groselj B, Hamdy FC, Kiltie AE (2013) The emerging role of histone deacetylase (HDAC) inhibitors in urological cancers. *BJU Int* **111**: 537–542.

Sharma S, Ksheersagar P, Sharma P (2009) Diagnosis and treatment of bladder cancer. *Am Fam Physician* **80**: 717–723.

Short SC, Giampieri S, Worku M, Alcaide-German M, Sioftanos G, Bourne S, Lio KI, Shaked-Rabi M, Martindale C (2011) Rad51 inhibition is an effective means of targeting DNA repair in glioma models and CD133+ tumor-derived cells. *Neuro Oncol* **13**: 487–499.

Shrivastav M, De Haro LP, Nickoloff JA (2008) Regulation of DNA double-strand break repair pathway choice. *Cell Res* **18**: 134–147.

Sievert KD, Amend B, Nagele U, Schilling D, Bedke J, Horstmann M, Hennenlotter J, Kruck S, Stenzl A (2009) Economic aspects of bladder cancer: what are the benefits and costs? *World J Urol* **27**: 295–300.

Singh NP, McCoy MT, Tice RR, Schneider EL (1988) A simple technique for quantitation of low levels of DNA damage in individual cells. *Exp Cell Res* **175**: 184–191.

Spiegel S, Milstien S, Grant S (2012) Endogenous modulators and pharmacological inhibitors of histone deacetylases in cancer therapy. *Oncogene* **31**: 537–551.

Steel G, McMillan T, Peacock J (1989) Letter to the Editor The 5Rs of Radiobiology. *Int J Radiat Biol* **56**: 1045–1048.

Stein JP, Skinner DG (2006) Radical cystectomy for invasive bladder cancer: long-term results of a standard procedure. *World J Urol* **24**: 296–304.

Stenzl A, Nagele U, Kuczyk M, Sievert K-D, Anastasiadis A, Seibold J, Corvin S (2005) Cystectomy – Technical Considerations in Male and Female Patients. *EAU Updat Ser* **3**: 138–146.

Stenzl A, Witjes JA, Compérat E, Cowan NC, Santis M De, Kuczyk M, Lebret T, Ribal MJ, Sherif A (2011) Guideline on Bladder Cancer Muscle-invasive and Metastatic (European Association of Urology).

Stewart GS, Maser RS, Stankovic T, Bressan DA, Kaplan MI, Jaspers NG, Raams A, Byrd PJ, Petrini JH, Taylor AM (1999) The DNA double-strand break repair gene hMRE11 is mutated in individuals with an ataxia-telangiectasia-like disorder. *Cell* **99**: 577–587.

Storch K, Eke I, Borgmann K, Krause M, Richter C, Becker K, Schröck E, Cordes N (2010) Three-dimensional cell growth confers radioresistance by chromatin density modification. *Cancer Res* **70**: 3925–3934.

Sumantran VN (2011) Cellular Chemosensitivity Assays: An Overview. In Cancer Cell Culture: Methods and Protocols, I.A. Cree, ed. (Totowa, NJ: Humana Press), pp. 219–236.

Surova O, Zhivotovsky B (2013) Various modes of cell death induced by DNA damage. *Oncogene* **32**: 3789–3797.

Sylvester RJ, van der Meijden APM, Oosterlinck W, Witjes JA, Bouffioux C, Denis L, Newling DWW, Kurth K (2006) Predicting recurrence and progression in individual patients with stage Ta T1 bladder cancer using EORTC risk tables: a combined analysis of 2596 patients from seven EORTC trials. *Eur Urol* **49**: 466–5; discussion 475–7.

Sylvester RJ, Oosterlinck W, van der MEIJDEN APM (2004) A single immediate postoperative instillation of chemotherapy decreases the risk of recurrence in patients with stage Ta T1 bladder cancer: a meta-analysis of published results of randomized clinical trials. *J Urol* **171**: 2186–2190.

Tate CR, Rhodes L V, Segar HC, Driver JL, Pounder FN, Burow ME, Collins-Burow BM (2012) Targeting triple-negative breast cancer cells with the histone deacetylase inhibitor panobinostat. *Breast Cancer Res BCR* **14**: R79.

Trujillo KM (1998) Nuclease Activities in a Complex of Human Recombination and DNA Repair Factors Rad50, Mre11, and p95. *J Biol Chem* **273**: 21447–21450.

Turney BW, Kerr M, Chitnis MM, Lodhia K, Wang Y, Riedemann J, Rochester M, Protheroe AS, Brewster SF, Macaulay VM (2012) Depletion of the type 1 IGF receptor delays repair of radiation-induced DNA double strand breaks. *Radiother Oncol* **103**: 402–409.

Uchisaka N, Takahashi N, Sato M, Kikuchi A, Mochizuki S, Imai K, Nonoyama S, Ohara O, Watanabe F, Mizutani S, Hanada R, Morio T (2009) Two brothers with ataxia-telangiectasia-like disorder with lung adenocarcinoma. *J Pediatr* **155**: 435–438.

Ungerstedt JS, Sowa Y, Xu W-S, Shao Y, Dokmanovic M, Perez G, Ngo L, Holmgren A, Jiang X, Marks PA (2005) Role of thioredoxin in the response of normal and transformed cells to histone deacetylase inhibitors. *Proc Natl Acad Sci U S A* **102**: 673–678.

Valerio M, Lhermitte B, Bauer J, Jichlinski P (2011) Metastatic primary adenocarcinoma of the bladder in a twenty-five years old woman. *Rare Tumors* **3**: e9.

VanderMolen KM, McCulloch W, Pearce CJ, Oberlies NH (2011) Romidepsin (Istodax, NSC 630176, FR901228, FK228, depsipeptide): a natural product recently approved for cutaneous T-cell lymphoma. *J Antibiot (Tokyo)* **64**: 525–531.

Vojtesek B, Dolezalova H, Lauerova L, Svitakova M, Havlis P, Kovarik J, Midgley C, Lane D (1995) Conformational changes in p53 analysed using new antibodies to the core DNA binding domain of the protein. *Oncogene* **10**: 389–393.

Wallmeroth A, Wagner U, Moch H, Gasser TC, Sauter G, Mihatsch MJ (1999) Patterns of metastasis in muscle-invasive bladder cancer (pT2-4): An autopsy study on 367 patients. *Urol Int* **62**: 69–75.

Waltes R, Kalb R, Gatei M, Kijas AW, Stumm M, Sobeck A, Wieland B, Varon R, Lerenthal Y, Lavin MF, Schindler D, Dörk T (2009) Human RAD50 deficiency in a Nijmegen breakage syndrome-like disorder. *Am J Hum Genet* **84**: 605–616.

Wang G, He J, Zhao J, Yun W, Xie C, Taub JW, Azmi A, Mohammad RM, Dong Y, Kong W, Guo Y, Ge Y (2012) Class I and class II histone deacetylases are potential therapeutic targets for treating pancreatic cancer. *PLoS One* **7**: e52095.

Wang M, Wu W, Wu W, Rosidi B, Zhang L, Wang H, Iliakis G (2006) PARP-1 and Ku compete for repair of DNA double strand breaks by distinct NHEJ pathways. *Nucleic Acids Res* **34**: 6170–6182.

Wang SC, Lin SH, Su LK, Hung MC (1997) Changes in BRCA2 expression during progression of the cell cycle. *Biochem Biophys Res Commun* **234**: 247–251.

Wang Z, Zang C, Cui K, Schones DE, Barski A, Peng W, Zhao K (2009) Genome-wide mapping of HATs and HDACs reveals distinct functions in active and inactive genes. *Cell* **138**: 1019–1031.

Whittaker SJ, Demierre M-F, Kim EJ, Rook AH, Lerner A, Duvic M, Scarisbrick J, Reddy S, Robak T, Becker JC, Samtsov A, McCulloch W, Kim YH (2010) Final results from a multicenter, international, pivotal study of romidepsin in refractory cutaneous T-cell lymphoma. *J Clin Oncol* **28**: 4485–4491.

Williams GJ, Lees-Miller SP, Tainer JA (2010) Mre11-Rad50-Nbs1 conformations and the control of sensing, signaling, and effector responses at DNA double-strand breaks. *DNA Repair (Amst)* **9**: 1299–1306.

Williams RS, Moncalian G, Williams JS, Yamada Y, Limbo O, Shin DS, Groocock LM, Cahill D, Hitomi C, Guenther G, Moiani D, Carney JP, Russell P, Tainer JA (2008) Mre11 dimers coordinate DNA end bridging and nuclease processing in double-strand-break repair. *Cell* **135**: 97–109.

Williams S V, Adams J, Coulter J, Summersgill BM, Shipley J, Knowles MA (2005) Assessment by M-FISH of karyotypic complexity and cytogenetic evolution in bladder cancer in vitro. *Genes Chromosomes Cancer* **43**: 315–328.

Wilson AJ, Holson E, Wagner F, Zhang Y-L, Fass DM, Haggarty SJ, Bhaskara S, Hiebert SW, Schreiber SL, Khabele D (2011) The DNA damage mark pH2AX differentiates the cytotoxic effects of small molecule HDAC inhibitors in ovarian cancer cells. *Cancer Biol Ther* **12**: 484–493.

Wilson PM, LaBonte MJ, Martin SC, Kuwahara ST, El-Khoueiry A, Lenz H-J, Ladner RD (2013) Sustained inhibition of deacetylases is required for the antitumor activity of the histone deactylase inhibitors panobinostat and vorinostat in models of colorectal cancer. *Invest New Drugs* **31**: 845–857.

Wouters BG, Begg AC (2009) Irradiation-induced damage and the DNA damage response. In Basic Clinical Radiobiology, M.C. Joiner, and A. van der Kogel, eds. (London: Hodder Arnold), pp. 11–26.

Wu X-R (2005) Urothelial tumorigenesis: a tale of divergent pathways. *Nat Rev Cancer* **5**: 713–725.

Xiao W, Graham PH, Hao J, Chang L, Ni J, Power CA, Dong Q, Kearsley JH, Li Y (2013) Combination Therapy with the Histone Deacetylase Inhibitor LBH589 and Radiation Is an Effective Regimen for Prostate Cancer Cells. *PLoS One* **8**: e74253.

Xu J, Reumers J, Couceiro JR, De Smet F, Gallardo R, Rudyak S, Cornelis A, Rozenski J, Zwolinska A, Marine J-C, Lambrechts D, Suh Y-A, Rousseau F, Schymkowitz J (2011a) Gain of function of mutant p53 by coaggregation with multiple tumor suppressors. *Nat Chem Biol* **7**: 285–295.

Xu XS, Wang L, Abrams J, Wang G (2011b) Histone deacetylases (HDACs) in XPC gene silencing and bladder cancer. *J Hematol Oncol* **4**: 1–11.

Yan W, Liu S, Xu E, Zhang J, Zhang Y, Chen X (2013) Histone deacetylase inhibitors suppress mutant p53 transcription via histone deacetylase 8. *Oncogene* **32**: 599–609.

Yee DS, Ishill NM, Lowrance WT, Herr HW, Elkin EB (2011) Ethnic differences in bladder cancer survival. *Urology* **78**: 544–549.

Yu X, Chen J (2004) DNA Damage-Induced Cell Cycle Checkpoint Control Requires CtIP , a Phosphorylation-Dependent Binding Partner of BRCA1 C-Terminal Domains. *Mol Cell Biol* **24**: 9478–9486.

Yuan Z, Zhang X, Sengupta N, Lane WS, Seto E (2007) SIRT1 regulates the function of the Nijmegen breakage syndrome protein. *Mol Cell* **27**: 149–162.

Zha S, Boboila C, Alt FW (2009) Mre11: roles in DNA repair beyond homologous recombination. *Nat Struct Mol Biol* **16**: 798–800.

Zhang F, Zhang T, Teng Z-H, Zhang R, Wang J-B, Mei Q-B (2009) Sensitization to gamma-irradiation-induced cell cycle arrest and apoptosis by the histone deacetylase inhibitor trichostatin A in non-small cell lung cancer (NSCLC) cells. *Cancer Biol Ther* **8**: 823–831.

Zhang Y, Carr T, Dimtchev A, Zaer N, Dritschilo A, Jung M (2007) Attenuated DNA damage repair by trichostatin A through BRCA1 suppression. *Radiat Res* **168**: 115–124.

Zhang Y, Lim CUK, Williams ES, Zhou J, Zhang Q, Fox MH, Bailey SM, Liber HL (2005) NBS1 Knockdown by Small Interfering RNA Increases Ionizing Radiation Mutagenesis and Telomere Association in Human Cells Ionizing Radiation Mutagenesis and Telomere. *Cancer Res* **65**: 5544–5553.

APPENDICES

Appendix A.

Table A.1. Cell lines *TP53* status, grade and stage characteristics.

Cell line	*TP53* status	Grade	Stage	Reference
RT112	wild-type	G2	Not recorded (1972)	(Masters *et al*, 1986; Williams *et al*, 2005)
CAL29	mutant	G4	T2	(Cattan *et al*, 2001)
T24	mutant	G3	Not recorded (1970)	(Bubenik *et al*, 1973)

Table A.2. Plating efficiencies for cell lines used in this thesis.

Cell line	Plating efficiency
RT112	0.59
CAL29	0.18
T24	0.58
Ku80KD	0.43
RAD51KD	0.58

Table A.3. The combination index analysis of 10 nM panobinostat in RT112 cells.

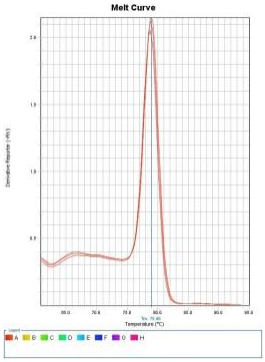
Dose (GY)	DMSO+IR Sfa	Sfb	SfaxSfb	PAN+IR Sfab	Effect
0	1	0,985187	0,985187	1	Sub-additive
2	0,741729		0,730742	0,73490752	Sub-additive
4	0,50475		0,497274	0,442596538	Supra-additive
6	0,272797		0,268756	0,171524437	Supra-additive
8	0,102697		0,101176	0,048118873	Supra-additive

Table A.4. The combination index analysis of 25 nM panobinostat in RT112 cells.

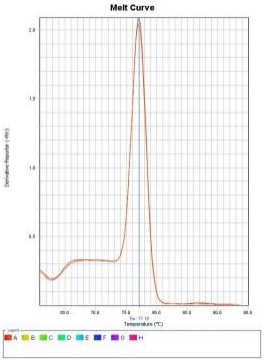
Dose (GY)	DMSO+IR Sfa	Sfb	SfaxSfb	PAN+IR Sfab	Effect
0	1	0,745654	0,745654	1	Sub-additive
2	0,741729		0,553073	0,711616	Sub-additive
4	0,50475		0,376369	0,348884	Supra-additive
6	0,272797		0,203412	0,105567	Supra-additive
8	0,102697		0,076576	0,015869	Supra-additive

Appendix B. Melting temperature profiles for *HDAC1-11* primers

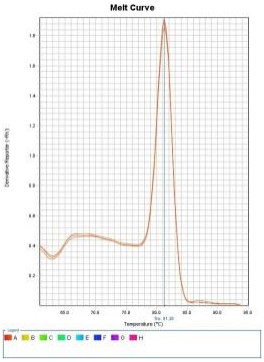
HDAC1



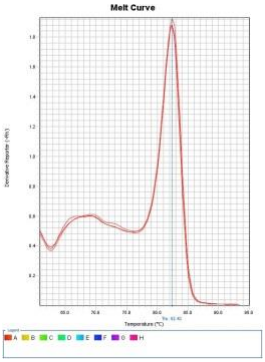
HDAC2



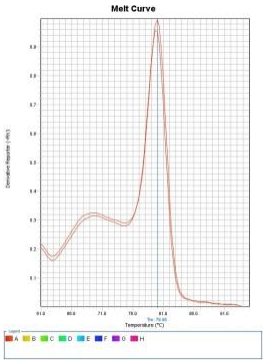
HDAC3



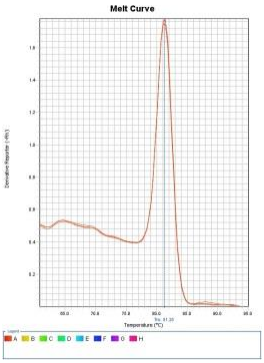
HDAC4



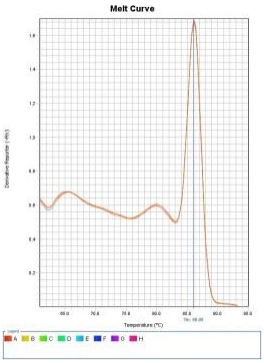
HDAC5



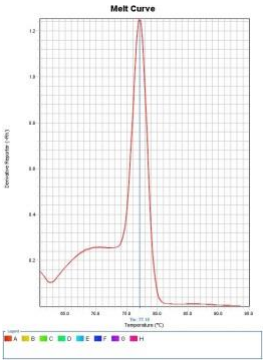
HDAC6



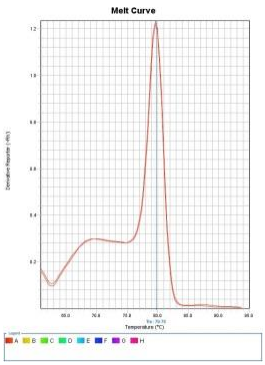
HDAC7



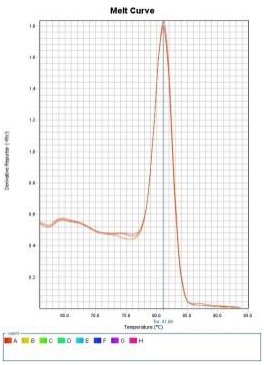
HDAC8



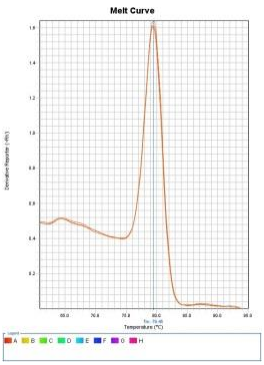
HDAC9



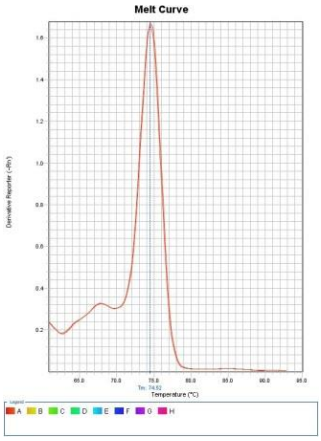
HDAC10



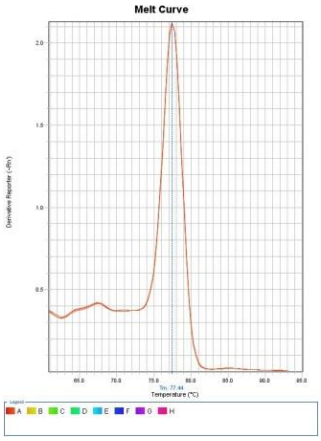
HDAC11



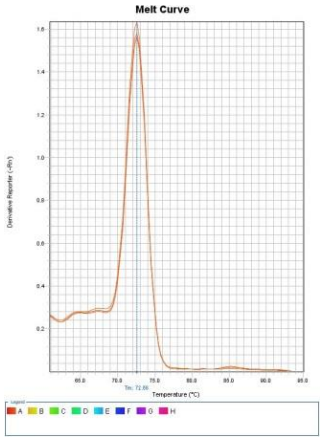
MRE11



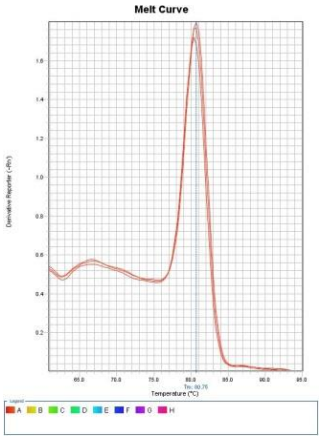
RAD50



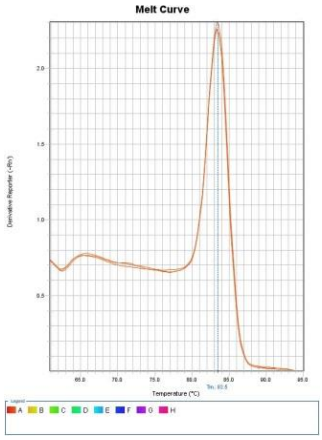
NBS1



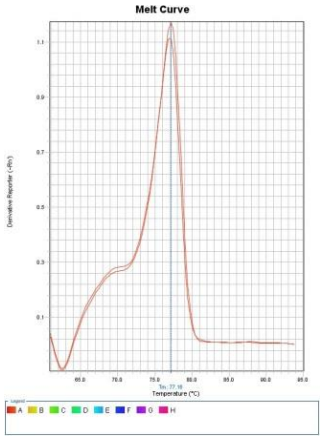
RAD51



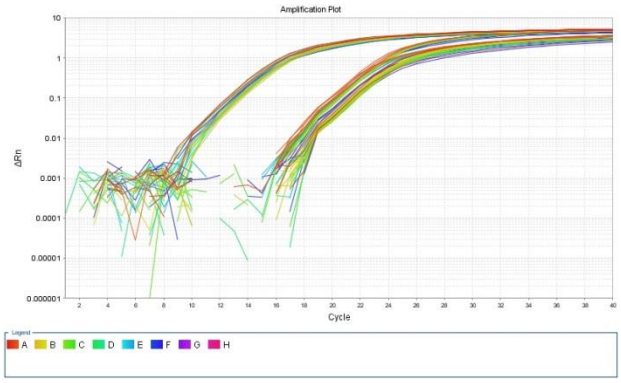
p53



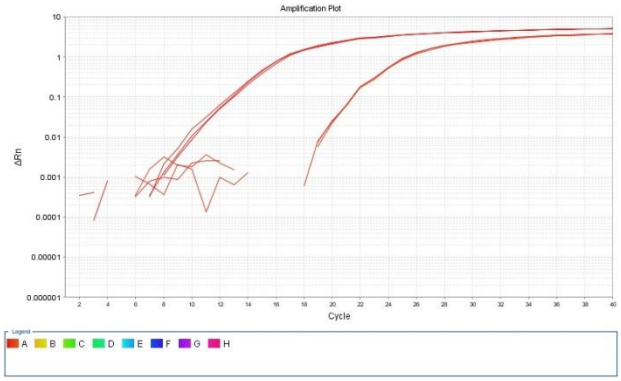
CtIP



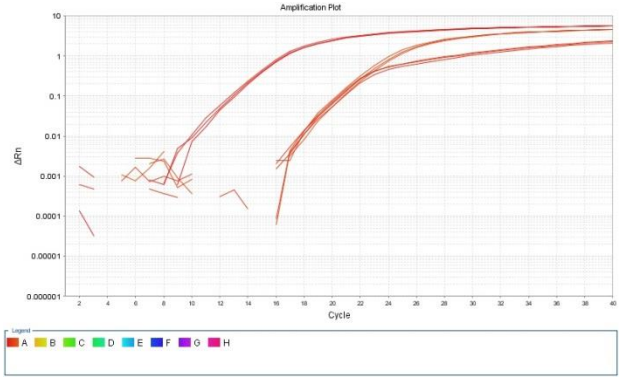
GAPDH and MRN complex qPCR amplification plot.



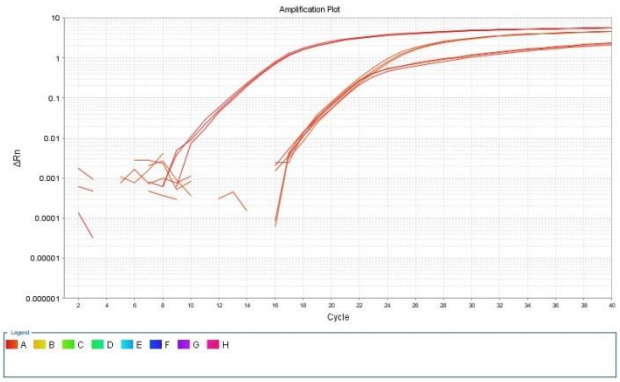
GAPDH and RAD51 qPCR amplification plot.



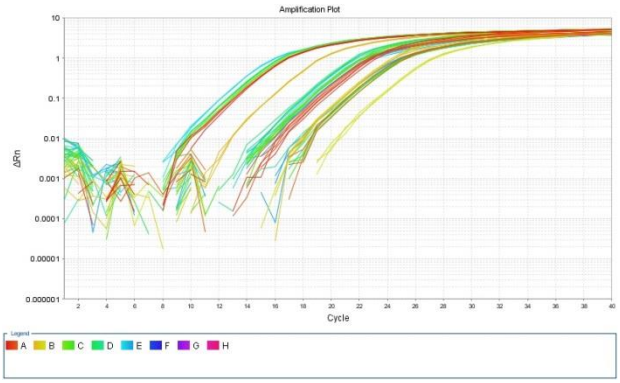
GAPDH, p53 and CtIP qPCR amplification plot.



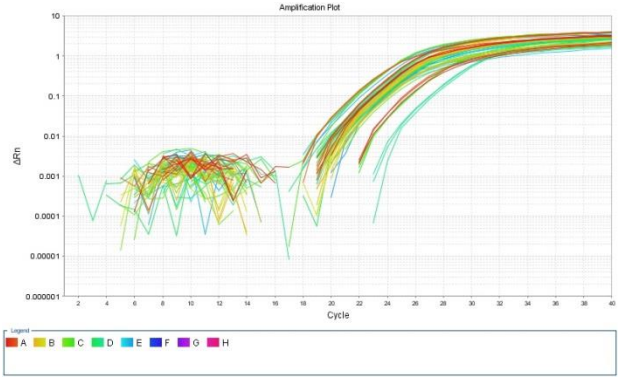
GAPDH, p53 and CtIP qPCR amplification plot.



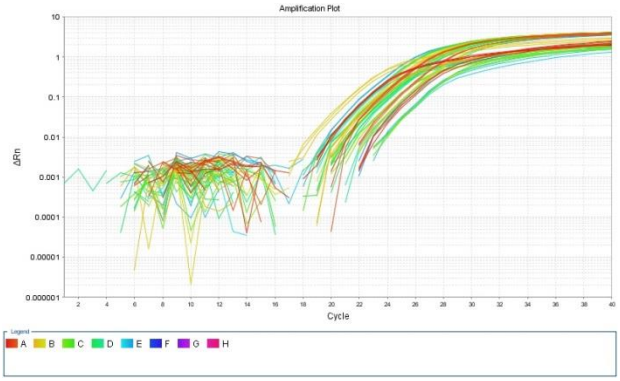
GAPDH, HDAC1, HDAC2 and HDAC3 qPCR amplification plot.



HDAC4, HDAC5, HDAC6 and HDAC7 qPCR amplification plot.



HDAC8, HDAC9, HDAC10 and HDAC11 qPCR amplification plot.



Appendix C. Published papers

1. Sharma NL, Groselj B, Hamdy FC, Kiltie AE (2013) The emerging role of HDAC inhibitors in urological cancers. *BJUi* **111**:537-542.
2. Groselj B, Sharma N, Hamdy FC, Kerr M, Kiltie AE (2013) Histone deacetylase inhibitors as radiosensitisers – effects on DNA damage signalling and repair. *Br J Cancer* **108**:748-754.
3. Qiao B, Kerr M, Groselj B, Teo MTW, Knowles MA, Bristow RG, Phillips RM, Kiltie AE (2013) Imatinib radiosensitisers bladder cancer by targeting homologous recombination. *Cancer Res* **73**:1611-1620.
4. Groselj B, Kerr M, Kiltie AE (2013) Radiosensitisation of bladder cancer cells by panobinostat is modulated by Ku80 expression. *Radiother Oncol*. DOI: 10.1016/j.radonc.2013.06.021.